To the Graduate Council:

I am submitting herewith a thesis written by Roger T. Steinberg entitled "Geology and Petrology of the Lost Creek Barite Mine, Union County, Tennessee." I recommend that it be accepted in partial fulfillment of the requirements for the degree of Master of Science, with a major in Geology.

Otto Kopp, Major Professor

We have read this thesis
and recommend its acceptance:

Lawrence A. Taylor

Kenneth P. Walker

Accepted for the Council:

Vice Chancellor
Graduate Studies and Research

GEOLOGY AND PETROLOGY OF THE LOST CREEK BARITE MINE, UNION COUNTY, TENNESSEE

A Thesis

Presented for the

Master of Science

Degree

The University of Tennessee, Knoxville

Roger T. Steinberg

June 1981

3051870

DEDICATION

This thesis is dedicated to my family, especially my Mom and Dad. I could not have done it without your continuing love and support. Thanks, Mom and Dad, Aunt Jean and Uncle Gordon, Barbara, Dick, and Susan.

ACKNOWLEDGMENTS

The writer wishes to extend his most sincere appreciation to Dr. Otto Kopp for his advice and unending support during my undergraduate and graduate work at the University of Tennessee.

A word of gratitude is also extended to Mr. Helmuth Wedow, formerly of the United States Geological Survey, who graciously offered his invaluable field assistance and counsel.

Special thanks to Dr. Lawrence Taylor and Dr. Kenneth Walker for their assistance and contributions to the finished product.

I am most grateful to Mr. Stuart Maher of the Tennessee Division of Geology who first introduced me to the Lost Creek deposit.

Thanks also to my many colleagues and friends, especially Dr. Clayton Breland and Dr. Habte Churnet, who assisted the writer on numerous occasions with technical problems. Field assistance was given by Mr. Roland Larsen, Mr. Gary Runyon, and Mr. Tom Stafford.

Imco Services, Inc., donated drill core which was essential to understanding the Lost Creek deposit. I am also grateful to Coastal Mining Company for the opportunity to complete the thesis.

Finally, I wish to thank my family who were always there when I needed them.

ABSTRACT

The geology and petrology of the Lost Creek barite mine, Union County, Tennessee, were investigated. The uppermost portion of the Mascot Dolomite (Lower Ordovician) and the lower portion of the Dot Formation (Middle Ordovician) are exposed in the Lost Creek area. Rocks of the Lower Ordovician are separated from those of the Middle Ordovician by the Knox unconformity.

The depositional regime for the Dot Formation portion of the Lost Creek section was peritidal (tidal flat and adjacent shallow water marine environments). The carbonate depositional regime of Andros Island, Bahamas, is considered to be a very approximate recent analogue.

Diagenesis of the Dot sediments included many specific events which can be woven into a paragenetic sequence. Most important of these events was dolomitization. Two distinct episodes of dolomitization are recognized. The first (Type I) occurred within a mixing zone of marine and fresh waters. A second episode (Type II) preceded and accompanied mineralization. Type II dolomite can be distinguished by its coarse grain size, luminescent zonation, and ferrous iron content. Much of the Type II dolomite occurs as void- or vug-fillings.

At Lost Creek, mineralization consists of barite with minor sulfides (pyrite, marcasite, sphalerite, galena, and chalcopyrite) and is associated with brecciation and Type II dolomitization. Unlike other Mississippi Valley-type deposits in east Tennessee, brecciation and mineralization are not confined to Lower Ordovician rocks but extend into basal Middle Ordovician beds. Mineralization within the Middle

Orodvician Dot Formation can be considered a diagenetic event, and was probably even syngenetic in part.

Mineralization, at least some brecciation, and Type II dolomitization resulted from mixing of the mineralizing fluids with formational waters (which themselves were the product of the earlier mixing of fresh and marine waters). Barite deposition may have been controlled by the cooling and oxidation of the sulfide-rich ore fluid by the formational solutions.

TABLE OF CONTENTS

CHAPTER		PAGE
I.	INTRODUCTION	1
	Purpose and Scope of Investigation	1
	Geologic Setting	4
	General Description of the Deposit	8
	History of Mining	11
	Methods of Study	12
	Field Work	12
	Lab Work	15
II.	STRUCTURAL GEOLOGY	20
	Breccia Body	20
	Knox Unconformity	24
	Other Structural Features	26
III.	STRATIGRAPHY, ENVIRONMENTS OF DEPOSITION, AND DIAGENESIS	30
	Introduction	30
	Stratigraphy	32
	Knox Group - Mascot Dolomite	32
	Chickamauga Group - Dot Formation	33
	Lost Creek Section and Lithologies	35
	Environments of Deposition of Dot Formation	37
	Peloid-Intraclast Grainstone/Packstone Lithology	37
	Lime Mudstone Lithology	44
	Skeletal Wackestone/Packstone Lithology	48
	Summary of Depositional Environments	50

CHAPTER PAGE

Diagenesis 50

Introduction 50

Formation of Framboidal Pyrite 51

Cementation 54

Neomorphism 63

Dolomitization 65

Type I dolomite 67

Type II dolomite 80

Dedolomitization 90

Silicification 91

Calcite Veining 93

Stylolitization 95

Occurrence of Non-Framboidal Pyrite 95

Summary of Diagenesis 96

IV. MINERALIZATION 98

Introduction 98

Barite Mineralization 98

Veins 98

Replacement Barite - Dolomitization Halo 101

Open-Space Filling Barite 111

Shell molds 111

Associated with the breccia body 111

Barite coatings 113

Barite cement 114

Syngenetic Barite 122

Barite Color Banding 127

CHAPTER PAGE

Sulfide Mineralization 129

Paragenesis 133

Origin and Timing of Brecciation 135

Chemistry of the Ore Fluid 140

Precipitation of Ore Minerals 140

Summary and Discussion 143

V. SUMMARY AND CONCLUSIONS 145

Recommendation for Further Work 146

REFERENCES 147

APPENDIX 159

VITA 165

LIST OF FIGURES

FIGURE		PAGE
1.	Index Map of Study Area from Maynardville (145-SE) T.V.A. - U.S.G.S. Quadrangle Map	2
2.	Map of East Tennessee Showing the Location of the Lost Creek Barite Mine, Union County, in Relation to Mining Districts of Mississippi Valley-Type	3
3.	Generalized Stratigraphic Column for the Lost Creek Area	6
4.	Location of the Lost Creek Barite Mine, Union County, Tennessee, in Relation to the Powell River District, an Unnamed Barite Prospect in Knox County, and the Oak Ridge Barite Occurrence in Anderson County	7
5.	View of the Lost Creek Barite Mine, Looking Northwest, Showing Pits and Small Mine Dumps Developed in the Dot Formation	9
6.	Northeast Corner of the Lost Creek Breccia Body, Showing Barite as Fragments and Coatings Around Fragments	9
7.	Geologic Map of the Lost Creek Barite Mine, Union County, Tennessee	13
8.	Map of Lost Creek Showing Location of Samples	16
9.	Portion of the Geologic Map of the Lost Creek Barite Mine Showing Sample Locations of All Breccia Samples	17
10.	Idealized Cross Section of the Lost Creek Barite Mine, Modified from Fagan (1969) and Carpenter et al. (1971)	22
11.	Idealized Cross Section of the Lost Creek Barite Mine Based on Drill Hole Data	25
12.	Base Map of the Lost Creek Barite Mine Showing Bedding Attitudes After Rotation to Remove Present Day Regional Dip	28
13.	Warped Block of Dolomitized Dot Formation Limestone from the Lost Creek Breccia	31
14.	Distribution of Lithologies with the Dot Formation Portion of the Lost Creek Section	36
15.	Peloid-Intraclast Grainstone	39

FIGURE		PAGE
16.	Laminoid Fenestrae Developed in the Basal Dot Sediments . . .	39
17.	Probable Mudcrack, Inferred to have Formed on a Channel Levee Backslope (Supratidal)	43
18.	Fossilferous Lime Mudstone, Containing Ostracod Valves and Trilobite Fragments	45
19.	Irregular Fenestrae Developed in Sediments of the Lime Mudstone Lithology	47
20.	Typical Biota of the Skeletal Wackestone/Packstone Lithology	49
21.	Relict Patches of Lime Sediment Within a Largely Dolomitized Peloid-Intraclastic Sediment	53
22.	Fresh Water Phreatic Calcite Cement as Void-Filling Spar . .	56
23.	Ferroan Calcite (C) and Ferroan Dolomite (D) Cements Occupying the Central Portions of a Void Initially Lined with Non-Ferroan Calcite Cement	59
24.	Molluscan Shell Mold Filled with Ferroan Dolomite Cement . .	61
25.	Interstitial, Relict Calcite in an Essentially Dolomitized Rock	68
26.	Relict Intraclasts and Sparry Cement in the Same Dolomitized Rock Depicted in Figure 25	70
27.	Skeletal Wackestone/Packstone, Representing Shallow Subtidal Deposition, that was Partially Dolomitized During Type I Dolomitization	75
28.	Schematic Representation of a Typical Mixing Zone in a Coastal Setting Where Meteoric Water Mixes with Marine Water	79
29.	Type II Dolomite (D) Associated with and Surrounded by Neomorphic Microspar that Developed Within an Ostracod Shell	81
30.	Ostracod Shell from the Dot Formation	83
31.	Irregular Fenestrae Cemented by Both Sparry Calcite and Type II Dolomite	85
32.	Colonial Coral Fragment Showing Two Stages of Cementation of Coralite Openings	85

FIGURE PAGE

33. Partially Silicified Coral Fragment 92

34. Paragenetic Sequence of Diagenetic Events Affecting Lost Creek Sediments (Dot Formation Only) 97

35. Hand Sample of Barite Vein Showing Distinct Dark Coloration of Associated Late Calcite (C) 100

36. Dolostone from the Dolomitization Halo 102

37. Dolostone from the Dolomitization Halo (Identical to Figure 36) with Crossed Nicols 104

38. Appearance of Typical Type I Dolostone with Cathodoluminescence 104

39. Appearance of Typical Type II Dolostone, Formed by Recrystallization of Type I Dolostone, with Cathodoluminescence 106

40. Typical Type II Vein-Filling Dolomite as it Appears When Using Cathodoluminescence 106

41. Replacement Barite Associated with the Dolomitization Halo 109

42. Barite Found Within the Living Chamber of an Ostracod 112

43. Sphalerite (SP) Precipitated as a Coating on a Barite Fragment (B) 115

44. Feathery Barite Which Occurs with Pink, Coarse-Grained Dolomite as Late Cement Between Breccia Fragments 117

45. Sphalerite Color Banding Found at Lost Creek 120

46. Colloform Sphalerite Which Precipitated Prior to (and Probably Partly Simultaneous with) Feathery Barite (Visible as White Mineral in the Interstices) 120

47. Possible Syngenetic Barite 123

48. Barite Occurrence Suggestive of Syngenetic Precipitation . . 125

49. Twinned Marcasite that Precipitated Subsequent to Formation of Pyrite (Euhedral Grain in Center) 131

50. Typical Sulfide Botryoid Showing Concentric Layers of Different Mineralogy 131

FIGURE PAGE

51. Replacement of Large Dolomite Grains (D) by Sphalerite (SP) and Marcasite (MC) 134

52. Paragenetic Sequence for Late Diagenetic Mineralization at the Lost Creek Barite Mine, Expanded from Figure 34 . . . 136

A-1 Control Points Used in Construction of Stratigraphic Framework 161

A-2 Example of Graphical Determination of Stratigraphic Position 163

CHAPTER I

INTRODUCTION

Purpose and Scope of Investigation

The Lost Creek barite mine is located in north-central Union County, Tennessee, on the Lost Creek embayment of Norris Reservoir (Tennessee Coordinates 712,400 N; 2,630,300 E) (Figure 1). The geologic setting is comparable to that of the large Mississippi Valley-type ore deposits, both barite and sphalerite, which are hosted by brecciated Lower Ordovician carbonate strata in east Tennessee (Figure 2). However, brecciation and mineralization at Lost Creek are not confined to Lower Ordovician rocks but extend into basal Middle Ordovician beds. This anomalous feature has prompted widespread speculation among area geologists for the past fifteen years (Wedow, personal communication, 1977). Even so, only two investigations of the deposit were undertaken prior to the present research (Fagan, 1969; Carpenter et al., 1971), and these were primarily descriptive.

This investigation considers the structure, stratigraphy, depositional and diagenetic environments, and ore mineralogy and textural relationships of the Lost Creek deposit. It is hoped that an evaluation of these parameters will lead to a better understanding of the genesis of the Lost Creek ore and ultimately of its relationship, if any, to other east Tennessee mineral deposits.

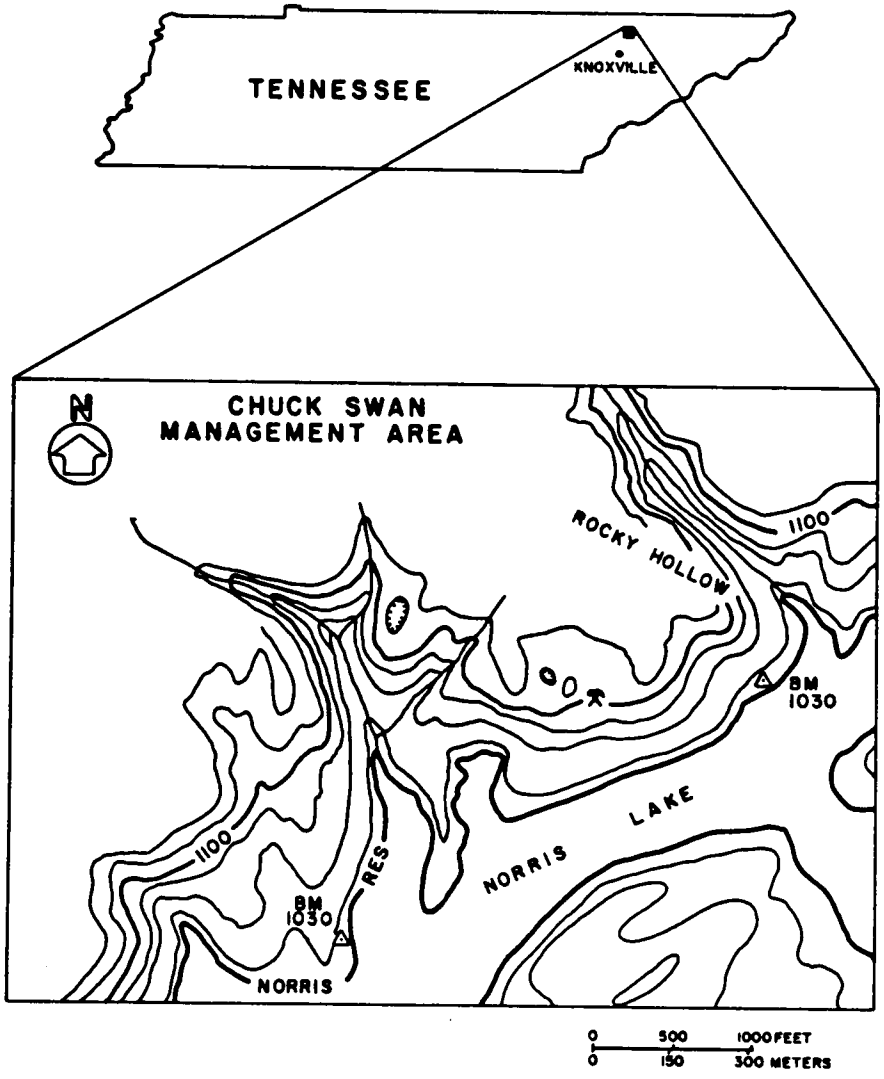


Figure 1. Index map of study area from Maynardville (145-SE) T.V.A.-U.S.G.S. quadrangle map. Crossed picks symbol in right-center marks mine location.

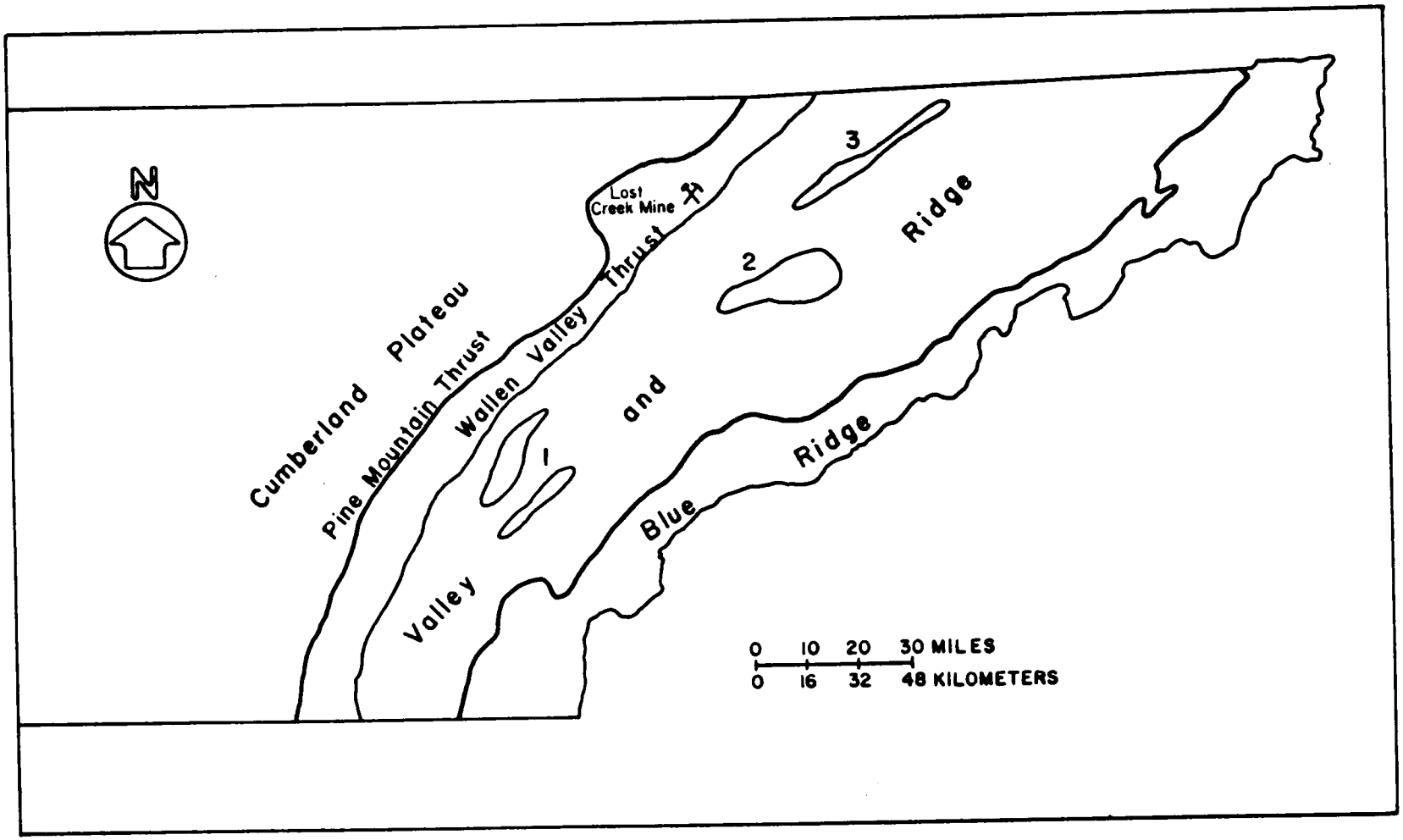


Figure 2. Map of East Tennessee showing the location of the Lost Creek barite mine, Union County, in relation to mining districts of Mississippi Valley-type. 1, Sweetwater barite district; 2, Mascot-Jefferson City zinc district; 3, Copper Ridge zinc district.

Geologic Setting

The Lost Creek barite mine lies on the southeasteast flank of the Powell Valley anticline within the northwesternmost fault block of the Valley and Ridge physiographic province of Tennessee. This fault block, much broader and less deformed than those farther southeast (Brokaw et al., 1966), is bounded by the Pine Mountain thrust fault to the northwest and by the Wallen Valley thrust on the southeast (see Figure 2).

Because of its characteristics, the Lost Creek mine can be classified loosely as a Mississippi Valley-type ore deposit. In east Tennessee the general characteristics of other Mississippi Valley-type deposits are as follows (Ohle, 1959; Maher, 1970; Hoagland, 1971):

1. A Lower Ordovician carbonate host.
2. Simple mineralogy (primarily sphalerite, barite, galena, fluorite, and pyrite in varying amounts, although usually not all together).
3. Simple wall rock mineralogy characterized by pervasive dolomitization.
4. Ore deposition at shallow depth occurring after lithification of the host rocks.
5. Ore deposition primarily as open-space fillings.
6. A fairly narrow stratigraphic range of mineralization.
7. Evidence of solution activity (primarily brecciation) predating and/or associated with mineralization.

With reference to the above features, and despite its Mississippi Valley-type label, the Lost Creek deposit appears strikingly

anomalous, primarily as a result of the age of the host rocks. Known mineralization at Lost Creek extends from the uppermost Lower Ordovician formation of the Knox Group (Mascot Dolomite) across the post-Knox unconformity (hereafter referred to simply as the Knox unconformity) into the basal strata of the Middle Ordovician Chickamauga Group (Dot Formation) (Figure 3). According to Maher (1970), Lost Creek is the only known occurrence of mineralization in Middle Ordovician rocks that has been mined in East Tennessee. Furthermore, as will be discussed later, the mineralization appears to have occurred prior to complete lithification of the Middle Ordovician portion of the host sediments.

The Lost Creek mine is anomalous not only for the age of the host rocks but also because of its apparent isolation with respect to other barite occurrences. Bordering the mine on the northeast is the Powell River district, a northeast-trending belt of small zinc and lead mines, prospects, and occurrences. These are hosted in Upper Cambrian and Lower Ordovician strata and are generally dissimilar to Mississippi Valley-type deposits of east Tennessee (Brokaw et al., 1966). Traces of barite have been found in only a few of the occurrences in the Powell River district (Maher, 1970) even though the region is one of the most extensively mineralized areas in eastern Tennessee (Brokaw et al. 1966). Other than these (in addition to the Lost Creek mine), barite has been reported (Maher, 1970) from only one small prospect and one occurrence, both in Knox residuum, from the six-county area centered in Union County (Figure 4).

As a result of its relative isolation, the Lost Creek deposit could be an excellent subject for a variety of geochemical studies. It might be particularly well suited for geochemical halo studies, unlike

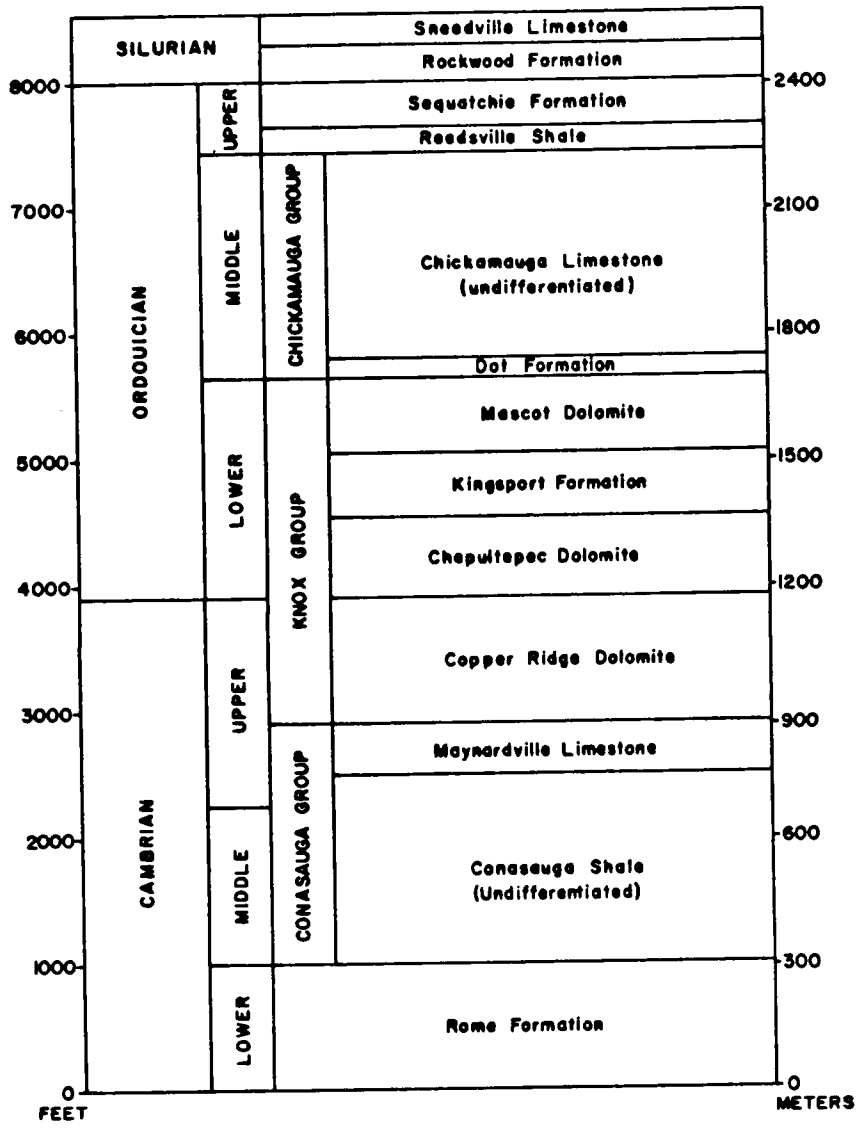


Figure 3. Generalized stratigraphic column for the Lost Creek area (from Rodgers, 1953; Finlayson, 1964; Blythe, 1967; and Harris, 1969).

Figure 3. Generalized stratigraphic column for the Lost Creek area (from Rodgers, 1953; Finlayson, 1964; Blythe, 1967; and Harris, (1969).

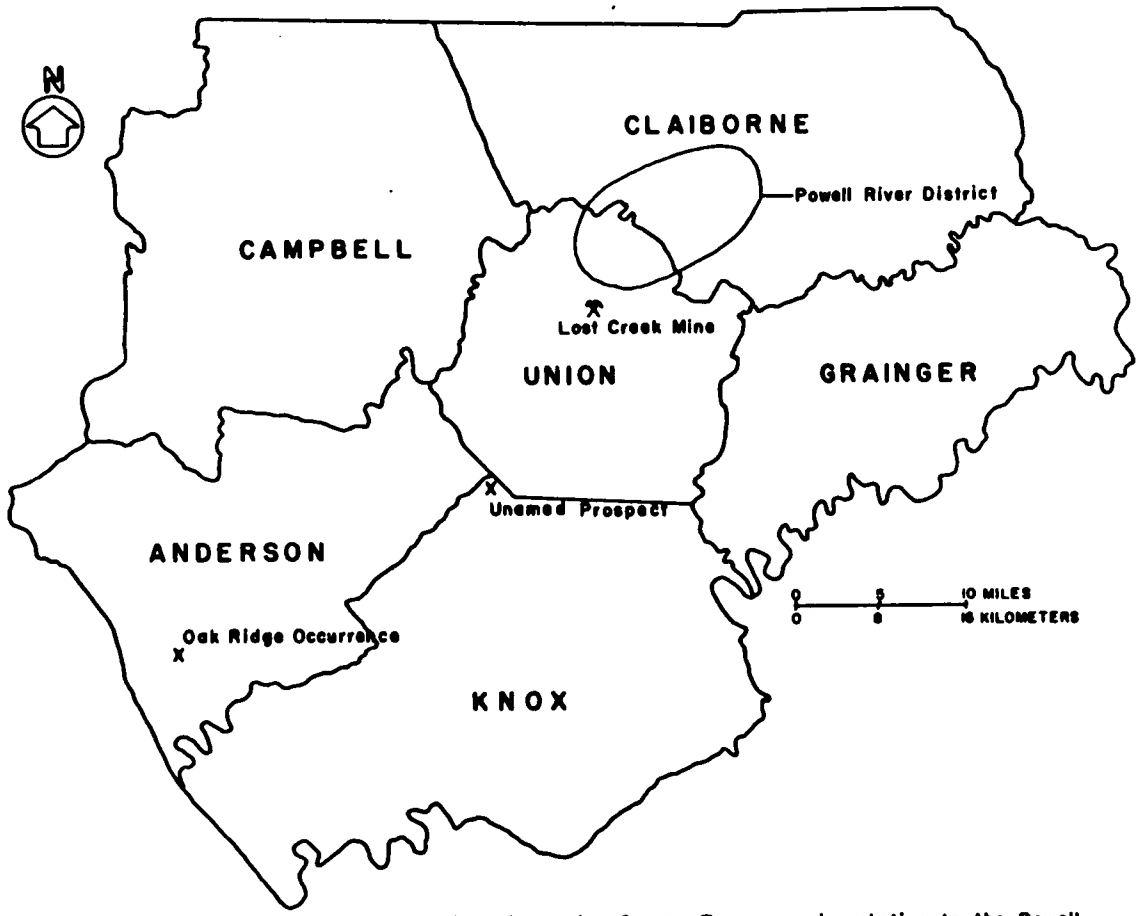


Figure 4. Location of the Lost Creek barite mine, Union County, Tennessee in relation to the Powell River District, an unnamed barite prospect in Knox County, and the Oak Ridge barite occurrence in Anderson County.

deposits which are part of a larger district and for which background values of trace and miner elements might be difficult to determine (Maher, personal communication, 1977).

General Description of the Deposit

The Lost Creek barite mine occupies a shallow depression, about 150 meters (500 feet) in diameter, which is developed on the dip slopes of the uppermost Mascot Dolomite and lowermost Dot Formation (Figure 5).

The Mascot is a fine-grained, tan to light gray dolostone. It is capped by white to light gray, massive procellaneous chert in the northeastern portion of the mine. The top of the Mascot, visible in several exposures, is marked by an unconformity. A pre-Middle Ordovician unconformity (Knox unconformity), such as found at Lost Creek, is a widespread feature of the regional stratigraphic section (Rodgers, 1953). Basal beds of the Dot Formation reflect the irregularities of this erosion surface and consist of a mixture of dolomitic chert conglomerates, and argillaceous and dolomitic limestones. Higher in the section the Dot Formation comprises massively bedded, bluish-gray aphanitic limestone.

Within the area of the mine are numerous small pits from which residual accumulations of barite were removed during past mining operations. Large boulders of country rock which presumably were also removed from these pits form scattered mine dumps (see Figure 5).

In bedrock, barite occurs as fracture-fillings associated with a small dolomitized breccia body. Within the breccia body itself barite is found primarily as discrete fragments and coatings developed on or almost completely surrounding other (lithic) fragments (Figure 6),

Figure 5. View of the Lost Creek barite mine, looking northwest, showing pits and small mine dumps developed in the Dot Formation. The topographic high in the center of the picture is a mineralized breccia body. Field of view is approximately 45 meters (150 feet).

Figure 6. Northeast corner of the Lost Creek breccia body, showing barite as fragments and coatings around fragments. Note hammer for scale.



Figure 5



Figure 6

clearly indicating that the processes of brecciation and mineralization were, at least in part, contemporaneous.

The breccia body stands in conspicuous topographic relief in the center of the mine (see Figure 5). In plan, it is nearly circular, approximately 45 meters (150 feet) in diameter, and lies entirely within the stratigraphic interval of the Dot Formation. Drill core recovered in 1979 by Imco Services, a division of Halliburton Company, has shown that at depth brecciation also involved the underlying Mascot Dolomite. An irregular dolomitization halo extends into the country rock around the breccia body.

Abundant intergrown pyrite and marcasite accompany the barite mineralization at Lost Creek. At the surface, most of the marcasite and pyrite have been oxidized to limonitic material. Minor amounts of sphalerite, galena, gangue calcite, and pink and white gangue dolomite as well as traces of chalcopyrite are also associated with the barite mineralization. Smithsonite occurs in surface exposures as an alteration product of sphalerite. Fluorite has not been found.

History of Mining

The first description of the barite mineralization at Lost Creek was given by Cullison and Scott (1935). They recognized the anomalous nature of the deposit, noting the occurrence of mineralization both above and below the Knox unconformity.

Actual mining of barite, which was originally found in residual accumulations that in places were more than 25 feet thick (Penhallegon, 1938), began at Lost Creek early in 1938. Gildersleeve (1946) noted

that the mine was still active in the summer of 1940. Although there are no records, Maher and Finlayson (1965) reported that total production was slight.

In 1965 W. L. Ball of Meigs County, Tennessee, reopened the deposit, installed a washer and jigs, and produced an estimated 2,500 tons of concentrates (Maher, 1970).

Imco Services leased the mineral rights in 1978. During August 1979, they initiated a drilling program, the first ever at Lost Creek, designed to evaluate the subsurface extent of brecciation and mineralization. Three vertical holes were drilled which brought up a combined total of 570 feet of core. No new reserves of barite were found.

Methods of Study

Field Work

The initial stages of this investigation consisted of several months of field work devoted to careful mapping, section measuring, sample collection, and detailed observation.

Although a generalized geologic map of the Lost Creek mine has been published (Fagan, 1969; Carpenter et al., 1971), the need for precise control of sample locations required greater accuracy. This was deemed particularly vital to possible later geochemical studies. Therefore, a new base map, drawn with the aid of a square grid on 15.24-meter (50-foot) centers, was prepared (Figure 7).

The grid itself was constructed using a 15.24-meter (50-foot) rope and a Brunton compass. Grid points were marked in the field with wooden stakes. Additional mapping control was provided by a network of approximately 25 plane-table points shot with a Gurley alidade. Several

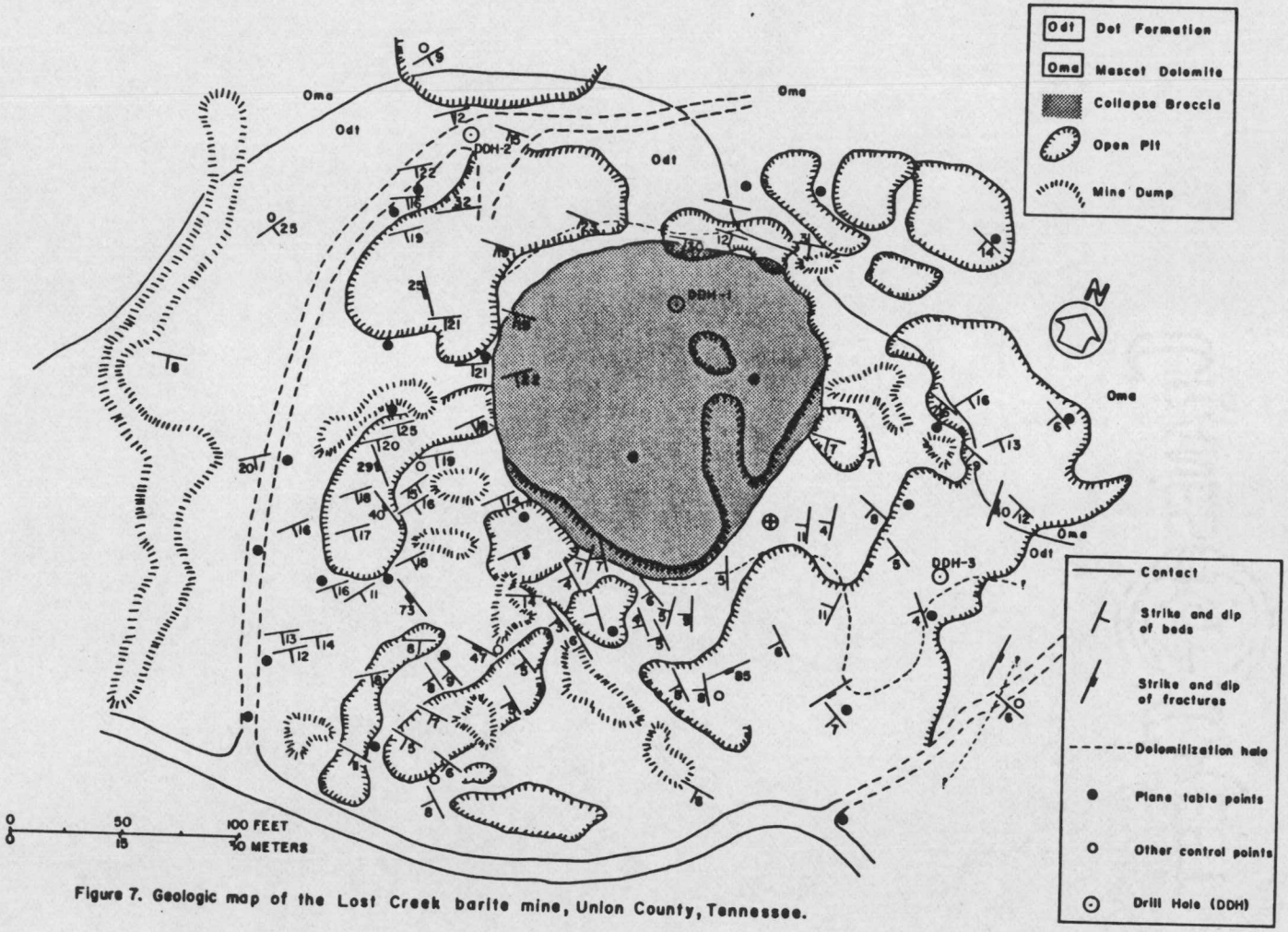


Figure 7. Geologic map of the Lost Creek barite mine, Union County, Tennessee.

other control points were located from these with the aid of a steel tape and Brunton compass (see Figure 7). As a result of this degree of control the base map is considered to be accurate to within ±5 feet.

The plane-table survey also proved instrumental in determining the extent of the stratigraphic section exposed at the mine. Within the area of the mine bedrock is primarily observed in numerous, largely discontinuous pits (see Figure 5). Even where the pits are continuous, bedding is generally massive and cannot be traced. Stratigraphic relationships of the bedrock exposures are further obscured by the slope of the land surface, which is in the same direction and at an angle approximating the dip of the strata.

Relative stratigraphic positions of the mapping control points of Figure 7 were calculated by projection. These projections were based on elevations, determined by plane tabling and hand leveling, and strikes and dips measured at or near those points. The mapping control points therefore also served as stratigraphic control points. (See the Appendix for a discussion of the probable accuracy of the resulting stratigraphic network.)

Sampling of rocks for both petrographic and possible geochemical studies progressed using this stratigraphic framework. Several factors were considered in selecting samples: (1) mesoscopic changes in lithology, (2) position within the stratigraphic framework, (3) interesting textures, and (4) goals of possible later geochemical analyses. The sample number and stratigraphic "up" direction were recorded on each sample at the time of collection.

A total of 231 rock and mineral samples were collected during this investigation. Of this total, 195 were collected for mesoscopic

and thin section study, while the rest were sampled for possible geochemical analysis. The locations for all samples except one geochemical control sample are given in Figure 8 and Figure 9 [control sample C-8 was collected along strike approximately 5.6 kilometers (3.5 miles) northeast of the mine location]. Relative stratigraphic positions of most of these samples were measured directly from the mapping control points using standard tape and compass procedures. The precise stratigraphic position could not be determined for any of the breccia samples.

Lab Work

Table 1 lists all samples from Figures 8 and 9, plus drill core samples, that were thin-sectioned. One hundred and nine standard 75 x 50 mm thin sections and 4 standard 50 x 25 mm polished thin sections were made initially. An additional 16 thin sections and 9 polished thin sections were made from selected drill core samples. (See Figure 7 for locations of drill holes.)

A portion of each thin section was stained with alizarin red S to distinguish between calcite and dolomite. A separate portion was stained with potassium ferricyanide to detect the presence of ferrous iron. These staining techniques are described in detail by Evamy (1963). Part of each thin section was left unstained.

In addition to transmitted-light microscopy of stained thin sections and reflected-light microscopy of polished thin sections, laboratory study also included examination of approximately 60 selected sections with cathodoluminescence. A Nuclide Corporation LUMINOSCOPE, Model ELM-2A, was used. This was mounted on a Bausch and Lomb microscope equipped with a 3.5x objective and a 10x hyperplane ocular.

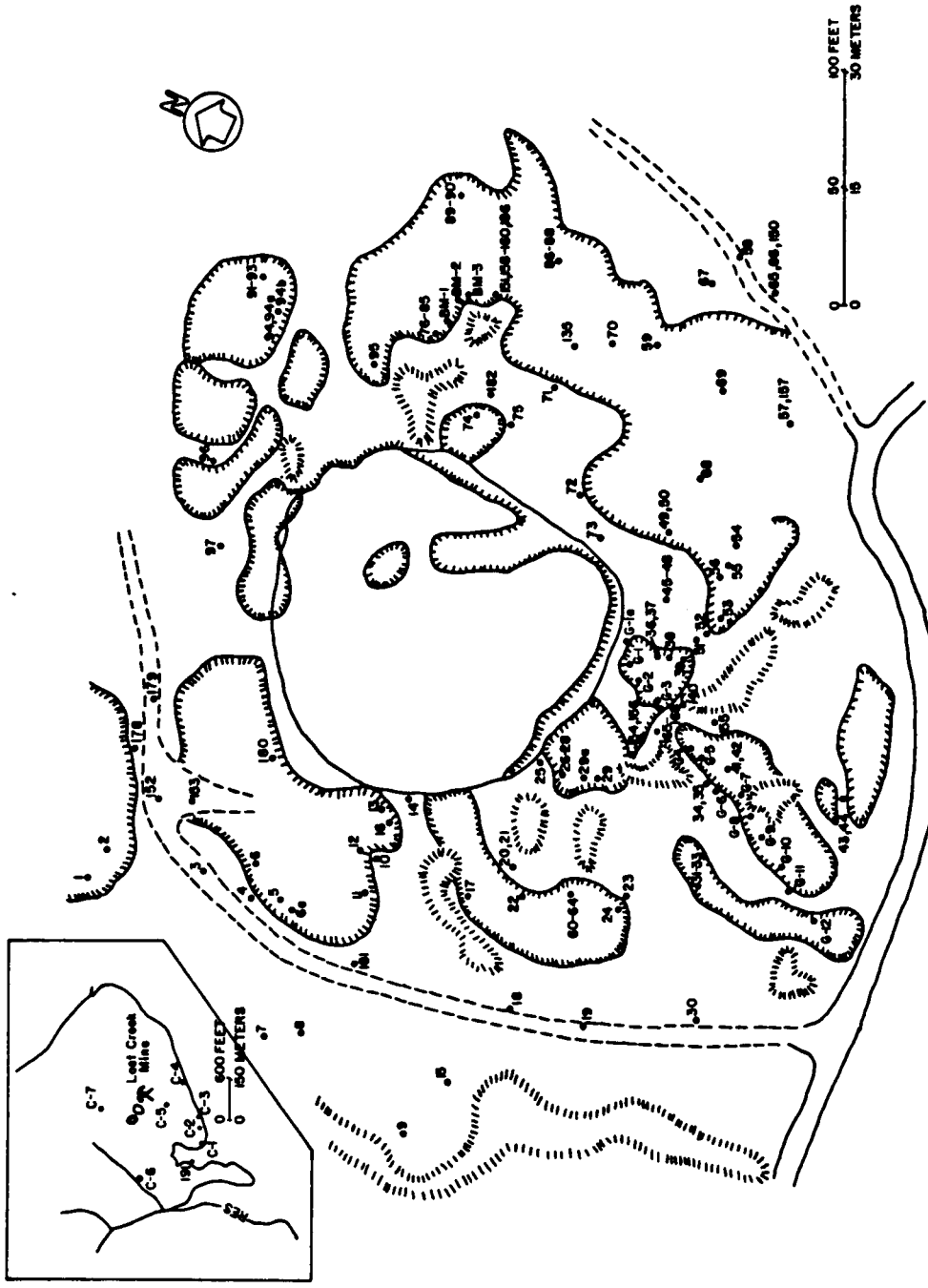


Figure 8. Map of Lost Creek showing location of samples. Inset shows location of control samples. Breccia sample locations are given in Figure 9.

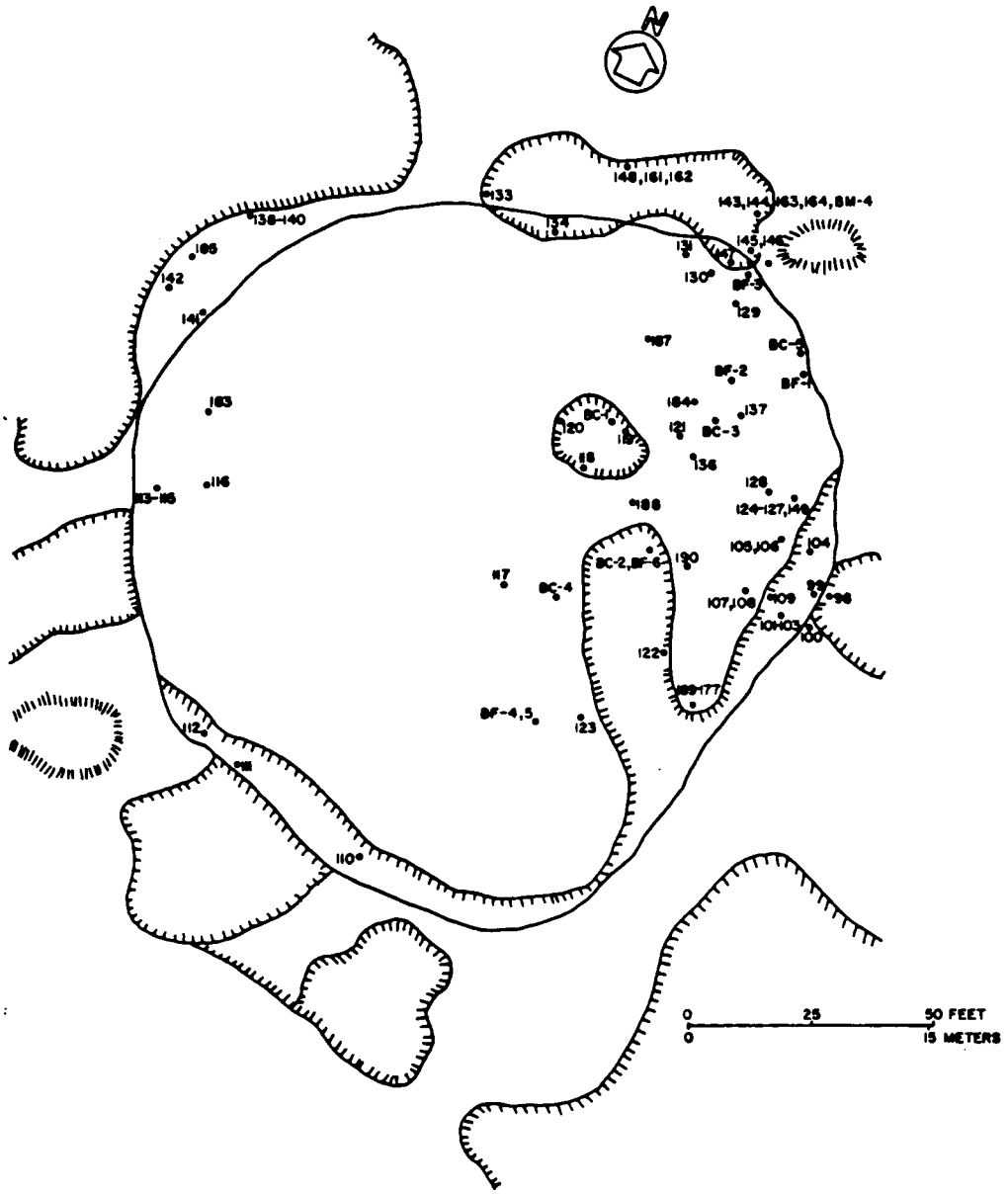


Figure 9. Portion of the geologic map of the Lost Creek barite mine showing sample locations of all breccia samples.

TABLE 1

LIST OF ALL SAMPLES, INCLUDING DRILL CORE SAMPLES, THAT WERE THIN-SECTIONED

Sample Number						
1	20	47	92	172	G-5	1-19*
2	21	55	94a	173*	G-6	1-20
3	22	60	94b	174*	G-7	1-27
4	23	61	115	175*	G-8	1-47
5	24	62	124	176*	G-9	1-51
6	25	63	136	178	G-10	1-58*
6a	26	64	137	179	G-11	1-91
7	27	65	138	180	G-12	1-123(2)*
8	28	66	152	181	C-3	1-125*
9	29	76	153	182	C-4	1-154*
10	29a	77	157	183	C-5	1-155
11	34	78	158	184	C-8	1-200
12	35	79	159	186	2-4	3-19*
13	36	80	165	190	2-7	3-56
14	37	81	166	191	2-11	3-180*
15	38	83	167	G-1a	2-13	3-191*
16	39	85	168	G-1	2-15	
17	40	89	169	G-2	2-19	
18	41	90	170	G-3(2)	1-8	
19	42	91	171	G-4	1-13	

*Indicates that a polished thin section was made.

Constant operating conditions were followed since the intensity of the luminescent colors is a function of these conditons (Ebers, 1976; Ebers and Kopp, 1979) as well as a function of certain intrinsic characteristics of the mineral (Nickel, 1978). Operating conditions were as follows: a current of 0.6 mA; a voltage of 10-12 kV; and a beam diameter of approximately 2 cm. Photographs were taken with Kodak Ektachrome Daylight film (ASA 400) exposed for 2 to 4 minutes.

Thin sections were described using the basic textural terminology of Friedman (1965) and carbonate rock classification of Dunham (1962).

CHAPTER II

STRUCTURAL GEOLOGY

Breccia Body

The most conspicuous structural feature at Lost Creek is the breccia body that forms an obvious topographic high in the central portion of the mine (see Figure 5, page 9). Parallel to and dipping away from the outer edge of this breccia body are numerous mineral-filled fractures averaging several centimeters in thickness (see Figure 7, page 13, for locations and attitudes measured on some of these fractures). The fractures arrayed in relatively concentric rings around the breccia occur in unbrecciated country rock. They are quite close together near the breccia body; however, the spacing between fractures increases and the fractures themselves dip more steeply with increasing distance from the periphery of the central core. The fractures essentially disappear within less than 30 meters (100 feet) from the breccia body. Fagan (1969) inferred a collapse origin for the Lost Creek breccia on the basis of similarities of this fracture pattern to that developed during massive cavern breakdown as described by Davies (1951). This interpretation is reinforced by the occurrence of nearly identical fracture patterns associated with mineralized breccia structures which have been proven to have formed by collapse (by the vertical displacement of marker beds) in the Mascot-Jefferson City zinc district (Crawford et al., 1971; McCormick et al., 1971).

Although common within the stratigraphic interval of the Dot Formation, fractures of this type are almost absent from Mascot

exposures. This may partially reflect the general scarcity of Mascot exposures, but is probably also indicative of a difference in response to stress. This latter interpretation is reinforced by the occurrence of other, smaller fractures associated with outcrops that expose the Knox unconformity. Near the unconformity the Mascot exhibits myriad, thin (1 mm or less) barite-filled fractures roughly parallel to bedding. The Dot, however, is relatively unaffected on this scale, even adjacent to the highly fractured Mascot Dolomite. These hairline fractures may not be related to brecciation but may represent stresses induced prior to brecciation or perhaps prior even to deposition of the Dot Formation. Considering the early onset of mineralization after transgression of the Middle Ordovician sea (see later, page 122) it is possible that such fractures could have remained open until filled with barite at that time.

Although barite is by far the most abundant mineral in the fracture-fillings at Lost Creek, dolomite, calcite, and pyrite are also found. Calcite is especially common farther from the brecciated central core and may be almost the sole constituent of the vein-fillings. Cross-cutting relationships between calcite veins and barite veins indicate multiple episodes of fracturing.

Drilling by Imco Services Company in August 1979 provided the first direct data concerning the subsurface configuration of the breccia body. Fagan (1969) and Carpenter et al. (1971) suggested that the surface exposures were but the tip of an iceberg that spread out laterally in the subsurface (Figure 10). Imco Services based their drill hole pattern on similar inferences derived from resistivity data. A

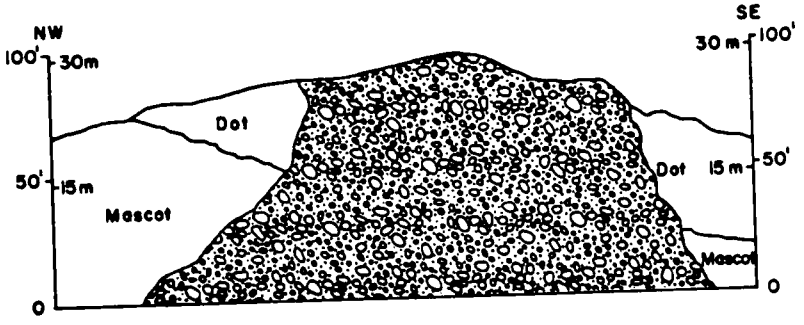


Figure 10. Idealized cross-section of the Lost Creek barite mine, modified from Fagan (1969) and Carpenter et al. (1971). Line of section is approximately NW-SE through the center of the breccia body.

Figure 10. Idealized cross section of the Lost Creek barite mine, modified from Fagan (1969) and Carpenter et al. (1971). Line of section is approximately NW-SE through the center of the breccia body.

resistivity survey had revealed a low resistance trend, believed to delineate subsurface brecciation, striking NW-SE across the breccia body (William Listerud, personal communication, 1979).

Of three holes drilled by Imco Services (see Figure 7, page 13, for locations), only DDH-1, located directly on top of the breccia body, penetrated significant additional brecciation. Mineralized crackle and rubble breccia was encountered along the entire 62-meter (204.5-foot) length of the hole. [In East Tennessee zinc company usage "rubble breccia" refers to breccias in which fragments have been rotated and displaced downwards. If separation and rotation of fragments is relatively minor, the term "crackle breccia" is used (Crawford et al., 1971).]

The uppermost breccia fragments of Mascot in DDH-1 appeared at a depth of 15 meters (50 feet) below collar elevation. This is 3 to 4 meters (10 to 15 feet) deeper than expected based on a projection of the unconformity from where it is exposed just north of the breccia, and may be additional evidence of a collapse origin for the Lost Creek breccia structure. An alternative explanation is that all or some of the difference is the result of irregularities developed on the unconformity.

DDH-2, northwest of the breccia body, brought up 49 meters (160 feet) of generally unfractured and unmineralized rock. The sparse fractures encountered were predominantly filled with pyrite and some barite and pink dolomite.

DDH-3, southeast of the breccia body, is more extensively fractured than DDH-2. Thin zones of rubble and crackle breccia occur throughout the 62 meter (205-foot) length of the drill hole. Pyrite was

again found to be the main fracture-filling mineral, with associated dolomite and traces of barite and sphalerite.

Figure 11 is an idealized cross-section of the Lost Creek mine based on drill hole information (compare to Figure 10). Drilling to date indicates that the Lost Creek breccia body is a relatively narrow, pipe-like structure. Perhaps that explains why the fracture pattern associated with the breccia body is relatively "tight" [i.e., why it doesn't extend very far into unbrecciated rock (see page 20)]. A broader breccia structure would likely have an associated broader fracture pattern. It might be possible that the breccia body is elongated in a NE-SW direction. Although drill hole data permit this interpretation, the concentric fracture pattern renders it unlikely. The fact that the rock penetrated by DDH-3 is more fractured than DDH-2 may indicate that the main breccia body (pipe structure or otherwise) extends further to the SE than it does to the NW.

Knox Unconformity

The Knox unconformity, which is a major regional disconformity (Rodgers, 1953), strongly influences the structural geology of the Lost Creek area. The relief developed on this paleo-erosional surface was considerable across the Valley and Ridge province of Tennessee (Harris, 1971). In the northwestern strike belts relief ranged up to 50 or 60 meters (approximately 200 feet).

At the mine itself, stratigraphic measurements document that at least 10.5 meters (35 feet) and perhaps as much as 13.5 meters (45 feet) or more of relief developed over a ground distance of less than

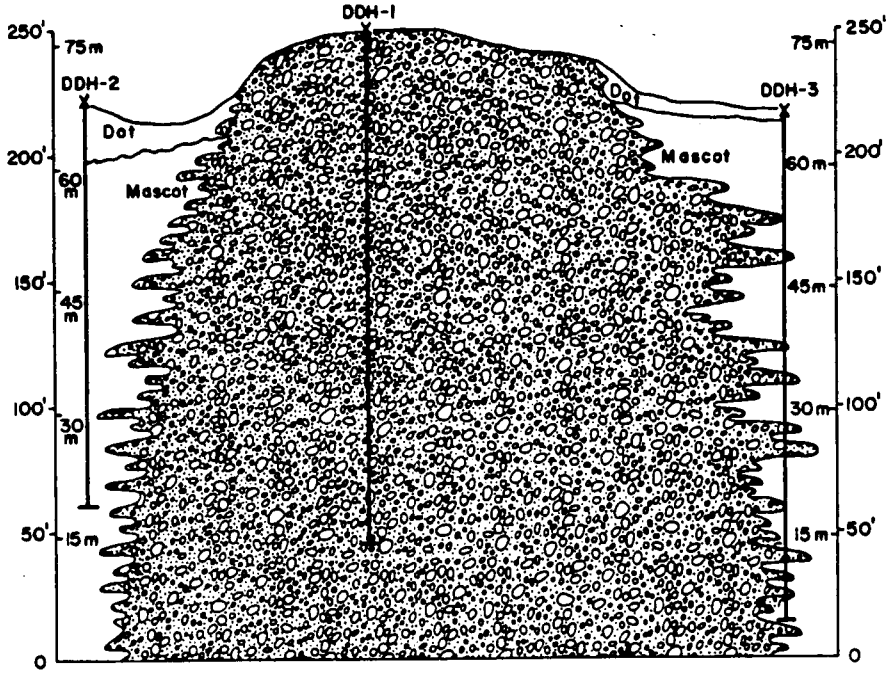


Figure 11. Idealized cross-section of the Lost Creek barite mine based on drill hole data. Line of section passes through DDH-2 and DDH-3 (see Figure 7, page 13).

76 meters (250 feet) (see the Appendix). The low point on this surface corresponds to the reentrant observed in the trace of the unconformity northwest of the breccia body (see Figure 7, page 13). This paleo-depression may have restricted the circulation of the intial Middle Ordovician transgressive sea, possibly resulting in an absence of fauna and therefore fossils in basal Dot sediments deposited within it (see later discussion, page 42).

The highest point on the surface of the unconformity is exposed immediately north of the breccia body. In general, the unconformity is relatively higher north, northeast, and east of the breccia body. Some of the relatively higher portions of the unconformity are capped by massive chert. This chert is residual Mascot chert, and was probably responsible for protecting those portions of the unconformable surface during the post-Knox erosional interval.

Other Structural Features

The average attitude of the beds west and northwest of the breccia body is N47^{o}E, 17^{o}SE (see Figure 7, page 13), which compares with the general regional orientation of bedding and major structural features. Beds adjacent to the breccia on the north strike more nearly east-west and dip more steeply toward the breccia, probably as a result of collapse associated with brecciation. The steeper dips may also reflect depositional dip on the uneven erosional surface of the Knox unconformity.

The other outcrops at the mine exhibit a NW-SE strike with a corresponding dip (quite shallow, 5 to 6^{o}) to the southwest. Because of the scarcity of exposures, except at the mine itself, the full extent

of beds with these anomalous attitudes is unknown, but they appear to be confined to the vicinity of the mine.

The contact between beds with a SE dip and those with a SW dip is not exposed; however, it is seemingly abrupt. Rocks dipping southwest are exposed adjacent to those dipping to the southeast. Although the origin of this contact (flexure) which strikes NE-SW is uncertain, it is reasonable to conclude that it may be related to the breccia body; i.e., the brecciation may have produced the structure, or the structure may have localized the brecciation. It is not likely that the structure post-dates brecciation since the breccia body was unaffected.

In either case, the structure would have formed prior to the late Paleozoic orogeny which tilted all beds into their present orientation. In order to remove the influence of this deformational event all measured bedding attitudes (see Figure 7, page 13) were rotated using a Schmidt Net so that the average "local" regional attitude of $N57^{\circ}E \pm 10^{\circ}$, $15^{\circ}SE \pm 3^{\circ}$ would be restored to horizontal (Figure 12). (This attitude is the average of 23 attitudes measured from Kingsport, Mascot and Dot outcrops peripheral to the mine, but at a distance far enough as to be unaffected by structures localized at the mine.)

The results, although quite interesting, are inconclusive. The NE-SW striking structural trend remains, although the shallow SW dips for rocks which strike NW-SE are all steeper and dip to the NW (approximately 14°). Beds that dipped to the SE prior to rotation exhibit a wide array of orientations. Resultant dips less than 4 or 5° can be considered to have been more or less restored to horizontal and are not shown in Figure 12. In general, the remaining beds dip toward the breccia body.

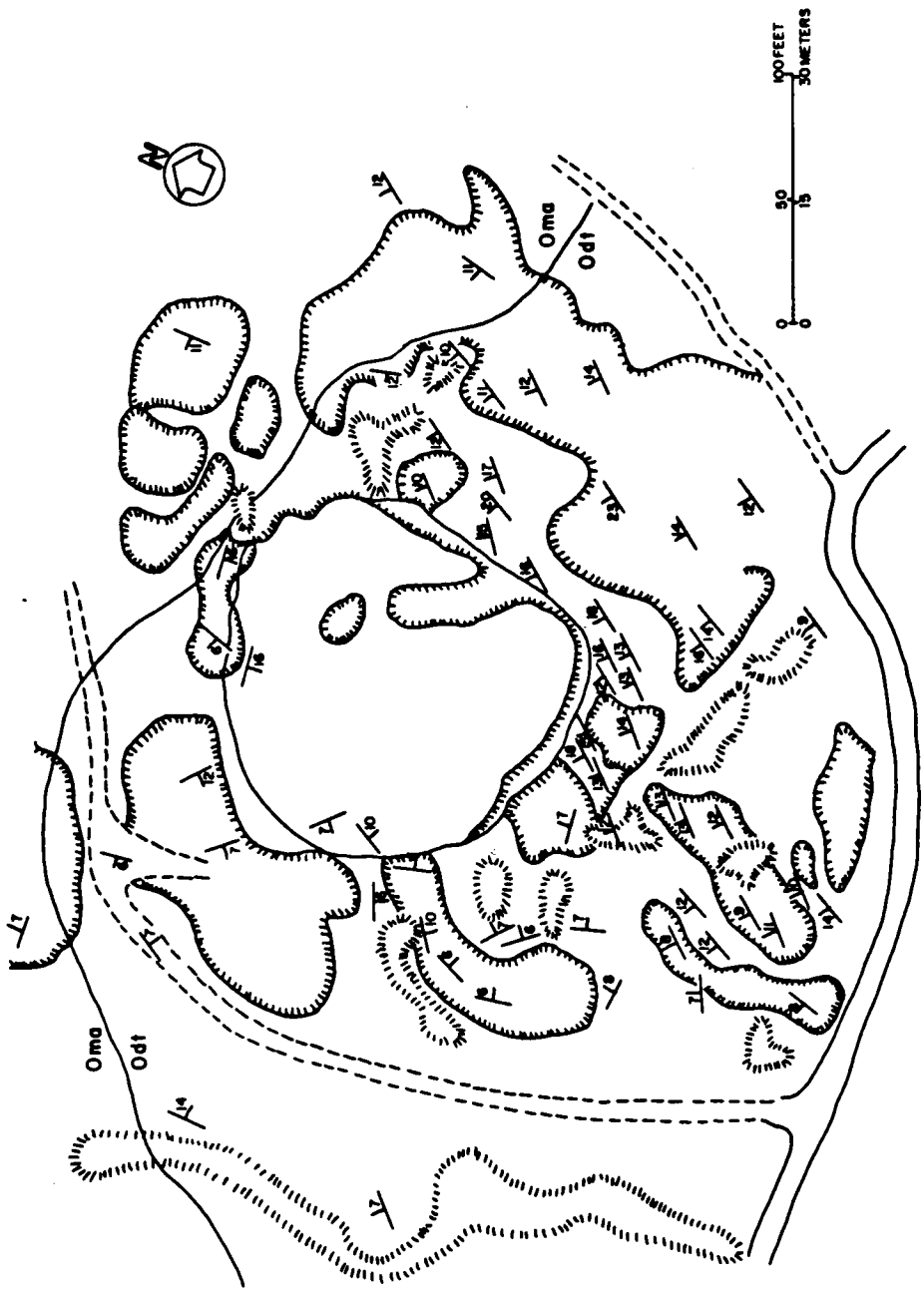


Figure 12. Base map of the Lost Creek barite mine showing bedding attitudes after rotation to remove present day regional dip.

It is possible that the anomalous SW dips are the result of depositional draping of sediments over the uneven erosion surface of the Knox unconformity. In fact, measurements on Mascot beds below the unconformity at an outcrop on the northeast side of the breccia (where the Dot above the unconformity has an attitude of N75^{o}W, 16^{o}SW) give an average strike of N38^{o}E and dip of 15^{o}SE. This would seem to support the idea of depositional dip for the anomalous Dot Formation attitudes since the Mascot attitudes are approximately equivalent to local regional measurements.

All other nearby exposures of Mascot, however, exhibit NW-trending strikes and SW dips (see Figure 7, page 13). These measured Mascot attitudes, plus the persistent nature of the SW-dipping attitudes of the Dot Formation at the mine seem to indicate that the SW dips are not the result of primary depositional dip. The discrepancy in attitudes of the Mascot may have been caused by the development of sink holes with resultant detachment, slumping, and rotation of entire blocks during exposure of the Knox surface to erosion prior to deposition of the Dot Formation. Similar effects can be observed in a modern sinkhole developed several hundred meters north of the mine.

CHAPTER III

STRATIGRAPHY, ENVIRONMENTS OF DEPOSITION, AND DIAGENESIS

Introduction

A primary concern of this investigation is to establish the stratigraphic sequence and determine the depositional and diagenetic environments for the host rocks exposed at the Lost Creek mine. The formations considered are the Lower Ordovician Mascot Dolomite, which is the uppermost formation of the Knox Group, and the overlying Dot Formation, which is the basal formation of the Middle Ordovician Chickamauga Group (see Figure 3, page 6).

This analysis is considered critical because previous investigators (Fagan 1969; Carpenter et al., 1971) suggested that the brecciation and associated mineralization occurred prior to complete lithification of the Middle Ordovician host sediments. Their hypothesis was based on the occurrence in the mineralized breccia of warped blocks of dolomitized Dot Formation limestone (Figure 13). They noted that these blocks do not show evidence of internal fracturing as might have resulted if brecciation occurred when the rocks were completely lithified and brittle. The somewhat rounded forms of many of the breccia blocks of the Dot Formation may lend additional support to this idea of pre-lithification brecciation. Rounding, however, has also been noted in ore-associated breccias developed in the Kingsport and Mascot formations of the Mascot-Jefferson City zinc district (Hoagland et al., 1965). These breccias are generally considered to have formed during an



Figure 13. Warped block of dolomitized Dot Formation limestone from the Lost Creek breccia. Block is to the left of the hammer, parallel to the handle.

erosional interval (Knox unconformity) long after substantial, if not complete, lithification of the brecciated rocks (Hoagland et al., 1965; Hill and Wedow, 1971). Dissolution by ore fluids may therefore have been responsible for the rounding of the breccia blocks, at least in the Mascot-Jefferson City zinc district. However, Churnet (1979) has related the brecciation of the nearly Copper Ridge zinc district to depositional and diagenetic processes. Further, Churnet speculates that some of the mineralization associated with brecciation was also earlier than the development of the Knox unconformity. Perhaps the rounded forms of the breccia blocks in ore breccias of the Mascot-Jefferson City district are also the result of early, pre-lithification brecciation.

The features described above imply that brecciation and mineralization at Lost Creek could actually have been penecontemporaneous with early diagenesis or even sedimentation, considering the generally early onset of lithification of carbonate sediments (Bathurst, 1975, p. 321). Therefore, it may be important to know just what the environments of deposition and diagenesis were for the Lost Creek sediments in order to fully understand the deposit.

Stratigraphy

Knox Group - Mascot Dolomite

In east Tennessee the Knox Group was first named by Safford (1869), who also included in this designation the underlying units that are now the Conasauga Group and the Rome Formation (see Figure 3, page 6). Keith (1901) essentially restricted the Knox Group to its present usage while mapping the region surrounding the Lost Creek mine.

The subdivision of the Knox Group has been the subject of controversy since the initial attempt by Ulrich (1911). In the Lost Creek area, the uppermost Knox unit was first mapped simply as Post-Longview beds (Cullison, 1937). Rodgers (1953) designated the uppermost Knox Formation on the northwestern side of the Valley and Ridge province as the Mascot Dolomite following the nomenclature of several earlier investigators, most notably Oder and Miller (1945) who supplied the original description. Harris (1969) redefined the boundaries of the Knox Group so that approximately 30 meters (100 feet) of the old Kingsport Formation are now included in the lower part of the Mascot Dolomite.

In the Lost Creek area, the thickness of the Mascot ranges from 120-180 meters (400-600 feet) (Finlayson, 1964) and is a function, in part, of the relief developed on the Knox unconformity.

Chickamauga Group - Dot Formation

Safford (1869) referred to the basal sequence of Middle Ordovician carbonates in east Tennessee as the Blue Limestone Member of his Trenton and Nashville Series. In the northwestern belts of the Valley and Ridge province Keith (1901) mapped these beds as part of the Chickamauga Limestone, a name first used by Hayes (1891) for a thick limestone sequence near Chattanooga, Tennessee.

By correlation with the earliest Middle Ordovician strata of central Tennessee, Ulrich (1911) designated the lower portion of Keith's Chickamauga limestone as the Stones River Group. Cullison (1937) mapped the basal Middle Ordovician strata in the Lost Creek area as the Murfreesboro Formation of the Stones River Group.

Rodgers (1953) replaced this terminology in the northwestern belts and called the lower 300 to 400 feet of the Middle Ordovician section simply Unit 1 of the Chickamauga Limestone. In the Lost Creek area Harris (1969) referred to the basal unit of the Chickamauga, which was elevated to group status in 1964 (Swingle, 1964), as the Dot Formation. Harris extended the name Dot from the same strike belt in southwest Virginia where Miller and Brosge' (1954) first used it to describe similar beds. A characteristic feature of the Dot is the occurrence of a red mudstone and shale facies which occupies the lowest depressions on the Knox unconformity (Harris, 1969). A typical example of this facies (Harris, 1969) can be found approximately 500 feet southwest along strike from the Lost Creek mine. A similar facies immediately above the Knox unconformity elsewhere in east Tennessee and Virginia has been referred to as the Blackford or Tumbez Formations by previous workers (Cooper and Prouty, 1943; Cooper, 1945). The term Blackford is preferred by Walker and coworkers at the University of Tennessee in their ongoing project to revise Ordovician stratigraphy in east Tennessee (Walker, personal communication, 1980).

A thin section examination of a sample of the Dot "mudstone" from the Lost Creek area (sample #191) revealed that these beds are actually argillaceous, fine-grained, hypidiotopic dolostones. The average grain size of the dolomite rhombs is approximately 30-60 . No relict calcite was observed.

The full areal extent and thickness of the Dot Formation have not been determined in the Lost Creek area. However, Blythe (1967) working in the same strike belt as Lost Creek but on the opposite

(northwestern) flank of the Powell Valley Anticline found the Dot to have a thickness of 104-145 feet.

Lost Creek Section and Lithologies

Rocks exposed in the area of the Lost Creek mine span approximately 42 meters (140 feet) of stratigraphic section, which includes approximately 6 meters (20 feet) of Mascot Dolomite and 36 meters (120 feet) of the overlying Dot Formation. Because of the relief developed on the unconformity at the top of the Knox Group (see page 8), the nature of the outcrops (see page 14), and the occurrence of several covered intervals, the Lost Creek measured section is actually a composite of several measured sections and drill core data. (Construction of the Lost Creek section is explained in detail in the Appendix). The vertical distribution of lithologies within the Dot Formation portion of the Lost Creek section is illustrated in Figure 14.

No attempt was made to categorize the various lithologies or depositional environments of the Mascot Dolomite. However, much of the Mascot exposed at Lost Creek consists of decimicron- and centimicron-sized hypidiotopic to idiotopoc dolostones. Laminations are common, and where fairly continuous, stand out in relief on weathered surfaces. In hand specimens and thin section these laminations are indistinct and consist of alternating thin (0.5-1.5 mm) dark layers and thicker (1-5 mm) light-colored layers. The coloration in the dark-colored bands resulted from the oxidation of very small (approximately 10) pyrite cubes. Lown (1978) suggested that similar laminations in Mascot dolostones from central Tennessee may be cryptalgal, which was defined by

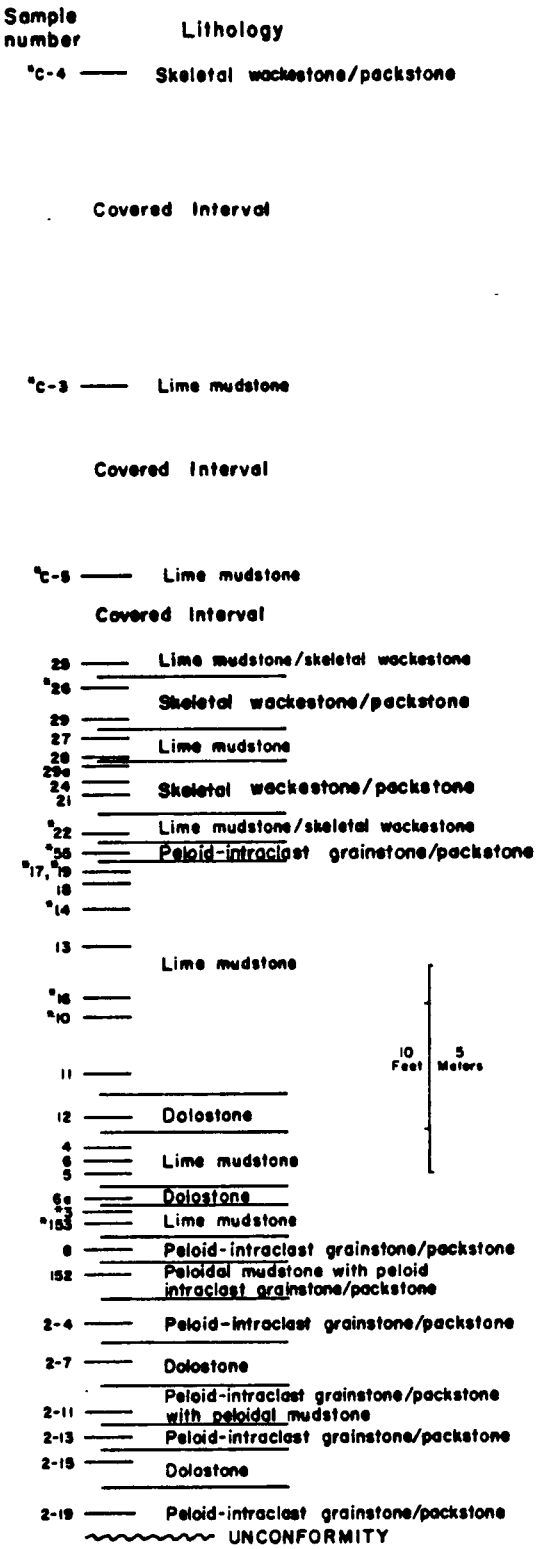


Figure 14. Distribution of lithologies within the Dot Formation portion of the Lost Creek section. Terminology after Dunham (1962).

Note: All samples except 2-19 and 2-13 are at least partially dolomitized. Those preceded by an asterisk (*) contain only scattered, small rhombs (discounting dolomite introduced by the mineralizing fluids, see page 78).

Aitken (1967) as "rock structures . . . believed to originate through the sediment binding and/or carbonate precipitating activities of non-skeletal algae."

The major lithologies of the Dot Formation are peloid-intraclast grainstone/packstone, lime mudstone, and skeletal wackestone/packstone. These lithologies commonly exhibit varying degrees of dolomitization. A minor dolostone lithology is also present. It resulted from complete or nearly complete dolomitization of precursor lime sediments (see page 69). Note that those samples assigned to the dolostone lithology of Figure 14 only include rocks so extensively dolomitized that the pre-dolomitization (depositional) lithology could not be determined. Some of the samples assigned to other lithologies would actually be dolostones by a strict definition. However, if the original rock type could still be distinguished, the sample was given that lithologic label. This approach is more practical to a discussion of depositional environments, especially considering the inferred timing of dolomitization. (The dolostone lithology will be considered in the following sections on diagenesis and mineralization.)

Environments of Deposition of Dot Formation

Peloid-Intraclast Grainstone/Packstone Lithology

Examples of this lithology, with two exceptions (see Figure 14 and page 120) were only observed in the basal 5-6 meters (15-20 feet) of section above the Knox unconformity. Hand specimens and thin sections of the lower units are unfossiliferous and exhibit distinctive modular structures attributable to pressure solution along non-sutured seams, or microstylolites (Logan and Semeniuk, 1976; Wanless, 1979). These

microstylolites (clay seams of Barrett, 1964, and horsetails of Roehl, 1967) are gently undulatory and of low relief. Individual seams are usually a few microns thick; however, these merge and diverge irregularly and form composite seams and swarms. These basal microstylolitic beds contain abundant decimicron-sized subangular quartz grains as stylocumulates. The quartz content, however, decreases markedly within the first few meters of section. Small, angular chert fragments are also especially common in the lowermost Dot sediments at Lost Creek.

Where microstylolites have not obscured original sedimentary structures, intraclasts and peloids can be seen to occur together, generally without size grading. The intraclasts are loosely packed, spherical to elliptical, and range in length from 0.2-2 mm (Figure 15). Peloids, which are presumably small micritic intraclasts, micritized skeletal debris, or fecal pellets (Bathurst, 1975, pages 84-87) are much smaller, averaging .04 mm in diameter, and are commonly spherical.

These peloid-intraclast lithologies contain a few zones, each approximately 5 mm thick, of well-defined layering consisting of interlaminated, clotted (or grumeleuse, see Bathurst, 1975, page 511) sediments and laminoid fenestrae (Figure 16). The intraclasts described above were probably derived from underlying clotted sediments which had developed some cohesion because of desiccation and binding action of algal mats. Although neomorphism and especially stylolitization have obscured the boundary relationships between intraclastic and clotted/fenestral sediments, as many as 5 separate fenestral zones have been observed in a single thin section (#2-19).

The laminoid fenestrae (see Tebbut et al., 1965, for a description of this terminology) are 0.1-0.2 mm high and at least 15-20 mm

Figure 15. Peloid-intraclast grainstone. Note the poor sorting, loose packing, and sparry interallochem calcite cement. Sample #2-19.

Figure 16. Laminoid fenestrae developed in the basal Dot sediments. Note sparry calcite cement filling fenestral voids. Sample #2-19.

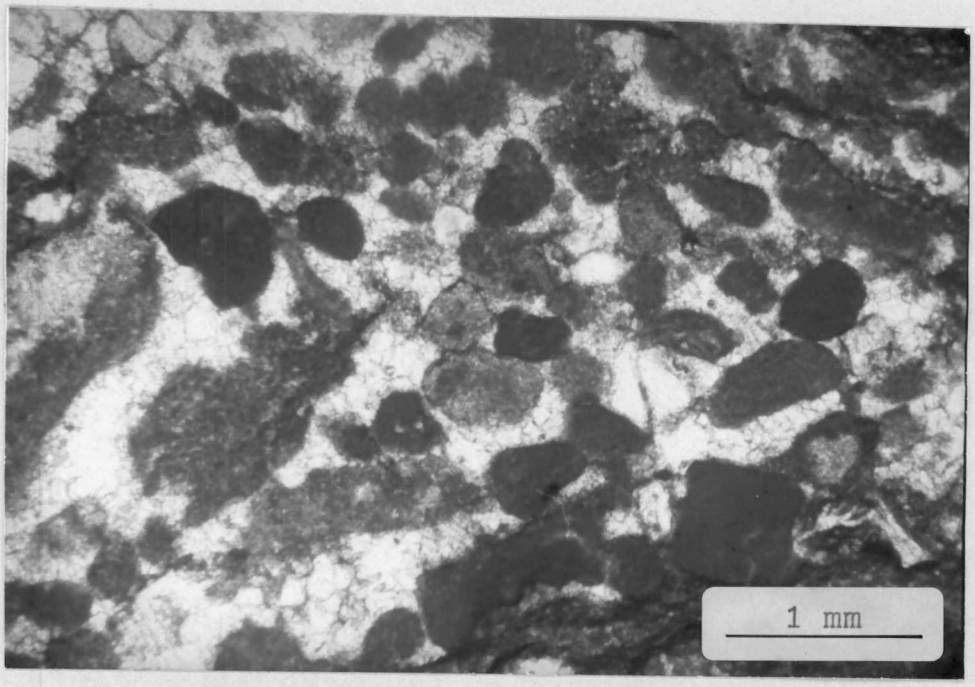


Figure 15

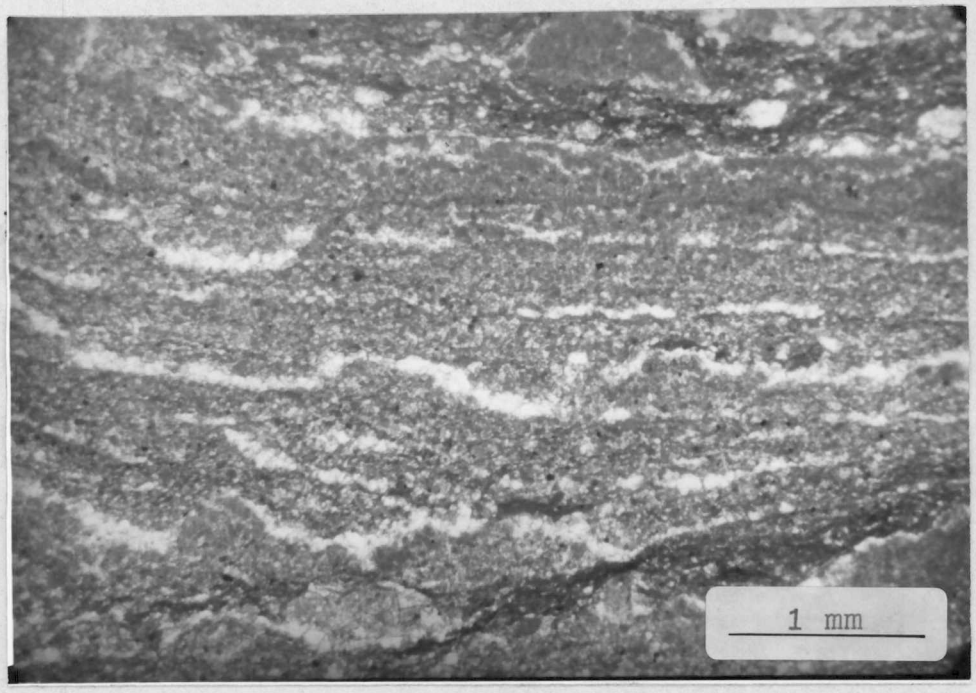


Figure 16

long. In size and shape the fenstrae are similar to laminoid fenestrae found in modern cryptalgal sediments (Logan, 1974). Overall, these fenestral zones resemble laminated supratidal deposits which form by a combination of mechanical deposition and algal mat activity on the modern tidal flats of Andros Island, Bahamas (Shinn et al., 1969; Hardie and Garrett, (1977). Similar deposits have also been documented in lowermost Middle Ordovician limestones from Virginia (Grover and Read, 1978). The intraclastic portions of the peloid-intraclast lithology are interpreted to have formed within the supratidal zone as well, probably by essentially in situ desiccation and deposition analogously to similar modern sediments found on Andros Island (Hardie and Ginsburg, 1977).

Grover and Read (1978) demonstrated the probability that "wet" climatic conditions existed in earliest Middle Ordovician time in southwestern Virginia. Walker (personal communication, 1979) has suggested that climatic conditions during the earliest Middle Ordovician in east Tennessee (during Dot deposition) were also "wet." In modern areas of high seasonal rainfall, such as the Bahamas, laminated, cryptalgal sediments can be expected to be most prolific in the supratidal zone (Shinn et al., 1969; Hoffman, 1973; Hardie and Ginsburg, 1977). This is because hypersaline conditions are unlikely to arise in a "wet" climate, thus allowing grazing and burrowing fauna to flourish in the intertidal zone. Algae are prevented from establishing mats by these algae-eating animals (Garrett, 1970).

That hypersalinity did not accompany the development of supratidal environments at Lost Creek is further suggested by the absence of diagenetic features which develop by prolonged exposure to evaporative, supratidal conditions. Evidence of caliche, evaporites, or (since in

a humid climate eventual dissolution of evaporites would have been likely) evaporite molds (Lucia, 1972; Ginsburg, 1975, page 234) has not been observed in the Lost Creek sediments. Also, no mudcracks have been found on the bedding surfaces of the Lost Creek outcrops (which expose considerable rock) or on bedding surfaces of core. Thin section study revealed only one example of a probable mudcrack (Figure 17), similar in size to those formed on channel levee backslopes (supratidal) on Andros Island (Hardie and Garrett, 1977). In fact, the only definite indication that any widespread desiccation occurred on the Lost Creek supratidal flats is the abundant desiccation intraclasts (described on page 38). Furthermore, interbedded fine-grained dolostones, which have often been cited as a priori evidence of supratidal formation and possible hypersaline conditions (Zenger, 1972), may have had quite different origins (see page 67).

With regard to the above discussion, the absence of fossils in the basal, supratidal Dot sediments may not be the result of hypersaline conditions. A paucity or absence of fauna could have been caused by lowered salinities (less than normal marine) which could have existed within the Lost Creek supratidal environments as a consequence of the interplay of the "wet" climate with other parameters of the depositional regime. Considering the relief developed on the Knox unconformity (see page 24), somewhat elevated salinities (though not hypersaline) could also have been produced solely or in part by restricted circulation.

In addition, non-hypersaline water is not the only requirement of marine organisms. Other needs include the availability of nutrients, the availability of sufficient dissolved oxygen in the water, and maintenance of a specific temperature range. The absence of fossils in the

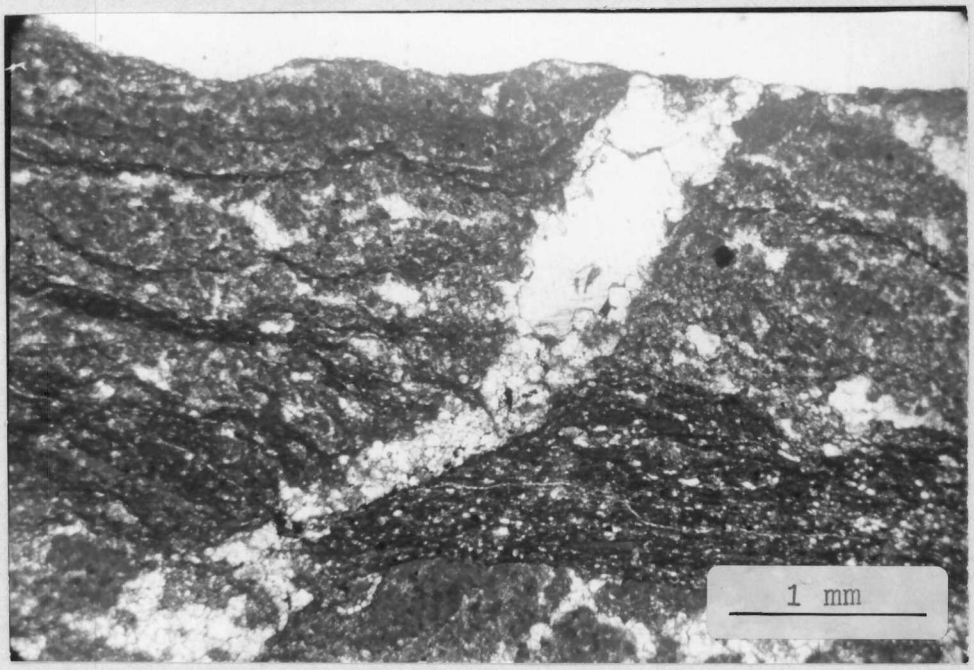


Figure 17. Probable mudcrack, inferred to have formed on a channel levee backslope (supratidal). Note sparry calcite cement in mudcrack. Sample #2-19.

lowermost Dot section may have resulted from unfavorable fluctuations of any one of these requirements (Burgess, 1968).

Sample #55 (see Figure 14, page 36), unlike other peloid-intraclast sediments, appears to have been size-graded, with large intraclasts grading upward to peloids and lime mud. Shinn (1973) found similar graded sediments as channel lag associated with tidal channels on the tidal flats of the Qatar Peninsula, Persian Gulf. Hardie and Garrett (1977) described nearly identical deposits from channel thalwegs on the Andros Island tidal flats. Sample #55 also contains skeletal debris, mainly ostracod shells, mixed with the intraclasts. The stratigraphic position of this sample places it within the intertidal zone (see the following discussion of the lime mudstone lithology).

Lime Mudstone Lithology

Lime mudstones, including clotted and peloidal subfacies, are the most abundant sediments of the Lost Creek section. This lithology is unlaminated, sometimes fenestral, and contains sparse fossil fragments. The most numerous fragments are whole and disarticulated ostracods (Figure 18). Fragmented skeletal grains of trilobites and gastropods occur occasionally. Brachiopod, bryozoan, and coral debris, as well as pelmatozoan grains, are rare and usually crushed and abraded as if transported some distance.

This faunal assemblage may indicate tidal flat deposition. Ostracods (and trilobites and gastropods as well) would have been capable of moving across the flats as dictated by tidal fluctuations. Since these are euryhaline animals they would have been able to tolerate salinity variations characteristic of this environment.

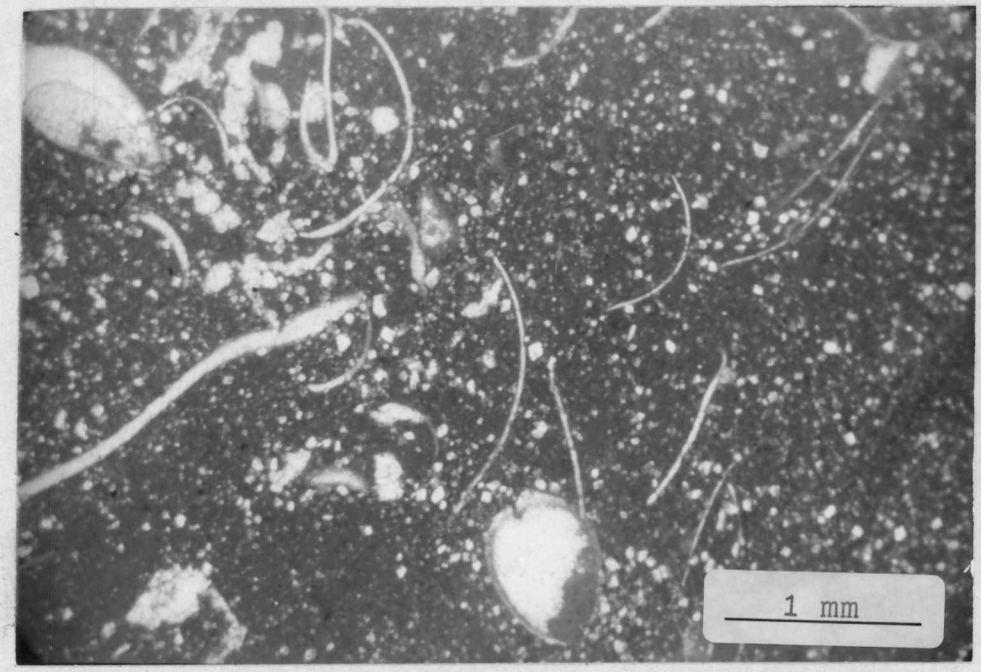


Figure 18. Fossiliferous lime mudstone, containing ostracod valves and trilobite fragments. This sediment, partially dolomitized, probably resulted from tidal flat deposition. Sample #11.

Although the mud portions of many of the rocks of this lithology are structureless (micrite of Folk, 1959), these commonly merge into grumeleuse, or clotted fabrics. The grumeleuse fabrics, in turn, are gradational with areas of peloidal packstone. These clotted fabrics contain abundant relatively thin (0.1 mm or less), anastomosing fenestrae. Grover and Read (1978) hypothesized that similar packstone facies formed from mud-supported sediments during diagenetic fenestral development. A simpler explanation is to consider clotted mudstones, and perhaps some micritic mudstones as well, to be peloidal packstones that coalesced due to compaction during early diagenesis. Shinn et al. (1969) reported that the intertidal flat sediments of Andros Island are composed predominantly of pellets.

A comparison of the fenestrae of the mudstones to those of the previously described peloid-intraclast grainstone/packstone lithofacies clearly shows that the fenestrae in the mudstones are more irregular in size and shape (Figure 19), often showing no preferred orientation relative to bedding. The fenestrae of the peloid-intraclast lithology, on the other hand, are longer, more planar, and parallel to bedding.

Fenestrae similar to those in the mudstone may form by decay of algal material in conjunction with diagenesis and lithification (Logan, 1974). They have also been formed experimentally by simple desiccation of lime mud (Shinn, 1968). The absence of other cryptalgal fabrics in the mudstone lithologies indicates that fenestrae formation probably resulted from alternate wetting and drying accompanying diagenesis. Although Shinn et al. (1969) consider similar fenestrae to be diagnostic of supratidal sediments, the lack of mudcracks and laminations, in addition to absence of abundant cryptalgal structures, suggests that

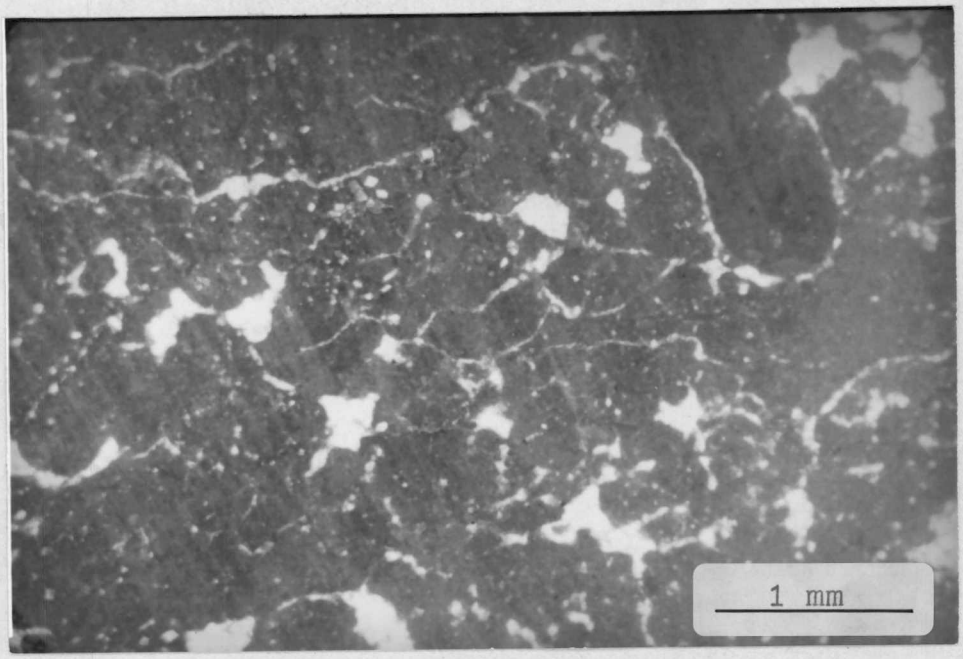


Figure 19. Irregular fenestrae developed in sediments of the lime mudstone lithology. These are inferred to have formed from strictly mechanical diagenetic processes such as wetting and drying. Sample #19.

most of the Lost Creek mudstone lithology was deposited within the intertidal zone, as suggested by Grover and Read (1978) for similar fenestral limestones of Virginia.

Rare tubular fenestrae, which may be preserved vertical burrows, are additional indicators of tidal flat sedimentation (Walker and Laporte, 1970).

Skeletal Wackestone/Packstone Lithology

This lithology is closely associated stratigraphically with the lime mudstone lithology. These two lithologies appear to be gradational as the fossil content of the mudstones increases and that of the skeletal wackestones decreases.

The biota of the skeletal limestones is abundant and diverse (Figure 20), and includes ostracods, pelmatozoan debris, trilobite fragments, bifoliate bryozoans, coral fragments, and algal remains (probably Hedstroemia). Laporte (1967) indicates that such diversity is the result of subtidal deposition, contrasted with tidal flats, where fossil types are few although individuals may be abundant. The largely unabraded nature of most of the skeletal grains indicates little or no transport from the primary environment.

Although no oncolites, which are excellent indicators of very shallow subtidal deposition (Benedict and Walker, 1978), were observed in this lithology, the marine biota indicates a subtidal origin, probably shallow, considering the repeated interfingering with tidal flat sediments (see Figure 14, page 36).

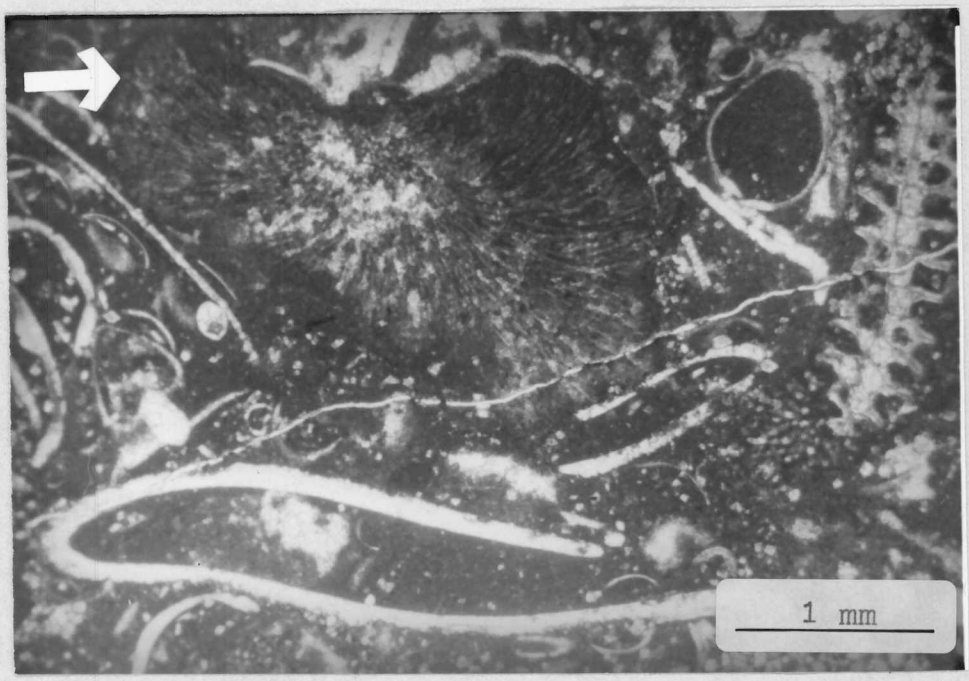


Figure 20. Typical biota of the skeletal wackestone/packstone lithology. The diversity and largely unabraded nature of most of the skeletal grains indicates subtidal deposition. The arrow indicates stratigraphic "up." Sample #24.

Summary of Depositional Environments

At Lost Creek the Dot Formation formed within a tidal flat and adjacent shallow water marine set of depositional environments (Peritidal Zone). This interpretation is consistent with the regional paleoenvironmental model proposed for the Middle Ordovician of east Tennessee as the result of the ongoing research program at the University of Tennessee (Walker, 1977). Overall, the unit is a transgressive sequence, developed above an extensive subaerial erosional surface, and overlain by extensive shelf-lagoon deposits (Walker, 1977).

A modern, direct analogue of the Lost Creek depositional regime does not exist. In several respects, brought out in the above discussion of depositional environments (and products of the environments), the setting of Andros Island, Bahamas (Shinn et al., 1969; Hardie, 1977), is the best, albeit very approximate, recent analogue.

Diagenesis

Introduction

The mineralogical, textural, and chemical changes which carbonate sediments undergo after deposition are defined as diagenesis (Friedman, 1964). Diagenesis, which begins at the sediment/water interface, includes all natural modifications that occur under normal outer crustal or surface conditions of pressure and temperature between the time of initial deposition and lithification (Twenhofel, 1939, page 254).

Post-lithification changes are sometimes considered to be diagenetic also, if the metamorphic threshold has not been crossed (Pray and Murray, 1965) and with the specific exclusion of weathering effects (Krumbein, 1942). A more rigorous definition of diagenesis

must include parameters defining the onset of the zeolite facies of regional metamorphism, which bridges the transition between diagenesis and greenschist facies metamorphism (Runnels, 1969).

Because of the large number of diagenetic environments, the wide array of textures produced within each environment, and the possibility of repeated changes in diagenetic environment during the history of a carbonate rock, establishing diagenetic sequences is generally complex (Longman, 1980). Nonetheless, paragenetic sequences of diagenetic events for carbonate units of widely varying geologic age and geographic distribution have been constructed by Neal (1969), Mossler (1971), Longman (1976), and Lyle (1977).

Petrographic examination of the Dot Formation limestones and dolostones reveals a variety of diagenetic features. One goal of this examination was to divide the diagenesis of the Lost Creek carbonates into distinct events. A discussion of individual diagenetic events and their petrographic characteristics follows. Details of paragenesis are added where necessary and eventually woven into an overall paragenetic sequence of diagenesis for the Lost Creek deposit. Diagenetic events are discussed in the approximate temporal sequence, from early to late, in which they occurred. The events considered are: (1) formation of framboidal pyrite, (2) cementation, (3) neomorphism, (4) dolomitization, (5) dedolomitization, (6) silicification, (7) calcite veining, and (8) stylolitization.

Formation of Framboidal Pyrite

Framboidal (sedimentary) pyrite (Rickard, 1970; Berner, 1970) forms as a result of the decay of organic matter under anaerobic

conditions (Park and Schot, 1968; Mossler, 1971). It has been demonstrated to be a syngenetic product in recent fine-grained sediments where reducing environments develop a few inches below the water/sediment interface (Love, 1964).

Framboidal pyrite is especially common in the lower portion of the Lost Creek section. Pyrite is commonly scattered throughout micritic sediments and concentrated along microstylolites. It is also associated with neomorphic and void-filling calcite spar. The pyrite associated with voids is concentrated along the outer boundaries of the voids. Since this calcite cement, based on its morphology and lack of ferrous iron content, is indicative of possible oxidizing conditions (see later section on cementation), the formation of pyrite, which began syngenetically within reduced lime sediments, must have been interrupted during cementation. Some of the pyrite concentrated along the margins of voids appears to have actually formed within the void itself (although this is difficult to determine in a 2-dimensional thin section). If true, then pyrite must have formed subsequent to cementation, perhaps as a result of micro-reducing environments.

In several samples (most notable #2-11) framboidal pyrite commonly surrounds areas of relict lime sediment in an otherwise dolomitized rock (Figure 21). The individual framboids are 10 microns or less in diameter. Under low power magnification the concentration of pyrite around relict limestone appears as a diffuse dark band. There is not, however, a one-to-one correspondence between relict limestone and framboidal pyrite, as some areas of relict calcite have no pyrite surrounding them, and there are also accumulations of framboidal pyrite elsewhere besides around relict limestone patches.

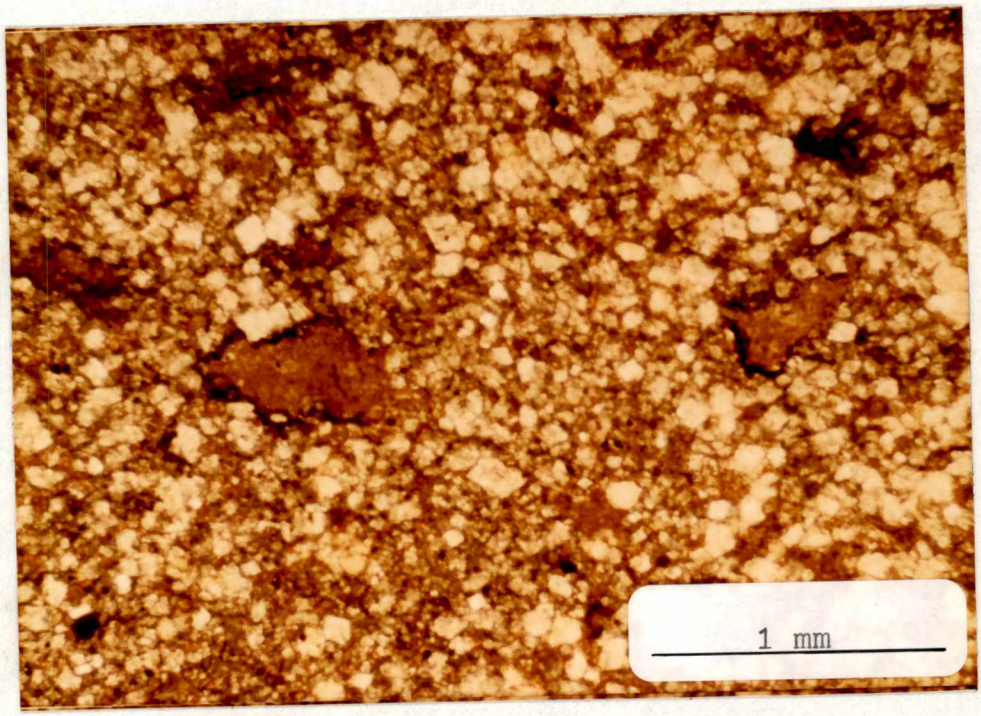


Figure 21. Relict patches of lime sediment within a largely dolomitized peloid-intraclastic sediment (stained with alizarin red S). Framboidal pyrite commonly surrounds these areas of relict calcite, and appears in this picture as a diffuse black band. Sample #2-11.

This pyrite may have precipitated in the vicinity of decomposing organic matter. The organic matter must have been "driven," before decomposition, as impurities, away from centers of dolomitization. A similar process can be observed in crystallizing halite (Gary Iversen, personal communication, 1980). Eventually, the organic material must have been reduced resulting in the formation of framboidal pyrite. The necessary reducing conditions were probably very local in scope, and perhaps only existed on a micro-scale. It would be difficult to imagine that pyrite, already formed, could accumulate in a similar manner. The significance of sample #2-11 is that it indicates an episode of formation of sedimentary pyrite after dolomitization.

To summarize, the formation of framboidal pyrite probably began pene-contemporaneously with deposition, was interrupted by sparry calcite cementation and dolomitization, and resumed again later, on a very small scale (after cementation and dolomitization), in an essentially lithified rock.

The abundance of framboidal pyrite in the lowermost Dot sediments indicates that despite the absence of organisms capable of leaving fossilized remains, organic matter must have been present. Perhaps it was derived chiefly from buried algal mats (see page 38).

Cementation

There is no evidence of either vadose or marine cementation in any of the sediments from Lost Creek [see, for example, Folk (1973), Folk and Land (1975), and Longman (1980) for criteria used in the recognition of these cements]. In sample #2-19, from just above the Knox unconformity, the loose packing of the intraclasts suggests early

cementation (see Figure 15, page 39). According to Steinen (1974) and Land (1970), carbonate diagenesis, including cementation, is more rapid in the freshwater phreatic environment than in either the vadose or marine phreatic realms. The morphology of the cement of #2-19 is also typical of meteoric phreatic (freshwater) cementation (Land, 1970; Folk, 1974; Badiozamani et al., 1977). Note, for example, Figure 22 which illustrates that the cement is equant and that individual crystals interlock and coarsen toward the center of the void. These features are all characteristic of meteoric phreatic cementation. However, Folk and Land (1975) point out that similar blocky, sparry calcite cement can also form in the deep subsurface environment where solutions, either connate or mixed with meteoric water, have lost Mg relative to Ca. This origin is possible, but unlikely for the Lost Creek cements, because many of the additional petrographic features and relationships described later during this discussion of diagenesis indicate a fresh-water (meteoric) phreatic origin. [The terms meteoric water and fresh water are used interchangeably in this paper following the practice of Longman (1980).]

In addition to occupying interallochem pore spaces, the fresh water cement of sample #2-19 also fills fenestrae (see Figure 16, page 40) and the mudcrack depicted in Figure 17 (page 43). Higher in the stratigraphic section similar blocky calcite is intimately associated with ferroan dolomite (revealed by staining) in vugs and voids (see later section on dolomitization). Some of the void-filling calcite cements from higher in the section are themselves ferroan (also revealed by staining). Why are both ferroan and nonferroan calcite cements found in the sediments of the Dot Formation? Why are the ferroan

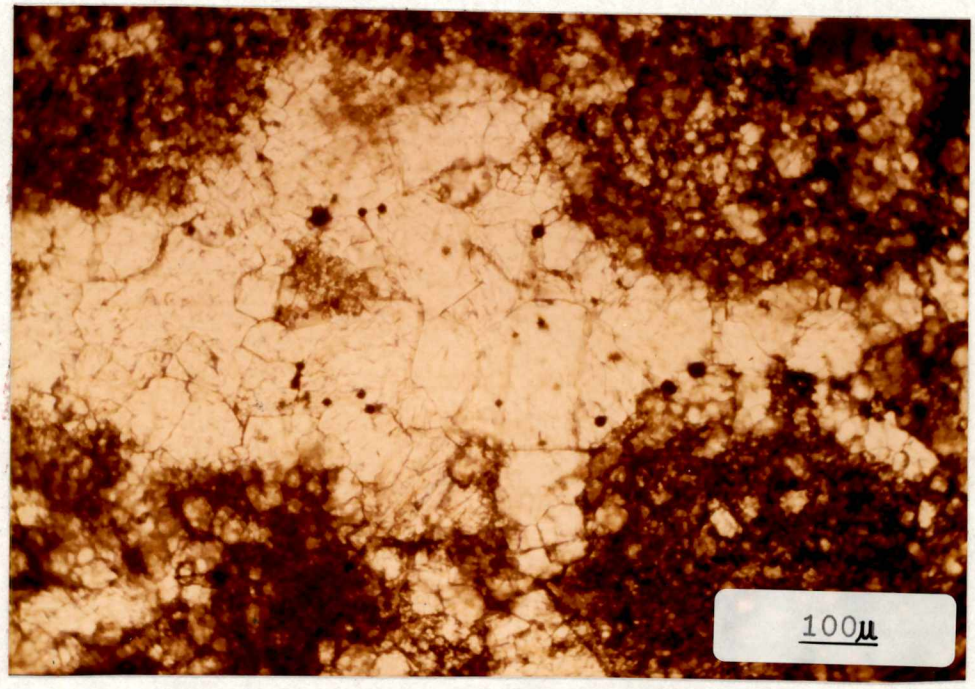


Figure 22. Fresh water phreatic calcite cement as void-filling spar. Sample #2-19. The void was an interallochem void.

calcite cements much less common? The most obvious hypothesis is that there was more than one episode of sparry calcite cementation. As will be shown later, this is true, but it is not in itself a complete explanation.

Ferroan calcite is often regarded as a late cement (Dickson, 1966). Oldershaw (1971) considered ferroan calcite cements to be burial cements produced during compaction by the process of pressure solution, which is most effective in clay-rich sediments. Leaching of iron from clay minerals may be the source of iron in the ferroan calcite cements. It is unlikely, however, that the ferroan calcite cements in the Dot Formation are burial cements. At Lost Creek the sediments that contain the greatest concentration of clays occur just above the Knox unconformity, and these sediments contain no ferroan calcite cement. (If the ferroan calcite cements are not burial cements then it would seem likely that the nonferroan calcite cements did not form in the deep subsurface either.)

Neal (1969) hypothesized that ferroan calcite cements from the Blackjack Creek Formation (Pennsylvanian) of Missouri were second-generation cements precipitated by circulating ground waters following subaerial exposure and partial lithification. According to Evamy (1963), the reducing conditions, under which ferrous iron is stable in carbonate terrains, occur widely below the water table and only rarely above it. Burgess (1979) agrees, noting that ferroan calcite is a common indicator of phreatic cementation, but is not restricted to the phreatic zone. Algal laminated sediments often have iron-rich cements and neomorphic microspar. It is known that algae thriving in the vadose zone can concentrate iron as a result of their life processes. This iron may

become incorporated into ferroan carbonates during later diagenesis and cementation but not in an oxidizing environment (Burgess, 1979). The algal laminated rocks from the Dot Formation, however (samples #2-19 and #2-4 are the best examples), without exception, contain no ferroan cement or ferroan microspar. It is therefore likely that the ferroan cements from rocks higher in the stratigraphic column, which are not even cryptalgal, are not vadose but phreatic.

On the other hand, flow paths of oxidizing water may arise below the water table in the absence of organic matter or because of a local absence of iron (Burgess, 1979). Other parameters which may produce oxidizing phreatic waters (or reducing vadose waters) include climate, distribution of ground water, and the presence of minerals which during oxidation may lower the Eh (Burgess, 1979).

The ferroan calcite cements in Lost Creek rocks are rather rare overall, but occur quite commonly in several samples (especially #11). Ferroan calcite cements generally occupy the centers of voids, indicating a change in the chemical environment during the final stages of void-filling cement precipitation (Figure 23). (The voids are commonly within ostracod shells, crinoid columnals, or other skeletal remains.) Ferroan dolomite cement also often occupies the centers of voids (see Figure 23). Other voids, even in the same samples that contain voids with ferroan calcite and/or ferroan dolomite cement, may be completely filled with non-ferroan calcite. These inconsistent relationships suggest that ferroan calcite is the result of very localized reducing environments within an otherwise oxidizing ground-water regime. With reference to calcite cementation, the reducing conditions existed only briefly during the final phases of precipitation.

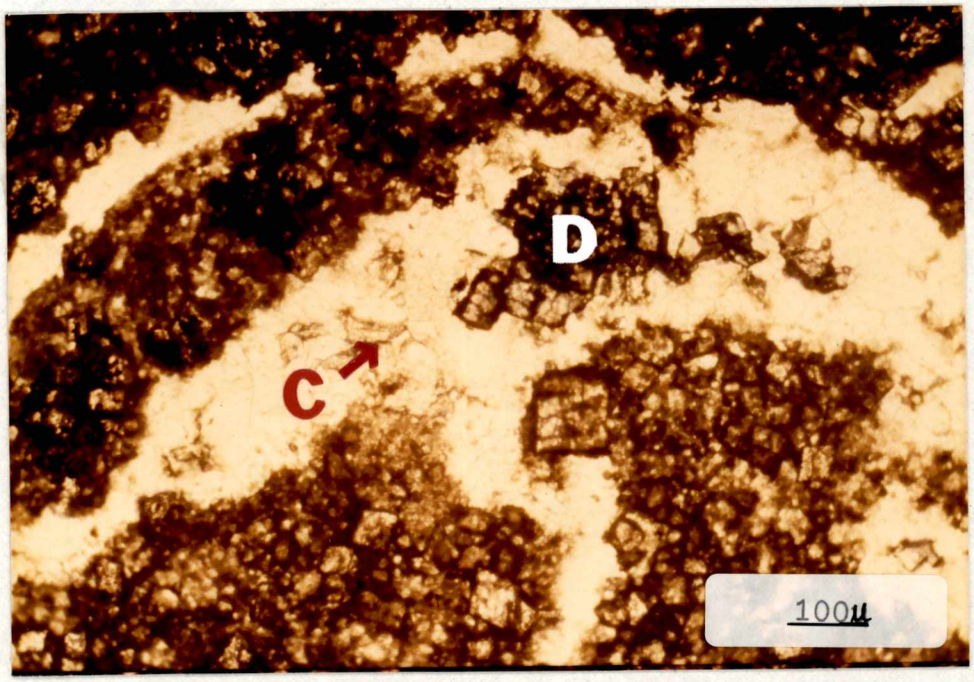


Figure 23. Ferroan calcite (C) and ferroan dolomite (D) cements occupying the central portions of a void initially lined with non-ferroan calcite cement. Stained with potassium ferricyanide. Sample #11.

In a later section on dolomitization it will be demonstrated that there were at least two and probably three distinct episodes of blocky calcite cementation. Ferroan calcite is found associated with only the last episode.

Evidence for an early episode of cementation, in addition to the loose packing of intraclasts in sample #2-19, is also found in sample #26. Molluscan shell molds are common (the shells themselves have been dissolved). These are predominantly filled with ferroan dolomite although minor calcite is also present (Figure 24). Obviously, selective solution/replacement of the aragonitic molluscan bioclasts occurred after initial cementation of the sediment, otherwise the molds would not have persisted. The absence of internal sedimentation suggests that void-filling by the ferroan dolomite and calcite closely followed creation of the voids. Two questions must be considered: When was the sediment cemented? When was the aragonite replaced?

The cement that could have preserved the molluscan shell molds may have been a marine cement (fibrous aragonite or Mg-calcite). There is, however, no evidence elsewhere in the Dot sediments for marine cementation. For instance, the interallochem pore spaces in #2-19, which would have existed immediately after deposition, contain only meteoric phreatic cement (see Figure 15, page 39). Perhaps the micropores in the sediment of #26, and throughout the section for that matter, also served as sites of meteoric phreatic cementation.

The timing of cementation of the sediment is less important if we consider that a mold of the aragonitic grain may have formed early, even without cementation of sediment, if the grain itself were coated with a layer of calcite cement. This layer would persist after the

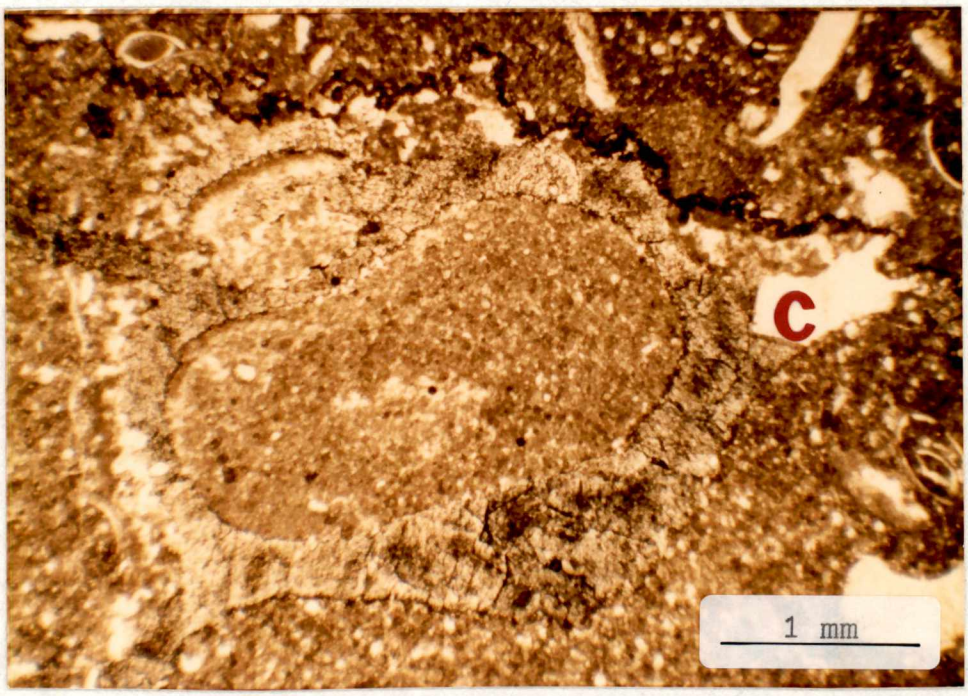


Figure 24. Molluscan shell mold filled with ferroan dolomite cement. Formation of mold indicates that solution--replacement of the aragonitic bioclast followed cementation of the sediment. Note the calcite grain (C) that accompanies the dolomite cement. Stained with potassium ferricyanide. Sample #26.

aragonite dissolved and would serve as a mold for later carbonate cements (Bathurst, 1975, page 327). Micrite envelopes, which were not observed in any samples from Lost Creek, more commonly serve as molds in this process.)

Grover and Read (1978) suggest that dissolution of aragonitic grains occurs in either marginal marine environments where waters become under-saturated with calcium carbonate because of the influx of continental waters, or under subaerial vadose conditions. Since there is no evidence of vadose diagenesis (based on parameters such as cement morphology) in the Lost Creek sediments, Grover and Read's first hypothesis may be the mechanism responsible for the dissolution of molluscan shells at Lost Creek. This idea of influxing continental (meteoric) waters has important implications for many of the diagenetic processes affecting Lost Creek sediments, especially dolomitization, as will be discussed later.

An idealized scheme for carbonate diagenesis (albeit vadose instead of phreatic) was suggested by Land et al. (1967). This scheme places the precipitation of calcite cement in intergranular and intragranular pores prior to the dissolution of aragonitic bioclasts. Apparently, a similar sequence may exist for meteoric phreatic diagenesis. Longman (1976) hypothesized that moving shallow subsurface ground water was responsible for dissolution of aragonitic shells in the Bromide Formation (Middle Ordovician) of Oklahoma, probably following cementation. The cement that preserves the shell molds in sample #26 (see Figure 24) from Lost Creek, whether in micropores in sediment, or as a coating around the aragonitic shells, is probably equivalent to the

initial, pre-dolomitic intergranular and void-filling cement observed in sample #2-19 (see page 53).

Neomorphism

Neomorphic microspar is a common feature in the Dot Formation sediments. Neomorphism, defined by Folk (1965) as "all transformations between one mineral and itself or a polymorph." Neomorphic processes are "wet" reactions that probably involve both dissolution and re-precipitation (Bathurst, 1975, page 476).

Neomorphic spar is most abundant in sample #2-19. Folk (1974) lists several mechanisms by which neomorphism of micrite to microspar can take place. All involve the removal of magnesium which prevents the normal growth of carbonate crystals (aragonite or calcite) beyond an equilibrium size of 2-3 microns. One mechanism, flushing of Mg by meteoric waters (see also Folk and Siedlecka, 1974), is attractive in regards to the Lost Creek sediments in general and sample #2-19 in particular. This sample, of course, is largely intraclastic (see page 39) and was therefore quite porous and presumably permeable, initially. Flushing also may explain why there is absolutely no dolomite in this sample (see later section on dolomitization). Since #2-19 is just above the Knox unconformity, emergent Knox terrain would have been nearby and would have served as a catchment area for large amounts of fresh water which could have been responsible for the flushing. The initial "wet" climatic conditions under which the Lost Creek sediments were deposited (see page 41) would have provided ample fresh water by precipitation. The neomorphic spar in sample #2-19 was possibly penecontemporaneous with the sparry cement in that sample, which also resulted from percolating fresh water (see section on cementation).

The presence of clays may aid the neomorphic process. Apparently, Mg ions are absorbed by clay minerals as waters percolate through the rock (Folk, 1974). The clay content of #2-19, while probably not a sole cause of the neomorphism, may therefore still have played an important role. According to Longman (1976), waters capable of neomorphosing aragonitic shells to calcite, or even capable of forming dolomite, may not be able to form microspar unless clay is present.

Higher in the stratigraphic section microspar is volumetrically fairly minor (because of less clay?). Comparable to the calcite cements, the microspar from this part of the section is also intimately associated with ferroan dolomite. Some of the microspar is ferroan, also (see discussion and illustrative figure in section on Type II dolomitization, page 80). There were probably several episodes of formation of microspar, just as there were several stages of sparry calcite cementation.

Neomorphic inversion of aragonite to calcite was considered in a previous section (on cementation), with reference to the aragonitic molluscan shells which were replaced by ferroan dolomite and calcite in sample #26 (Figure 24). One addition to the prior discussion must be made here. Bathurst (1975, page 359) points out that the formation of neomorphic microspar occurs during the same stage of vadose diagenesis as the dissolution of aragonitic bioclasts. There is no evidence for vadose diagenesis at Lost Creek (see pages 57-62). It was previously hypothesized, however, (page 51) that for both vadose diagenesis and meteoric phreatic diagenesis (evidence for which <u>is</u> found at Lost Creek) the dissolution of aragonitic bioclasts occurred after cementation. If the timing of microspar formation for both diagenetic environments is also similar, then the microspar seen in sample #2-19 must have

formed after cementation also. This is in contrast to the hypothesis of formation of microspar penecontemporaneous with cementation (see page 62). Perhaps, however, penecontemporaneous may still be a proper term if one allows it to cover a fairly broad range of time, i.e., both syn- and post-1st episode sparry calcite cementation.

Dolomitization

It is not the intent of this paper to review the literature on models of dolomitization; nevertheless, some discussion will be unavoidable. This is especially true considering the widespread occurrence of dolomite in the Lost Creek sediments, its many modes of occurrence, and its importance to a fuller understanding of the processes of diagenesis and mineralization.

Churnet (1979) has summarized the conditions that favor extensive dolomitization: (1) ample available Mg^{++}, (2) increase in Mg/Ca ratio, (3) decrease in P_{CO_2}, (4) increase in temperature, and (5) dilution or concentration of seawater-derived solutions. These factors can act singly or in combination to produce dolomitization.

A careful petrographic study of the Lost Creek sections reveals two major "types" of dolomite. These are distinguishable not only because of intrinsic petrographic characteristics of individual grains but on the basis of textural relationships as well. For convenience, these two "types" of dolomite will hereafter be referred to as Type I, or earlier, and Type II, or later, which, as will be demonstrated, followed the formation of Type I. Table 2 compares the general characteristics of each. [An additional "type" of dolomite, distinctive but volumetrically minor, was introduced with the mineralizing fluids. It will be considered later (see page 114).]

TABLE 2

COMPARISON OF EARLIER "TYPE I" DOLOMITE
AND LATER "TYPE II" DOLOMITE

Criteria	Type I Dolomite	Type II Dolomite
Grain size	Lower size limit 10-30 microns Upper size limit 100-130 microns	Range up to 500-600 microns
Extinction property	Individual grains generally show unit extinction	Mainly sweeping extinction
Staining (with potassium ferricyanide)	May have thin, outer ferroan rim	Generally ferroan throughout
Zoning	May have cloudy centers	Often have cloudy centers
	Predominantly unzoned when viewed with cathodoluminescence; may have thin, irregular luminescent band along outer margin	Mostly zoned; often many concentric luminescent bands
Fabric	Idiotopic to hypidiotopic	Xenotopic (anhedral masses)
	Generally no inclusions (rare, relict calcite inclusions)	Many inclusions of Type I dolomite
Occurrence	Complete or partial dolomitization of precursor lime sediments, post-cementation but pre-mineralization	Mainly void- and vug-fillings associated with mineralization

Type I dolomite. An examination of the distribution of lithologies at Lost Creek (see Figure 14, page 36) reveals an alteration of dolostone and limestone in the basal part of the section. Samples #2-19 and #2-13, essentially intraclastic grainstones containing no dolomite, sandwich a horizon that has been essentially completely dolomitized (sample #2-15). This alternation of Type I dolostone and limestone is seen higher in the section as well. It must be noted, however, that #2-19 and #2-13 are the only completely undolomitized limestones in the section. All other limestone lithologies are at least partially dolomitized. There are, however, several other examples, similar to #2-15, of completely dolomitized rock (dolostone lithology) in the section.

The dolostones referred to above, and the dolomitic portions of limestones as well, are primarily idiotopic to hypidiotopic. The lower size limit of the dolomite rhombs ranges from approximately 10 to 30 microns, whereas the upper size limit ranges from approximately 100 to 130 microns. Generally, the rhombs have a thin, outer ferroan rim (revealed by staining). Larger rhombs may have cloudy centers. The luminescent properties of Type I dolomite will be considered in a later section.

The timing of this dolomitization is probably post-cementation and post-neomorphism. This is suggested by samples such as #2-11 and #2-4 that are only partially dolomitized. Calcite (micrite and spar) in partially dolomitized samples is not a product of dedolomitization, rather, it may be a relict left after dolomitization. Most of the dolomite rhombs, as noted above, are euhedral. The calcite is interstitial and does not embay the rhombs as it would if it were replacing the dolomite (Figure 25).

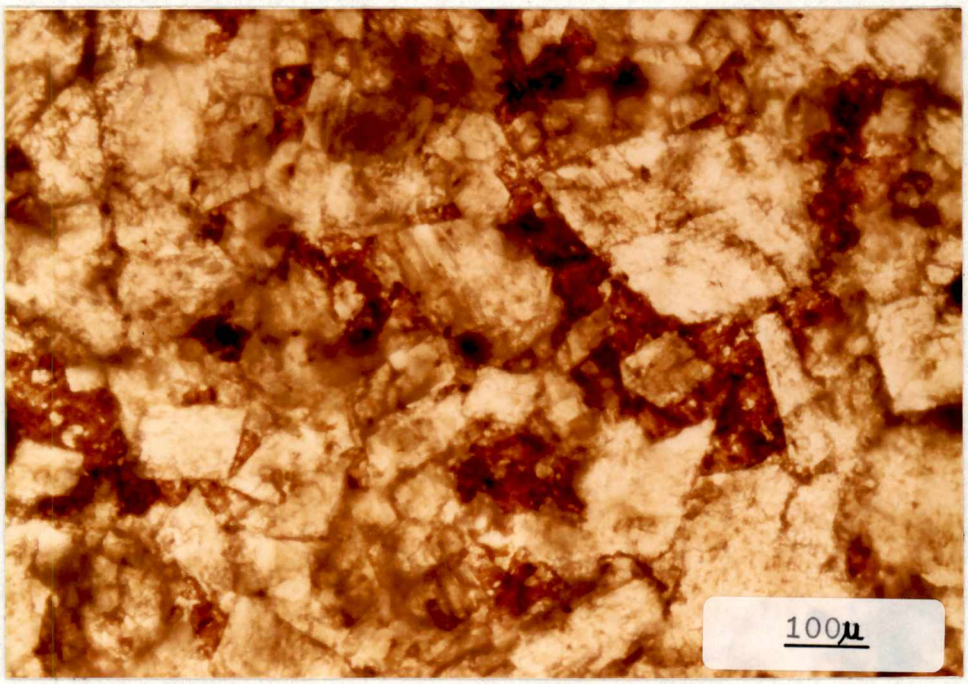


Figure 25. Interstitial, relict calcite in an essentially dolomitized rock. Stained with alizarin red S. Sample #2-11.

Relict structures are visible also. In sample #2-11, which is estimated to contain at least 70% dolomite overall, relict peloidal structures can be observed in patches of relict micrite. The peloids are identical in size and shape to the peloids described previously that are found as constituents of the peloid-intraclast lithologies (see page 37). Another area of relict calcite in #2-11 contains relict intraclasts set in relict spar, which presumably is cement (Figure 26). The relict micrite intraclasts themselves are partially dolomitized. The selective dolomitization of lime mud (micrite), because of its greater surface area and therefore reactivity, is well documented (Murray and Lucia, 1967; Neal, 1969).

Sample #2-4, also extensively dolomitized, contains several recognizable zones of spar-filled laminoid fenestrae and peloid-intraclast sediments. Even sample #2-7, which lies between #2-11 and #2-4 and which is essentially completely dolomitized, contains a few small patches of relict calcite, invariably spar. Apparently, all micrite and most of the spar in this sample have been dolomitized. This interpretation is based on the recognition that the lowermost 5 meters of section at Lost Creek are composed of either dolostone or peloid-intraclast grainstone/packstone ranging from completely undolomitized sediments to extensively dolomitized samples containing only scattered recognizable limestone relicts. This suggests that the dolostones were also peloid-intraclast grainstone/packstones prior to dolomitization. Dolomitization is therefore seen to have been a process activated <u>after</u> (not penecontemporaneous with) deposition and probably after most cementation.

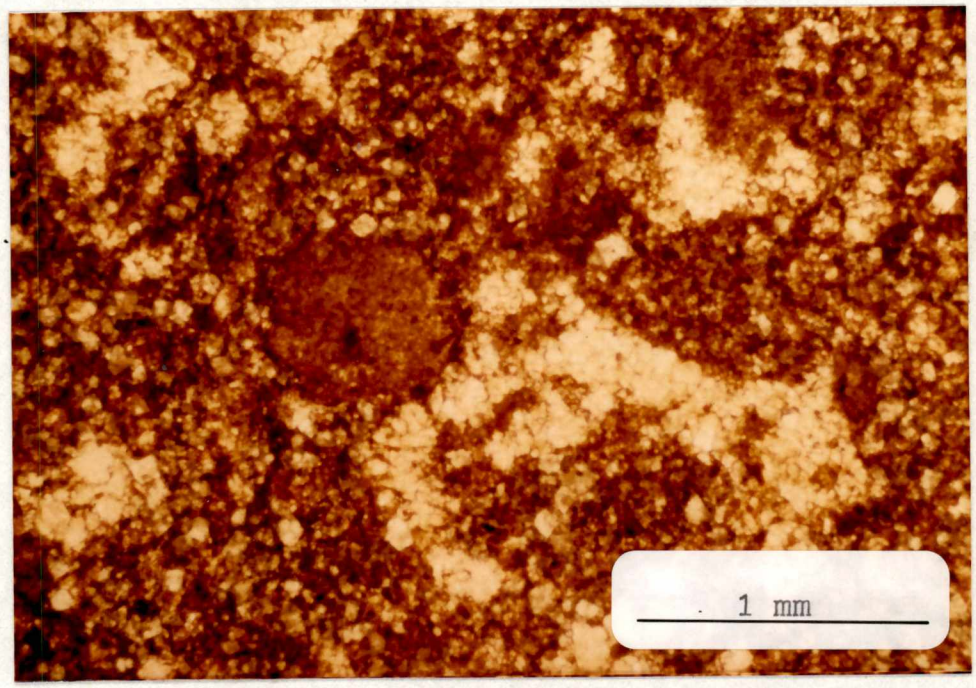


Figure 26. Relict intraclasts and sparry cement in the same dolomitized rock depicted in Figure 25 above. Note that the relict intraclasts are themselves partially dolomitized. Stained with alizarin red S. Sample #2-11.

Furthermore, the dolomitization did not act upon all sediments uniformly. In fact, the lowermost Lost Creek sediments are notable for their widely varying dolomite content.

A very few of the rhombs of the Type I dolomite contain calcite inclusions (revealed by staining). These are also interpreted to be relict, and not the result of dedolomitization.

Some of the relict calcite (but not the relict calcite, noted above, within dolomite rhombs) contains dolomite inclusions (revealed by staining). These may be either very small rhombs (less than 10 microns long) or tiny blobs. There are several possible origins for these dolomite inclusions:

1. They represent nucleii of dolomitization that did not grow any larger.

2. They are evidence of cementation in a mixing zone alternating between fresh water and marine or hypersaline conditions (Folk and Siedlecka, 1974) in which the solutions were saturated with respect to both calcite and dolomite (Churnet, 1979).

3. They are actually relict, and the calcite is a product of dedolomitization. This is very unlikely, considering the rhomb-shaped morphology of some of the "relicts" and the above discussion concerning dedolomitization.

4. They are the result of later alteration of high-Mg calcite inclusions (Meyers and Lohmann, 1978). This is not likely, otherwise the sparry calcite of #2-13 and #2-19 should also contain dolomite inclusions, since presumably this spar is similar in original composition to the relict spar in samples, such as #2-11, that do contain dolomite inclusions. (As has been noted previuosly, samples #2-13,

#2-19, and #2-11 are all peloid-intraclast grainstones/packstones separated stratigraphically by only several meters of section and were probably deposited under similar conditions. Diagenetic conditions were probably similar also.)

As will be explained below, perhaps either 1 or 2, or both 1 and 2 may be the processes responsible for the dolomite inclusions.

The alternating nature of the lithologies (limestone alternating with dolostone) from the lower portion of the Lost Creek section indicates a possible sedimentological or early diagenetic control of the process of Type I dolomitization. The depositional regime of Andros Island in the Bahamas has previously been noted as an approximate analogue in certain important respects, such as climate, to that of the Lost Creek sediments (see page 41). It is logical to assume that if the environments of deposition are somewhat comparable, then the diagenetic environments might be also. Therefore, an examination of the occurrence of dolomite on Andros Island is necessary at this point.

In the Bahamas, dolomite is a penecontemporaneous replacement product of pelletal material washed into supratidal areas. The pellets are not dolomitized in the intertidal zone, where they are assumed to have been produced by gastropods (Bathurst, 1975).

According to Shinn et al. (1969) dolomite (over 5%) is present only in the various subdivisions of the supratidal zone. The highest concentrations of dolomite occur in lithified surface crusts only a few inches above normal high-tide level. On levees, the highest dolomite content occurs on the flanks farthest from the channel (Shinn et al., 1969). The grain size of the Andros Island dolomite (actually a protodolomite) is extremely small, always less than 3 microns (Shinn et al.,

(1965). Shinn et al. (1969) consider the restriction of dolomite formation at Andros Island to supratidal environments to have important geological implications. The dolomitic sediments are invariably associated with diagnostic sedimentary structures such as algal and nonalgal laminations, desiccation features, and birdseye vugs. Recently, dolomite of different origins has been found at some depths in levees (Gebelein, 1977). This occurrence will be considered later (see page 77).

The processes commonly envisioned for the formation of the Andros Island dolomite, capillary concentration (Shinn et al., 1965) or evaporative pumping (Hsü and Siegenthaler, 1969) both involve concentration of interstitial water by evaporation. Both processes are complex and poorly understood. What is even more important, in terms of this discussion, is that both processes are hypothesized to be operative penecontemporaneously with lime mud deposition. Therefore, they cannot be responsible for the formation of Type I dolomite at Lost Creek, as this dolomite is clearly post-sedimentation and probably post-cementation as well (see page 67). Furthermore, some sediments in which (analogously to Andros Island) the greatest concentration of dolomite should be found (the cryptalgal sediments of sample #2-19) are precisely those which contain no dolomite.

Type I dolomite is also found in rocks higher in the section than those that have been considered so far in this discussion on dolomitization. In sample #153, dolomite rhombs seem to be concentrated especially along microstylolites. Logan and Semeniuk (1976) and Wanless (1979) discuss the growth of dolomite rhombs associated with the development of microstylolites. There is, however, no dolomite associated with sample #2-19, which contains abundant microstylolites. Also,

there are numerous small dolomite rhombs scattered throughout the micritic portions of #153, unassociated with microstylolites, but identical in size and shape to rhombs that are associated with microstylolites. Therefore, the dolomite rhombs which are concentrated with microstylolites are considered to be simply stylocumulates.

Sample #24 is a skeletal wackestone/packstone containing abundant, relatively unabraded fossils interpreted to be representative of very shallow subtidal deposition (see page 46). Small, Type I dolomite rhombs are abundant throughout this sample, replacing both micrite and some skeletal fragments (such as ostracod valves) as well (Figure 27). Note that enclaves of relatively undolomitized micrite frequently remain within the interiors of fragments such as trilobite spines and ostracods.

Obviously, the dolomite in sample #24 could not have been the result of evaporative concentration withn a supratidal environment. Even for those sediments at Lost Creek that can be demonstrated to be supratidal there is poor correspondence between expected sites of dolomitization (using the Andros Island model) and actual occurrence of dolomitization. Given the scarcity of desiccation features at Lost Creek, other than rounded intraclasts in the lowermost portions (and, possibly, irregular fenestrae from intertidal sediments), it is even doubtful that sufficient evaporation could have occurred to propel a dolomitizing mechanism such as that proposed by Shinn et al. (1965) or Hsü and Siegenthaler (1969). (A Persian Gulf model of dolomitization is therefore totally untenable as well.)

The formation of the Type I dolomite in sample #24 requires the existence of a process which is not operative only at the depositional surface. Deeper dolomitization was once thought to demand a seepage

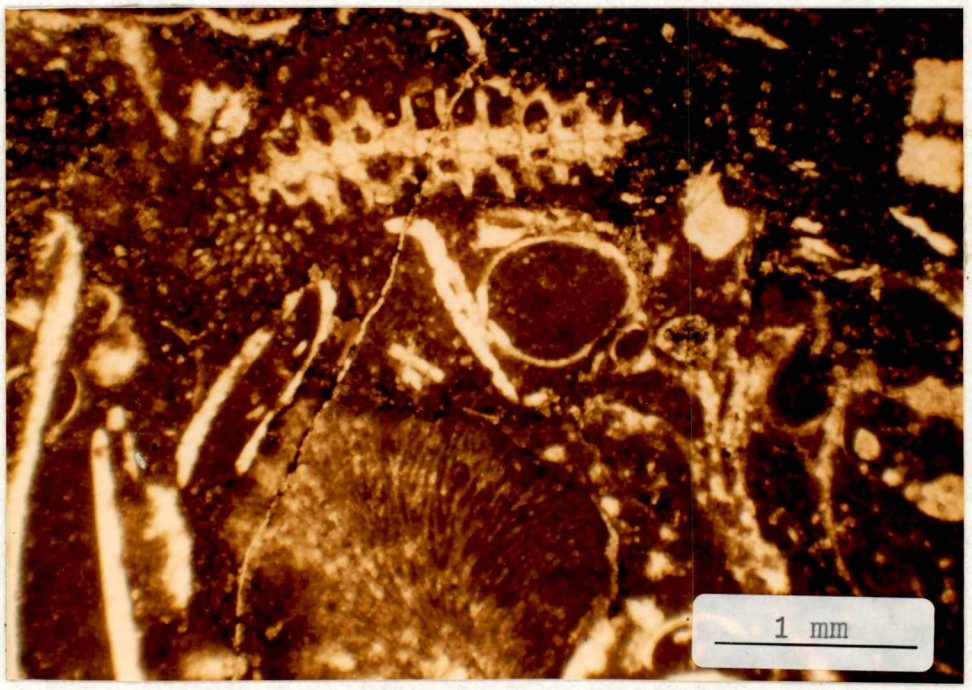


Figure 27. Skeletal wackestone/packstone, representing shallow subtidal deposition, that was partially dolomitized during Type I dolomitization. Note especially the many small rhombs in the upper right corner. Stained with potassium ferricyanide. Sample #24.

reflux circulation (Adams and Rhodes, 1960) such as that postulated for the island of Bonaire in the southern Caribbean (Deffeyes et al., 1965). Reflux is an easily understood concept, but is hydrologically unlikely and requires the precipitation of vast quantities of gypsum (Hsü and Siegenthaler, 1969; Land et al., 1975). Also, it has been demonstrated during later detailed study of the proposed modern example of reflux, Bonaire, that reflux may in fact exist only as a conceptual model (Hsü and Siegenthaler, 1969). Again, there is little evidence to suggest that the postulated conditions of intense desiccation, evaporation, and hypersaline waters necessary to produce a refluxing brine existed during deposition of the Dot sediments (see page 42).

Another recent model capable of fairly early diagenetic dolomitization, such as required at Lost Creek, is solution cannibalization (Goodell and Garman, 1969). While it is undoubtedly an operable process (Land et al., 1975), it requires the dissolution of considerable quantities of subaerially exposed limestones to produce dolomitization. The emergent Knox terrain consists wholly of dolostone near the Lost Creek area. Dolostone probably would not be subject to enough dissolution over the time interval necessary to dolomitize the nearby Dot sediments during diagenesis. The process, however, cannot be ruled out.

Gebelein (1977) has recently proposed another mechanism for the dolomitization of the Andros Island sediments, which, by analogy, may be applicable to the Lost Creek rocks. He suggested that the dolomitization is actually the result of subsurface mixing of high-alkalinity meteoric waters (derived from dissolution of carbonates and organic decomposition) with low alkalinity, high ionic strength sea waters. Dolomitization is massive and cuts across sedimentary facies boundaries. Beach

ridges act as the input areas for rainwater and serve as the localizing mechanism for the development of fresh-water lenses within the tidal-flat sediments.

Churnet (1979) concluded, based on trace element data, that both fine- and coarse-grained dolostones from Knox Group rocks of the Copper Ridge zinc district may have formed by a mixing of fresh and marine waters. He further suggested that the length of time of mixing may be the controlling factor of grain size. Other workers who suggested the possibility of dolomitization by mixing fresh and saline waters are Hanshaw et al. (1971), Land (1973), Badiozamani (1973), Folk and Siedlecka (1974), Folk and Land (1975), Plummer (1975), and Longman (1980).

Perhaps the dolomite of Type I at Lost Creek also formed as the result of the mixing of fresh and marine waters, apparently post-cementation but prior to the complete occlusion of porosity and permeability. As discussed previously, the emergent Knox terrain could have served as the input area for fresh water. Also, flushing by meteoric waters has been previously suggested as the mechanism for both cementation by sparry calcite and neomorphism in Dot sediments. A mixing hypothesis may explain why there is absolutely no dolomite in several samples from immediately above the Knox unconformity. Perhaps all marine water was simply flushed out of these sediments because they are so porous or because of their close proximity to the input area of the fresh water (if the mixing zone was operative quite early). Thus, the depositional environment influenced the formation of dolomite indirectly through the creation of <u>porosity</u> and <u>permeability</u>.

According to Murray and Lucia (1967), dolomite has a stronger tendency to replace rocks which were originally deposited as lime mud containing sand-sized particles (wackestone), or carbonate sand with interstitial lime mud (packstones) than to replace grainstones. Illing (1959) also emphasized permeability variations as the control for dolomite selectivity. He suggested that if cementation preceded dolomitization, the rocks that were most highly cemented (such as grainstones) were those least dolomitized.

Churnet (1979) reported that theoretical considerations involving the mixing of fresh and marine water demonstrate that dolomitization is possible for mixtures containing between 10-40 wt. % of marine water. Neomorphism of limestone is feasible for mixtures between 40-60 wt. % marine water. The general paragenetic sequence so far established for the Lost Creek sediments is: deposition formation of sedimentary pyrite cementation and neomorphism neomorphism Type I dolomitization. Considering that the sparry calcite cement observed in Lost Creek sediments requires essentially fresh water conditions, Churnet's theoretical calculations, and the above paragenetic sequence, it becomes apparent that the proposed Lost Creek mixing zone was subject to several fluctuations in relative percentages of fresh and marine waters.

A schematic representation of a typical mixing zone, where meteoric water mixes with marine water in a coastal setting, modified after Knauth (1979), is shown in Figure 28. Through time, with either overall transgression or regression, a wedge-shaped dolostone lens would be produced by this mixing zone.

Since only one small section was examined during this study, it was not possible to construct fence diagrams or facies cross-sections.

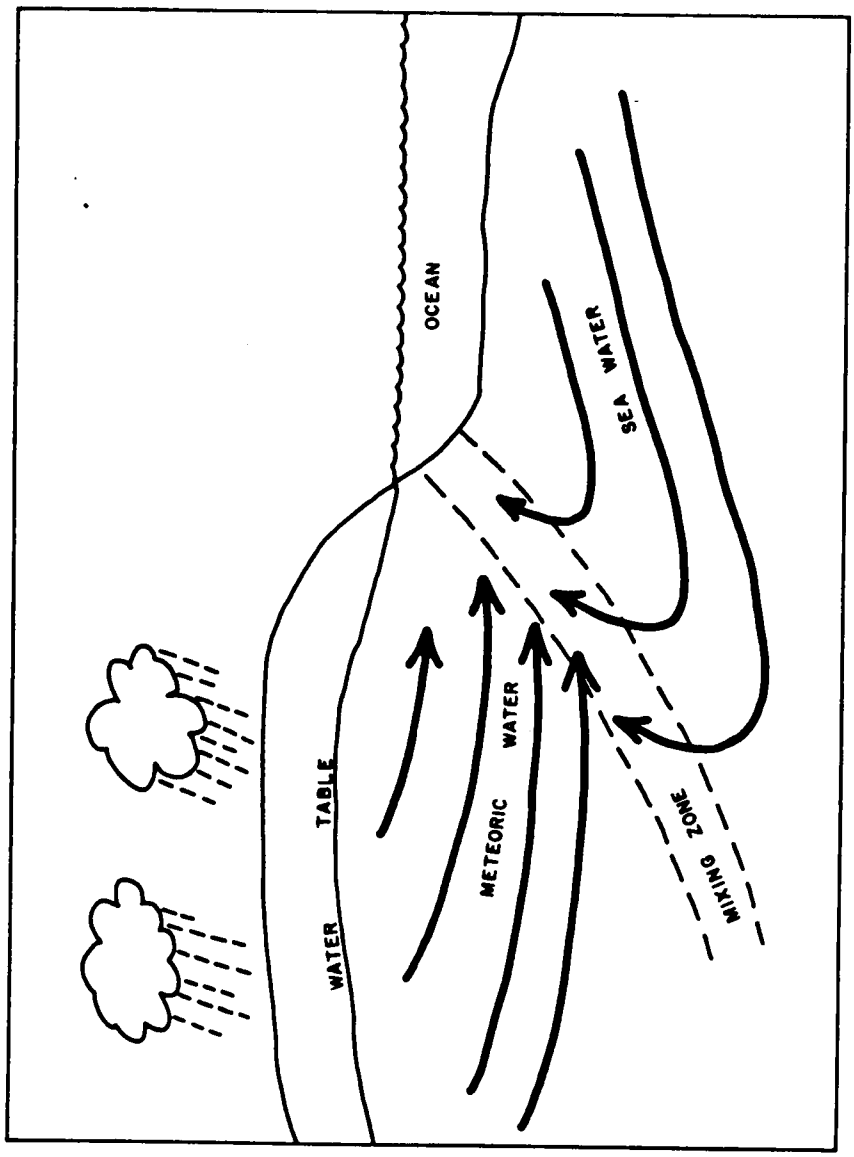


Figure 28. Schematic representation of a typical mixing zone in a coastal setting where meteoric water mixes with marine water. Modified from Knauth (1979).

It is therefore not possible to determine the geometric relationships between limestone and dolostone and whether an overall cross-cutting limestone/dolostone interface may exist, perhaps on a scale larger than discernible by study of 42 meters (140 feet) of section.

Finally, it should be noted that the samples from highest in the Lost Creek section (#C-3 and #C-4) comparable to the lowest (#2-19 and #2-13) contain almost no Type I dolomite. Perhaps by this time transgression had occurred to the extent that a near-shore mixing zone was too distant to produce dolomite in the sediments of #C-3 anc #C-4.

Type II dolomite. Type II dolomite is easily distinguished from Type I. Generally, Type II dolomite occurs in anhedral masses, seemingly ferroan throughout (based on staining), and exhibits sweeping extinction. Individual crystals within the masses range up to 500-600 microns in length. Type II dolomite crystals are sometimes zoned and often have cloudy centers. Although the origin of these cloudy centers is unknown, Sibley (1979) attributed similar cloudy centers in dolomite to molds and inclusions of calcite. Luminescence reveals that quite often even the anhedral masses (that appear ferroan throughout when stained) contain many growth zones (see later, page 103).

Type II dolomite may occur as discrete masses replacing micritic sediments. Usually, however, it occurs as a void-filling cement, generally associated with sparry calcite (see Figure 23, page 59). Type II dolomite is sometimes associated with neomorphic microspar (Figure 29).

Veins cutting both Dot and Mascot lithologies often contain Type II dolomite. In sample #6a, Type II dolomite heals a fracture that cuts a dolostone, composed of Type I dolomite, of the Dot

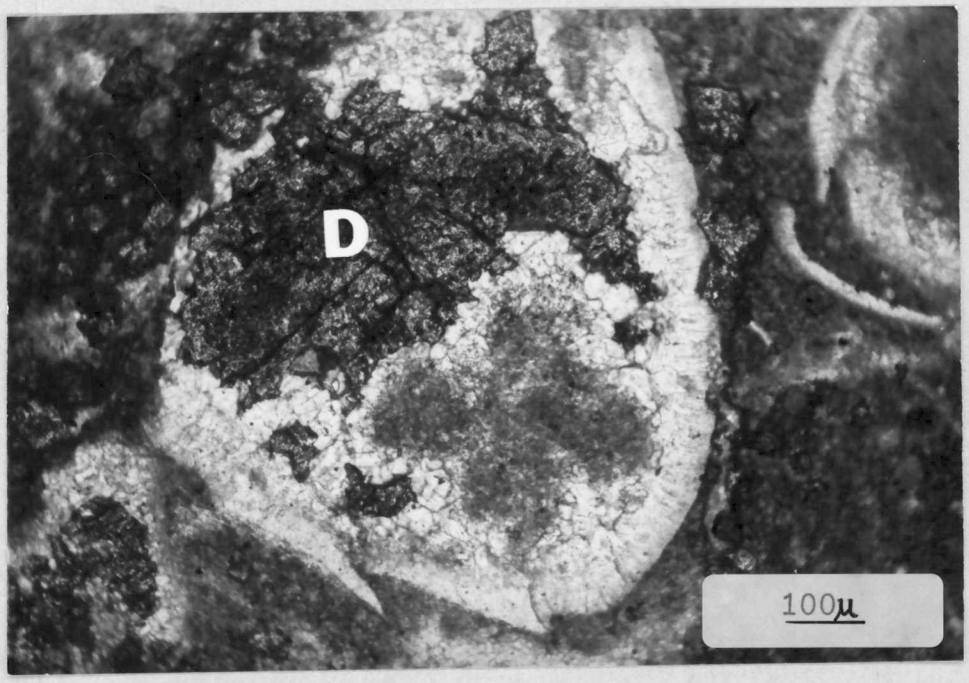


Figure 29. Type II dolomite (D) associated with and surrounded by neomorphic microspar that developed within an ostracod shell. Stained with potassium ferricyanide. Sample #29.

Formation. This indicates that Type II dolomite is later than Type I. Furthermore, the vein in sample #6a also contains barite, which links Type II dolomite with mineralization. The association of Type II dolomite with mineralization is considered further in the section on mineralization. For now, it is sufficient to realize that the ferroan dolomite was probably introduced with the ore fluid, and at some time after the introduction of all previously discussed postdepositional alteration materials.

Type II dolomite also occurs as a poorly defined dolomitization halo surrounding, as well as affecting, the central brecciated core of the Lost Creek deposit (see Figure 7, page 13, for the configuration of the dolomitization halo). The dolomitization halo forms a distinct dolostone lithology quite unlike the dolostone lithology that resulted from Type I dolomitization. The dolomitization halo is considered further in a later section (page 101).

As mentioned above, it appears that Type II dolomite is later than Type I. Figure 30 further supports this conclusion. A paragenetic sequence for this figure is easily discernible: deposition, with fossil debris (such as the ostracod shell depicted here) geopetal filling (note that this geopetal fill seems to be in two distinct layers, the earlier one containing Type I dolomite rhombs) sparry calcite cement, as a fringe on the inside of the ostracod valve as well as thinly covering the geopetal sediment ferroan Type II dolomite, probably penecontemporaneous with the sparry calcite that fills the rest of the void. This demonstrates there were at least two episodes of sparry calcite cementation following the formation of Type I dolomite (which itself

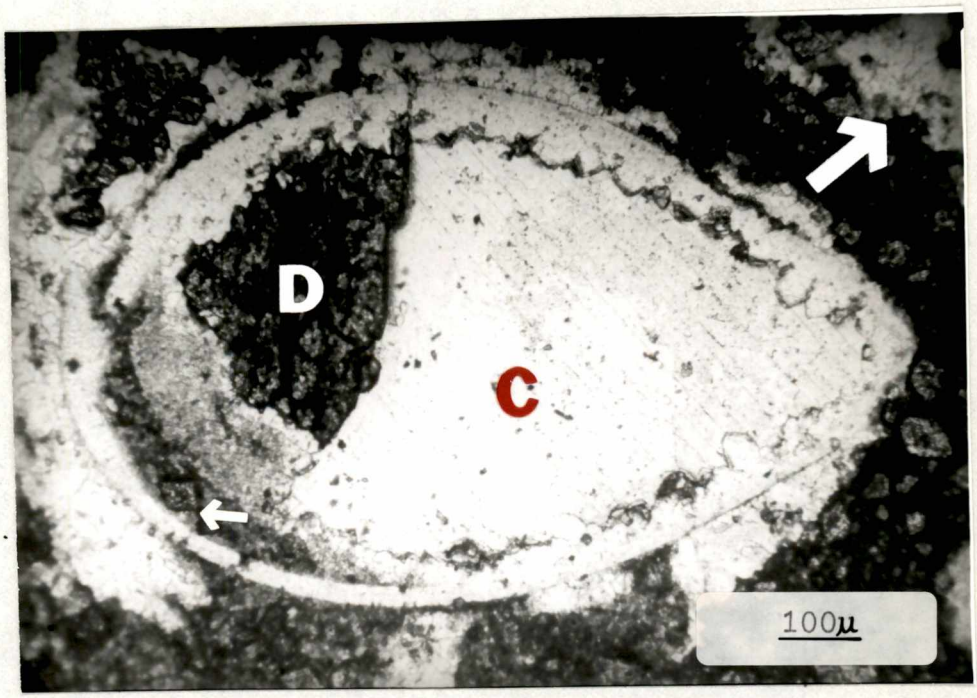


Figure 30. Ostracod shell from the Dot Formation. The paragenetic sequence for material infilling the shell is as follows:

1. Deposition.

2. First geopetal sediment, partially dolomitized by Type I dolomitization (small arrow points to dolomite rhomb).

3. Second geopetal sediment, undolomitized.

4. Sparry calcite cement as a fringe lining the inside of the ostracod valve and thinly covering the geopetal sediment.

5. Penecontemporaneous ferroan, Type II dolomite (D) and sparry calcite (C) cement which fills the remaining void space. Large arrow indicates stratigraphic "up." Stained with potassium ferricyanide. Sample #11.

followed an episode of cementation, see page 67). Type II ferroan dolomite is apparently temporally and spatially associated with the third episode of cementation.

In addition to filling the ostracod shell of Figure 30 the third episode of cement, consisting of intergrown Type II ferroan dolomite and sparry calcite, can also be observed filling irregular fenestrae (Figure 31), within molds of molluscan shells (Figure 24, page 61), and within irregular voids. These latter may be solution-enlarged molds of aragonitic shells which have been modified beyond recognition, or simply dissolution vugs.

Sometimes the third episode of cement consists of only ferroan dolomite, as observed in sample #26 within the living chambers of a coral (Figure 32). Similarly, a third episode of cement consisting strictly of sparry calcite may be present, as observed in other living chambers of the coral depicted in Figure 32. As mentioned previously (page 55), this late-stage calcite cement is sometimes ferroan. It may be that the ferrous iron in the ferroan calcite cements originates from the same source as the iron in the Type II ferroan dolomite, i.e., introduced with the mineralizing fluids.

It is possible that the void-filling ferroan dolomite is a replacement of void-filling calcite. There are, however, at least two reasons why this is unlikely:

1. Neal (1969) has published an order of susceptibility of some Pennsylvania carbonate constituents to dolomitization. The apparent order is mud matrix ferroan calcite sparry cement and bioclasts nonferroan calcite spar nonferroan calcite bioclasts. Considering

Figure 31. Irregular fenestrae cemented by both sparry calcite and Type II dolomite. Note that only the dolomite (D) fills the larger, irregular voids, whereas calcite (stained) generally fills thinner fenestrae connecting the larger voids. Stained with alizarin red S. Sample #19.

Figure 32. Colonial coral fragment showing two stages of cementation of corallite openings:

1. Fringe of sparry calcite.

2. Filling of central portion by either more sparry calcite or ferroan Type II dolomite (dark). Stained with potassium ferricyanide. Sample #26.

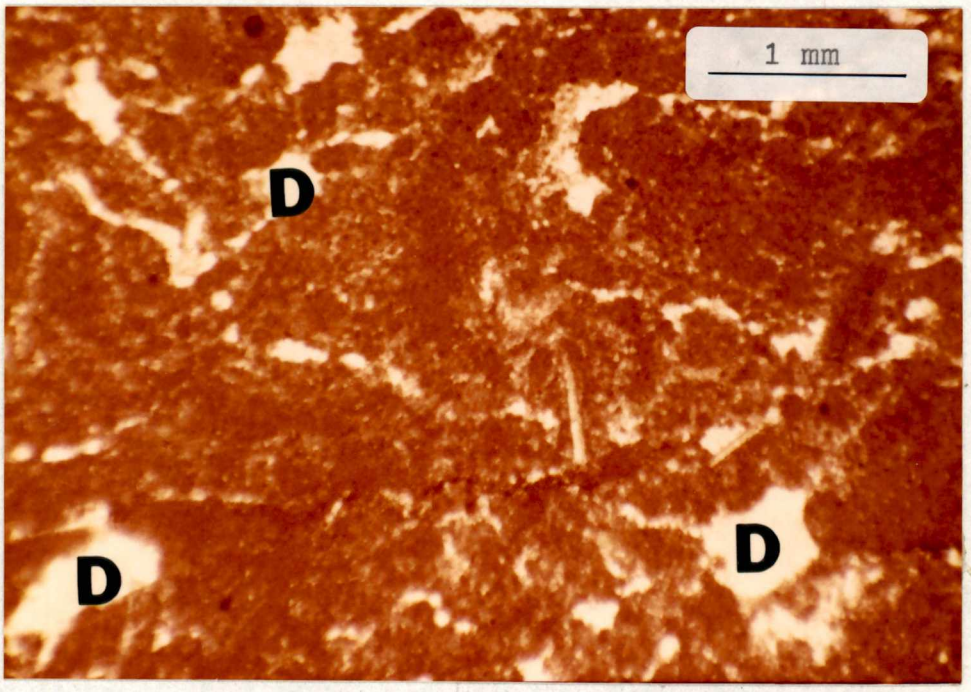


Figure 31

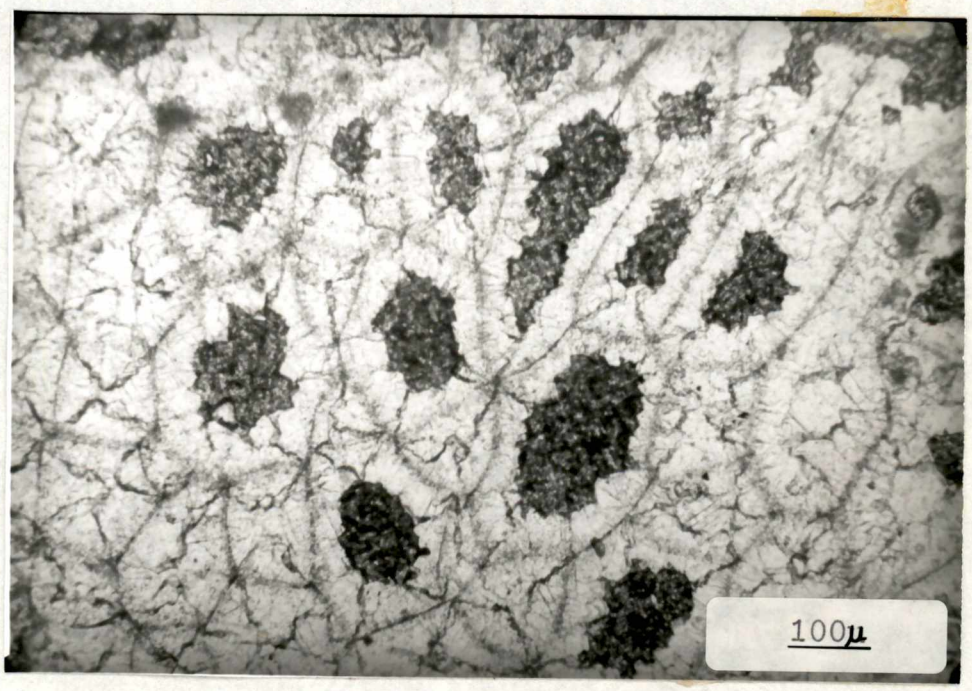


Figure 32

Neal's scheme, it is not likely that the ferroan dolomite would preferentially replace sparry calcite and leave most of the micritic portion of the rocks unreplaced.

2. The contacts between ferroan dolomite and sparry calcite are generally sharp. This is probably indicative of equilibrium conditions, maybe even co-precipitation (Churnet, 1979), and certainly not typical of replacive relationships.

The inconsistent relationships displayed by the third episode of cement, which may be composed of ferroan dolomite alone, calcite alone (sometimes ferroan) or a mixture of dolomite and calcite (sometimes ferroan) indicates that Type II dolomitization, like Type I, probably also resulted from a mixing of solutions. The fluids hypothesized to have produced Type II dolomite are mineralizing solutions and pore fluids that persisted through this stage of diagenesis [As demonstrated in the previous section on Type I dolomite, these pore fluids were themselves the result of mixing, presumably marine water with fresh water. Where extensive flushing by fresh water accompanied the earlier mixing, it is probable that the resulting formational fluids (later mixed with the mineralizing solutions) were largely fresh water also.] Lown (1978) hypothesized that similar inconsistent relationships between sparry calcite cementation and dolomitization indicated the mixing of two solutions.

The magnesium ions necessary for dolomitization may have been delivered to the site of dolomitization by the mineralizing fluids. It is also possible that the source of the magnesium was the formational waters, although ultimately derived from the carbonate aquifer. Bogacz et al. (1975) claimed that the passage of mineralizing solutions through

a dolostone aquifer (such as the Knox Group?) will lead to dolomitization by mobilization of and mixing with the ground waters of the aquifer. Although Bogacz et al. do not speculate on the geochemical mechanism that could produce the dolomitization, the important point of their model is that it recognizes the dual nature of the fluid responsible--part ore fluid and part formational fluid.

The timing and distribution of the ferroan dolomite is critical, considering its probable link with mineralizing fluids. The lowest stratigraphic occurrence of Type II dolomite within the Dot Formation is in sample #153 (see Figure 14, page 36). Type II dolomite is relatively scarce until the mudstones in the section are encountered (sample #11 is stratigraphically the lowest of these mudstones). There are several possible explanations for this distribution:

1. The Type II ferroan dolomite was simply not introduced until after deposition and cementation of the lower sediments of the section, whereas it was introduced before complete cementation of higher sediments.

2. Ferroan dolomite was introduced with mineralizing fluids, but these fluids simply did not migrate to the area of the deposit where Dot sediments stratigraphically below sample #153 occur (these are all core samples from DDH-2). However, this hypothesis suffers because bedrock samples containing ferroan dolomite are only a few meters away from DDH-2. In addition, sample #1, from the Mascot, contains Type II ferroan dolomite in fractures and was taken from an outcrop even further northwest of the deposit than the location of DDH-2.

3. The ferroan Type II dolomite is essentially late diagenetic with reference to all portions of the Dot stratigraphic section. This

may explain why Type II dolomite is never found as an interallochem cement. Interallochem cements are considered to be early diagenetic and comprise the first discernable episode of cementation in the Dot sediments (see the prior section on cementation). As an example, sample #55, an intraclastic grainstone (see Figure 14, page 36), contains only calcite as interallochem cement, even though it is surrounded (both stratigraphically and geographically) by rocks containing abundant void-filling ferroan dolomite cement.

The absence of ferroan dolomite in samples from stratigraphically below sample #153 is probably the result of an absence of voids that remained open beyond the first episode of dolomitization (Type I). One might ask why the fenestrae of sample #19 (see Figure 31), for example, were not similarly completely cemented prior to the introduction of ferroan dolomite.

The fenestrae of sample #19, however, are not cryptalgal features (see page 46), like those of sample #2-19, and perhaps did not even open until after early diagenesis. Also, a close microscopic examination of these fenestrae shows that generally the ferroan dolomite fills areas within fenestrae where the fenestrae open into wider, irregular shapes. This indicates that the narrower portions of the fenestrae were cemented, perhaps by the first episode of calcite cement, prior to the introduction of ferroan dolomite.

Based on the above discussion, Type II dolomite is considered to be later diagenetic, i.e., post-lithification and post-Type I dolomitization, and associated with mineralization. The actual timing is unknown; however, the absence of internal sediment in shell molds

(formed after cementation, see page 60) such as depicted in Figure 24 (page 61) indicates that the ferroan dolomite cement was precipitated shortly after the creation of the void.

Dedolomitization

Experimental work (DeGroot, 1967) has shown that three conditions must be met for effective dedolomitization:

1. A high rate of water flow capable of removing Mg^{++}, thereby keeping the Ca^{++}/Mg^{++} ratio of the water constantly high.

2. A carbon dioxide partial pressure somewhat less than 0.5 atmospheres.

3. Temperatures not greater than $50^{o}C$.

The last two conditions indicate that dedolomitization is a near-surface process often attributable to weathering phenomena (Mossler, 1971). At Lost Creek, dedolomite is associated with calcite fractures that cut ferroan void-filling dolomite cements. Limonite is intimately associated with the dedolomite. Evamy (1963) explained a similar association of dedolomitization of ferroan dolomite and limonite by hypothesizing that during the dedolomitization process excess ferrous ions would be expelled from the dolomite lattice and re-precipitated as colloidal hydroxide. Apparently, ferrous iron, because of its ionic radius, can substitute for magnesium ions in dolomite more readily than it can exchange for calcium ions in calcite. Eventually, the colloidal ferric hydroxide will "age" to limonite. The limonite will either permeate the newly formed calcite crystals (Evamy, 1963) or accumulate as films and clotted amorphous aggregates at grain boundaries (Wolfe, 1970). Only the latter mode of occurrence is seen at Lost Creek.

The general timing of the formation of this dedolomite can be estimated. Cross-cutting relationships indicate that the calcite veinlets with dedolomite are younger than all other diagenetic features, with the exception of stylolites. Since dedolomitization is a near-surface process, but because this dedolomitization is older than stylolitization, it could not have occurred during the present erosional interval. Dedolomitization is inferred to have occurred prior to the accumulation of a thick sequence of sediments during the initial depositional and diagenetic interval. The relative timing of the calcite veinlet itself is also established by this line of reasoning.

Dedolomitization that may be associated with recent weathering is also found at Lost Creek. Calcite, with associated limonite (see above), has replaced vein-filling Type II dolomite along cleavages and crystal boundaries. This mode of occurrence can be observed in veins from both the Dot and Mascot outcrops.

A final point of interest is that one of the conditions necessary for dedolomitization, namely a high rate of water flow, is exactly what might be expected under the mixing-zone conditions hypothesized to have existed during Dot sedimentation and diagenesis.

Silicification

Several examples of minor silicification were noted during this petrographic study. Silicification of carbonate can be observed in sample #25 (Figure 33). Lutecite (see Wilson, 1966) has replaced a portion of a coral fragment. Because the lutecite contains several small relict calcite inclusions, the silicification must have been post-cementation (i.e., post-precipitation of sparry calcite in living

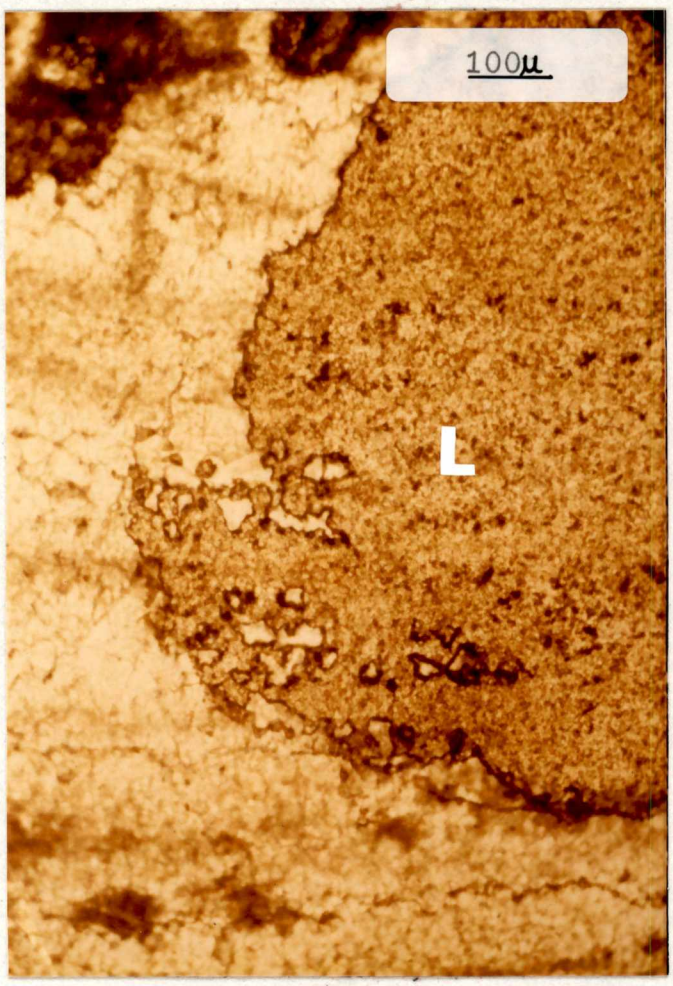


Figure 33. Partially silicified coral fragment. Formation of lutecite (L) was post-cementation. Sample #25.

chambers, which is a 3rd-episode cement). In areas of silicification where Type II dolomitization has occurred, these calcite inclusions may be replaced by ferroan dolomite. This relationship clearly establishes the timing of silicification as post-third-episode calcite cementation and pre-Type II dolomitization. The possibility of more extensive, selective replacement of sparry calcite by ferroan dolomite, previously discussed on page 84, is also indicated.

Silicification related to mineralization has not been observed at Lost Creek during this study.

Calcite Veining

Misik (1971) listed the processes which may lead to development of calcite veinlets in carbonate rocks:

1. Mutual withdrawal of discrete blocks of bedrock.
2. Mutual approach or compression of blocks.
3. Lateral shifting of bedrock blocks.
4. Recrystallization.

The scope of the present study renders determination of the processes involved in the formation of calcite veins at Lost Creek tentative in most cases. However, a determination of origin is not required for a discussion of the age relations of the veinlets relative to the overall diagenetic sequence.

Calcite veinlets, based on intersecting relationships, are generally younger than all other diagenetic features except for stylolites. Dissolution accompanying the stylolitization causes an offset to develop in veins transected by a stylolite. Sometimes, however, a calcite vein, especially a relatively thick vein, may cross-cut a relatively thin

stylolite. The offset along the stylolite indicates that formation of the veinlet was post-stylolite and caused by lateral shifting.

Calcite veinlets, presumed to be related to brecciation and mineralization, can be distinguished from other veinlets. Veinlets associated with brecciation and mineralization are irregular in shape and maintain irregular boundaries with the host rock. They are often quite thick (up to several cm) and may contain other minersls, such as dolomite, pyrite, and barite. The irregular boundaries are inferred to have resulted from vein filling prior to complete lithification of the host rocks. Alternatively, these boundaries may indicate that dissolution was active. In several samples, vein-filling calcite (or barite) seems to merge with adjacent calcite-cemented fenestrae in the host rock.

Calcite veinlets not associated with mineralization are generally thinner, with sharper host-rock boundaries, and contain no other minerals. Timing of these veinlets was probably after complete lithification, based not only on the sharpness of the vein boundaries but on the occurrence of associated micro-breccias that exhibit very angular "breccia blocks."

That these other veinlets are unassociated with mineralization is further demonstrated by their occurrence in sample #C-3, which was presumably well removed from the area of influence of brecciation associated with mineralization (see Figure 8, page 16). In addition, these other calcite fractures generally occur in subparallel swarms, and intersect bedding at approximately 30^{o}. These features suggest that such veinlets may be related to late Paleozoic tectonism.

Stylolitization

The timing and processes responsible for the formation of stylolites are matters of some disagreement (Park and Schot, 1968; Bathurst, 1975, pages 468-473). At Lost Creek, stylolitization is inferred to have been generally later than all other diagenetic processes (with the exception of weathering phenomenon, although these are not usually considered diagenetic) based on cross-cutting relationships.

In Sample #2-19 areas of sparry calcite cement are truncated against microstylolites. Microstylolites also outline the margins of sparry areas, indicating that spar is relatively less susceptible than micrite to dissolution during stylolitization.

The relationships and timing of calcite veining and stylolitization have been discussed in the previous section on calcite veining. The main point of the discussion is that a few calcite veins post-dated presumed early stylolitization. Stylolitization was probably a long-lived process, beginning in late diagenesis and persisting for an unspecified time after lithification.

Occurrence of Non-Framboidal Pyrite

Pyrite occurs in several other morphologies and associations besides framboidal. Discrete, subhedral to euhedral crystals, up to 1 mm in diameter, are found disseminated in several samples. Most large pyrite crystals are clearly post-Type II dolomite, although others seem to predate Type II dolomite. The relatively large size and inconsistent relationships to Type II ferroan dolomite indicate that these scattered pyrite crystals may be related to mineralization. Other pyrite, definitely associated with mineralization in veins and as breccia matrix, will be discussed in a later section on mineralization.

Summary of Diagenesis

The paragenetic sequence for the diagenetic events discussed in the previous section is summarized in Figure 34. Note that mineralization is considered a diagenetic event. Mineralization will be discussed in the following section of this paper. The band representing the span of mineralization in Figure 34 will be expanded in the next section so that individual events associated with mineralization can also be placed into a paragenetic sequence.

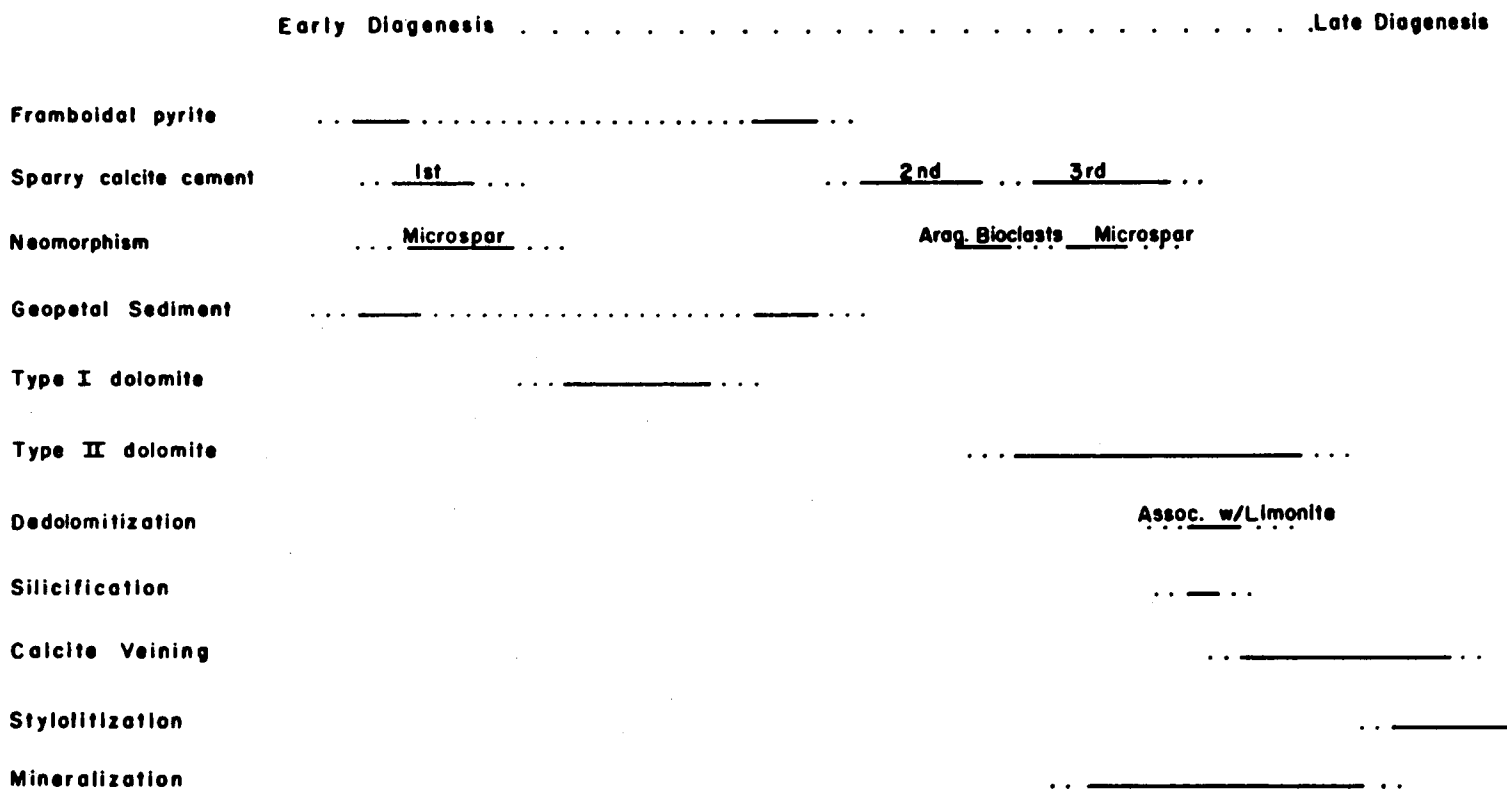


Figure 34. Paragenetic sequence of diagenetic events affecting Lost Creek sediments (Dot Formation only).

CHAPTER IV

MINERALIZATION

Introduction

Certain aspects of the Lost Creek mineralization have been mentioned briefly in previous sections. This chapter deals with the subject directly, and will consider the following topics:

1. Morphology and occurrence of barite, including its relationship to other minerals, including sulfides, precipitated by the mineralizing fluids.

2. Relationships and textures exhibited by sulfide minerals, including sphalerite, galena, pyrite, marcasite, and chalcopyrite.

3. Paragenesis, largely a synthesis of 1 and 2 above.

4. Origin and timing of the brecciation with which the mineralization is associated.

5. Nature of the ore fluid, and possible mechanisms of transport and precipitation of ore minerals.

Barite Mineralization

Veins

At Lost Creek, barite is the most abundant mineral in veins and fractures associated with brecciation and mineralization (see page 94 for criteria distinguishing ore-associated fractures from non-ore associated fractures). It was suggested (page 94) that the sediments of the Dot Formation were not completely lithified at the time of

fracture filling. Furthermore, cross-cutting relationships (see page 21) indicate more than one episode of fracturing and subsequent filling of fractures.

Multiple episodes of fracture filling may account for the variable mineralogy observed within the fractures. In a general paragenetic sequence the first mineral to precipitate within veins was ferroan, Type II dolomite (see pages 80-89). The dolomite occurs as relatively small, scattered crystals adjacent to the walls of veins. Thus, barite mineralization was preceded by Type II dolomitization. Type II dolomite includes not only fracture filling such as described above, but also void filling of all sorts (see pages 84-87), recrystallization of Type I dolostones, and dolomitization of limestones. The two latter processes will be discussed below.

Initial calcite precipitation followed Type II ferroan dolomite and preceded barite deposition. Open-space growth of barite resulted in bladed grains with sharp crystal face terminations. Calcite is also found filling the last voids that remained in the centers of veins after barite deposition. In hand specimens, the late calcite is recognized by its distinctive dark bluish gray coloration (Figure 35). Ferroan calcite that is sometimes observed in the small irregular voids between barite blades may be even later than the dark calcite. Precipitation of iron sulfides (intergrown pyrite and marcasite) generally followed barite deposition prior to late calcite precipitation.

Some veins depart from the paragenetic scheme outlined above and consist only of barite, or barite and calcite, or almost entirely of calcite. These may have opened after initial precipitation of Type II dolomite in earlier formed fractures. Other veins consist only of

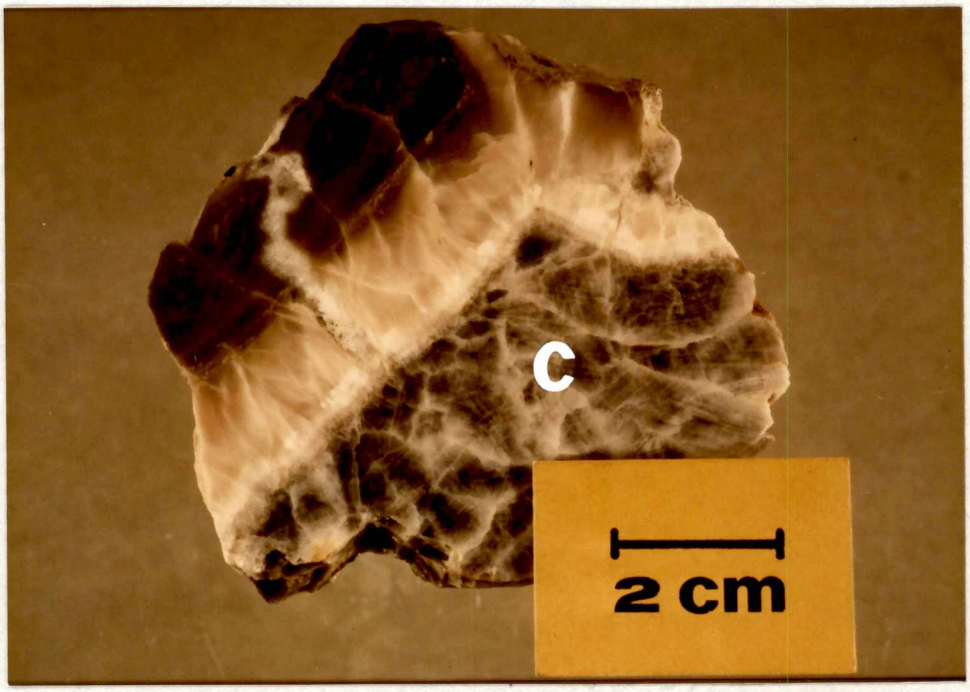


Figure 35. Hand sample of barite vein showing distinct dark coloration of associated late calcite (C). Note also the color banding of the barite--grayish brown (earliest), pink, and white (latest).

Type II dolomite, or dolomite and barite minus calcite. Rarely, Type II dolomite may be observed with dark calcite in the centers of veins.

These associations are difficult to explain based on timing of fracturing and fracture filling alone. Perhaps the mineralogy of veins reflects a local derivation of the Mg^{++} of the ferroan dolomite and the Ca^{++} of the calcite vein fillings. On microscopic and macroscopic scales proportions of dolomite and calcite in veins tend to reflect host-rock composition. In veins developed in limestone, calcite generally predominates over dolomite, whereas ferroan dolomite is the sole carbonate constituent of veins found in dolostones of both the Mascot and Dot Formations. Perhaps the timing of fracturing and host-rock composition together control the composition of vein fillings. In addition, variables of the precipitating environment, such as pH or Eh, or compositional differences of the ore fluid over short lateral or vertical distances might also lead to mineralogical variation of even penecontemporaneous vein fillings.

Replacement Barite - Dolomitization Halo

At Lost Creek, barite also occurs as a replacement of Type I dolomite associated with a dolomitization halo of Type II dolomite. A brief discussion of the halo is therefore necessary at this point.

Recrystallization of Type I dolostone and dolomitization of limestones has produced an irregular envelope of Type II dolomite around the deposit (i.e., around the breccia body, see Figure 7, page 13). Near the breccia body, especially to the north and northeast, the halo was formed largely by recrystallization of Type I dolostone. Figure 36 is a thin section of a dolostone from the halo northeast of the breccia

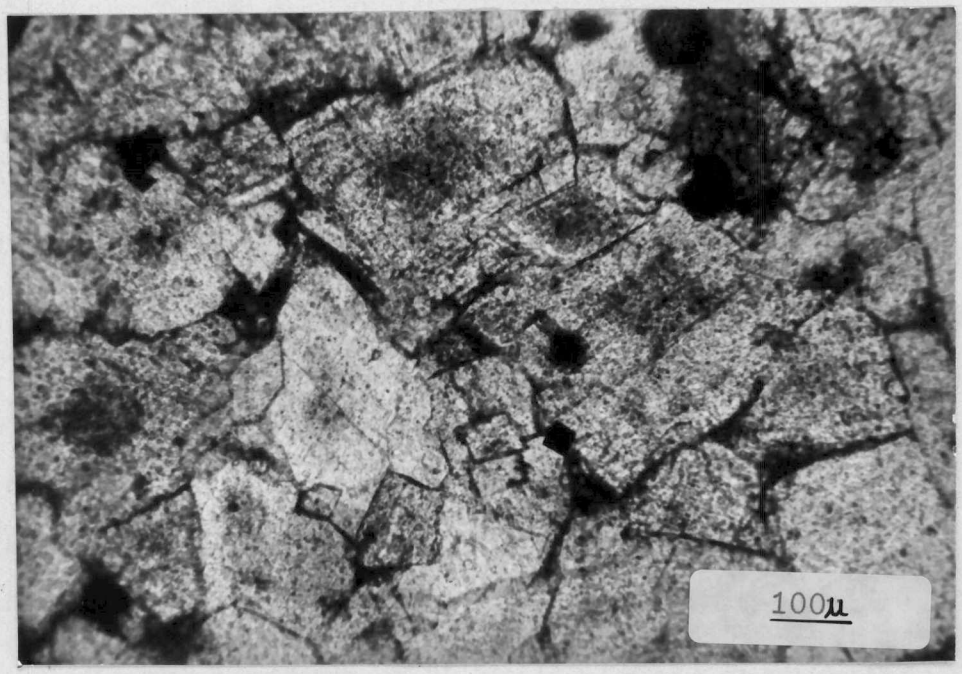


Figure 36. Dolostone from the dolomitization halo. This dolostone, composed of Type II dolomite, was formed by recrystallization of Type I dolostone. Sample #80.

core (sample #80). Relict Type I dolomite rhombs are visible within the larger, recrystallized, anhedral Type II dolomite grains under crossed nicols (Figure 37). Apparently, the recrystallization process did not involve complete dissolution of all precursor Type I dolomite rhombs. Preservation of the Type I rhombs within overgrowths of Type II dolomite is further clarified upon examination by luminescence. Figure 38 is a thin section of a Type I dolostone (sample #2-15). Note the single luminescent band, often parallel to crystal boundaries, which is associated with individual dolomite rhombs. The irregular edges of the luminescent bands may indicate non-equilibrium precipitation (Posey, 1976).

Type II dolostones, which formed by recrystallization of Type I dolostones, are also quite distinctive when using cathodoluminescence. Type II dolomite is characterized by many luminescent bands (Figure 39). These bands frequently cut across grain boundaries indicating co-precipitation (or co-recrystallization) of adjacent grains. Cathodoluminescence also reveals that many of the large, anhedral dolomite grains are overgrowths on smaller, Type I dolomite rhombs. These often form the core of the larger grains or occur as scattered inclusions.

The above interpretations are reinforced by comparison with Figure 40 which depicts vein filling Type II dolomite as it appears under cathodoluminescent light (sample #1, from the Mascot Dolomite). Note the many luminescent zones typical of Type II dolomite and the total absence of luminescent inclusions. Whereas open-space filling Type II dolomite (in veins or vugs) contains no inclusions, it is characteristic of Type II dolomite of replacement origin.

Figure 40 is also quite interesting because of the halo associated with veins of Type II dolomite. This effect, best developed in

Figure 37. Dolostone from the dolomitization halo (identical to Figure 36) with crossed nicols. Note the relict Type I dolomite rhombs which occur as inclusions within the Type II dolomite grains. Sample #80.

Figure 38. Appearance of typical Type I dolostone with cathodoluminescence. Note the single luminescent band, often parallel to crystal boundaries, which is associated with individual dolomite rhombs Non-equilibrium precipitation is suggested by the irregular edges of the luminescent bands. Sample #2-15.

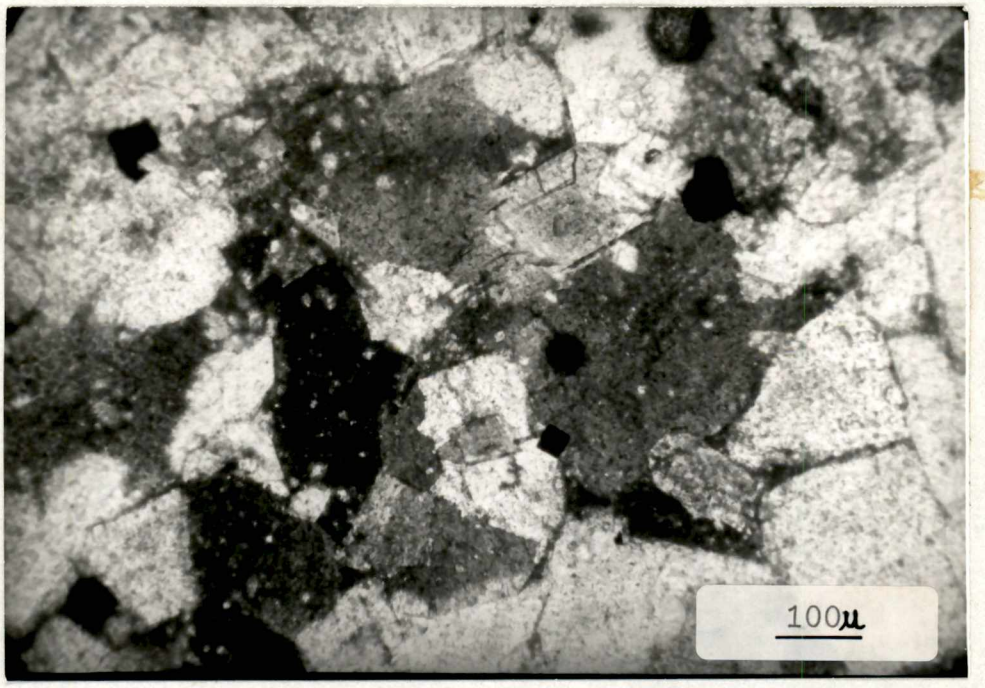


Figure 37

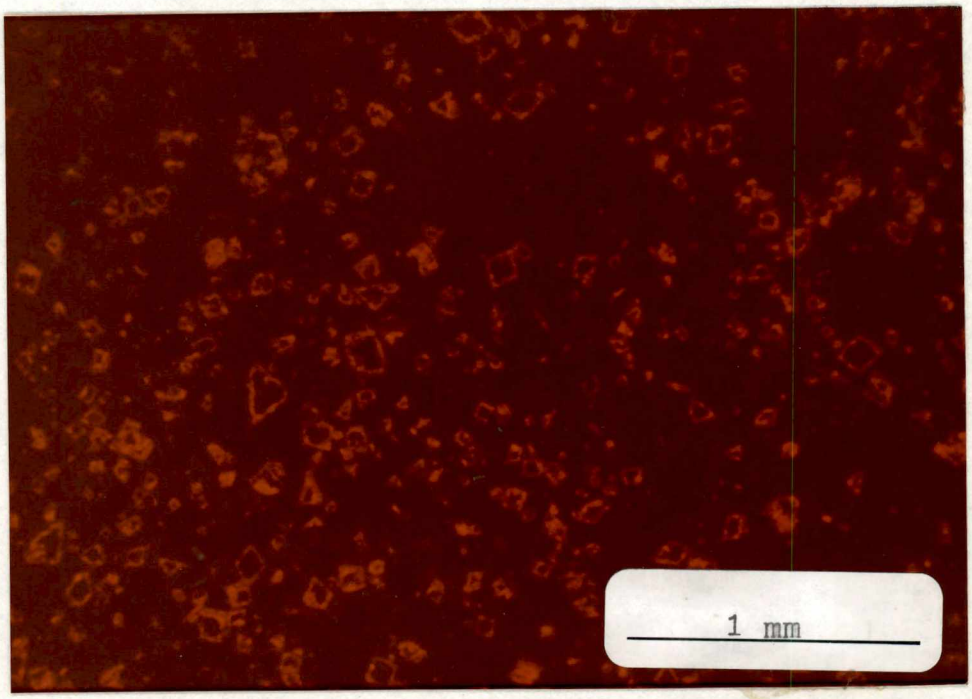


Figure 38

Figure 39. Appearance of typical Type II dolostone, formed by recrystallization of Type I dolostone, with cathodoluminescence. Type II dolomite is characterized by many luminescent bands. Note that relict Type I dolomite rhombs often occur as inclusions within and form the core of larger, anhedral Type II overgrowths. Sample #66.

Figure 40. Typical Type II vein-filling dolomite as it appears when using cathodoluminescence. Note the many luminescent zones typical of Type II dolomite and the total absence of luminescent inclusions. Sample #1.

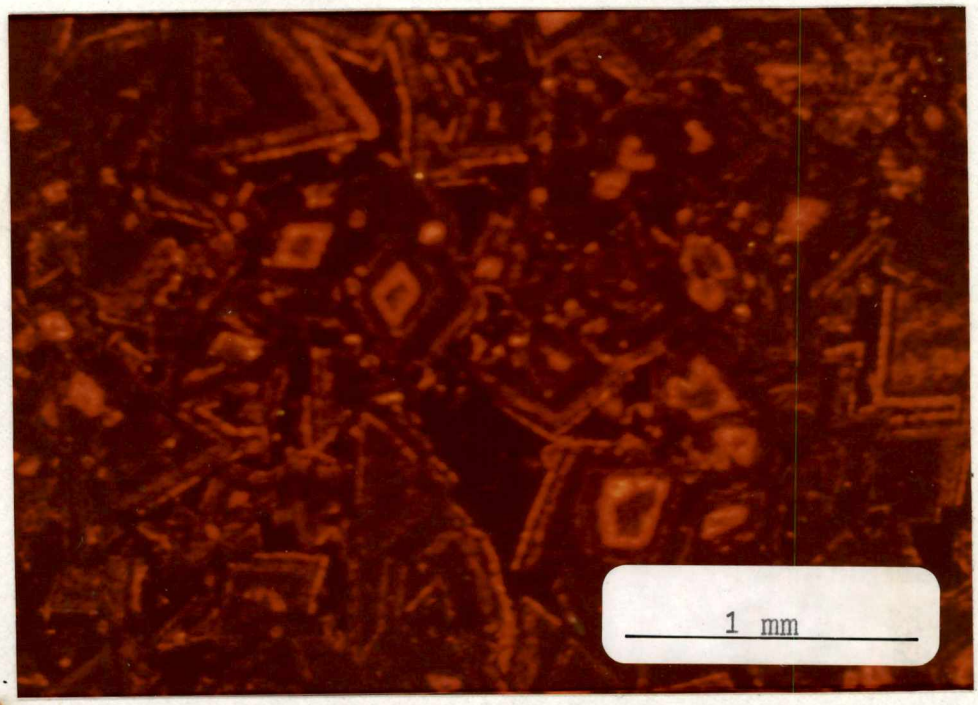


Figure 39

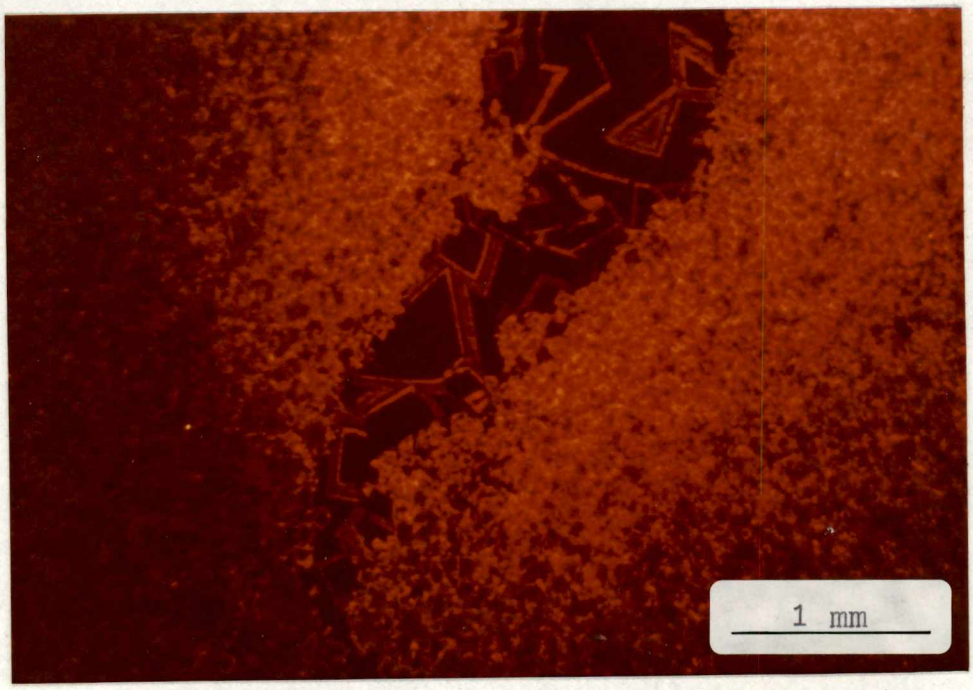


Figure 40

sample #1, indicates that the Type II dolomitization fluids were relatively enriched in a cathodoluminescence activator ion.

Preliminary work suggest that it may not be possible to correlate the cathodoluminescent banding of Type II dolomite. Occasionally, samples collected close together (within several meters, vertically or laterally) may exhibit similar luminescent banding. However, widely separated samples show no discernible patterns, differing greatly in the number of luminescent bands, relative band width, and relative intensities of individual bands. It may be that this is partly the result of comparing apples and oranges, i.e., vein filling Type II dolomite with Type II dolomite of the dolomitization halo, or with Type II dolomite cementing breccia fragments. The variety of modes of occurrence of Type II dolomite greatly complicates any efforts to determine a "dolomite stratigraphy" (see Meyers, 1974, and Ebers and Kopp, 1979) based on luminescent zonation, although it is precisely this variety which would render such determinations extremely valuable.

Typical replacement barite associated with the dolomitization halo is illustrated in Figure 41 (sample #78). A careful examination of the barite rosettes in sample #78 reveals that many of them contain small inclusions of Type I dolomite identical to the inclusions found within Type II dolomite of the halo. Several areas of the rock contain both barite and Type II dolomite, apparently as penecontemporaneous intergrowths replacing Type I dolomite.

An outlier of the dolomitization halo described above occurs east of the breccia body (see Figure 7, page 13). In that area of the deposit, dolomitization has affected sediments that were chiefly limestones. The line of demarcation separating relatively undolomitized

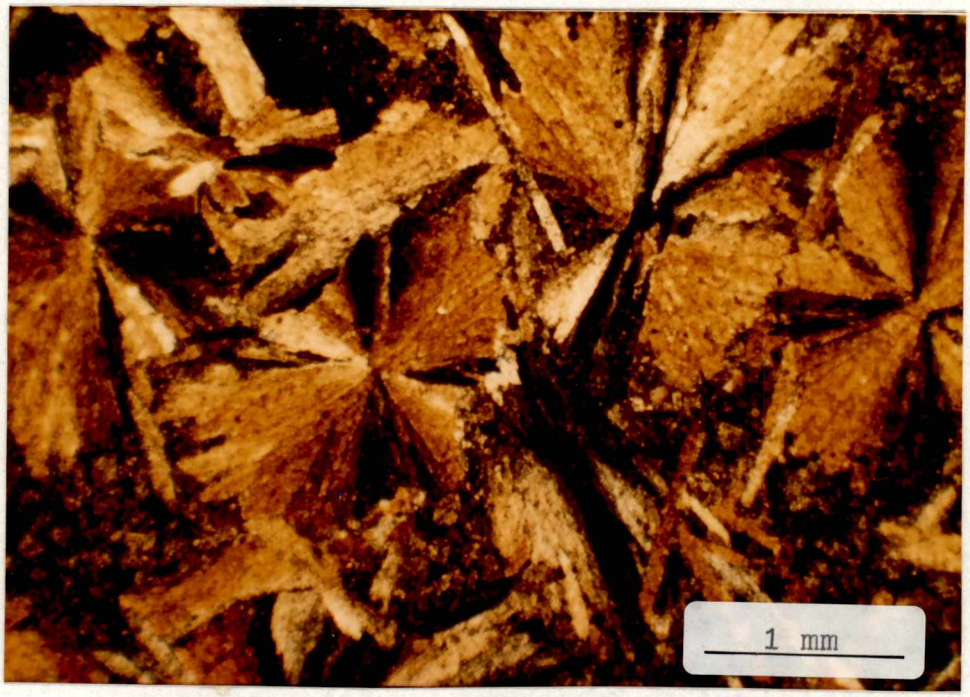


Figure 41. Replacement barite associated with the dolomitization halo. Relict Type I dolomite occurs both between barite rosettes and as inclusions within the rosettes. Crossed nicols. Sample #78.

limestone from Type II dolostone is sharp; samples of each can be collected just centimeters apart.

Barite, as irregularly scattered rosettes, may also replace undolomitized limestone. Replacement is strongly suggested by the numerous calcite inclusions found within individual barite needles of the rosettes.

Rocks of the Mascot Formation within the dolomitization halo have also been recrystallized. The process of recrystallization greatly increased the grain size of the dolomites, although very irregularly, and resulted in a mottled rock containing grains ranging in size from several microns to several hundred microns. Vugs are abundant and filled with jasperoid (see Lovering, 1972). Jasperoid appears whitish in hand samples but brown in thin section. It is probable that the jasperoid formed by mobilization and reprecipitation of silica originally found within the Mascot as chert. Thin stringers of barite can often be seen veining the vug-filling jasperoid.

Coarse, secondary dolomite, similar to the Lost Creek halo, is also found associated with the zinc deposits in east Tennessee. There it replaces limestone beds in the lower portions of the mineralized breccias [and can occur in a similar fashion unassociated with mineralization (Wedow, personal communication, 1980)]. Initial dolomitization is believed to be pre-ore (Hoagland et al., 1965; Hoagland, 1967) and has been ascribed to the same hydrothermal fluids which later became mineralizing solutions (Hill, 1969). Apparently, the earlier dolomitizing fluids at Lost Creek also became mineralizing fluids, based on the close timing of Type II dolomitization and barite precipitation (of which more will be said below).

Open-Space Filling Barite

Barite that was precipitated in the open space of veins has already been described (pages 98-101). Petrographic study has revealed several other modes of barite open-space filling.

Shell molds. Barite is found occasionally filling molds of shells, solution-enlarged molds of shells, and within the living chambers of shells (Figure 42), similarly to Type II, ferroan dolomite (see page 60). That both barite and Type II dolomite would precipitate as cement within shell molds is further evidence of their close paragenetic association. Furthermore, since the introduction of the Type II dolomite was a late diagenetic event, this mode of barite mineralization must have been a late diagenetic as well.

Solution-replacement of aragonitic molluscan shells has resulted in the baritization of many actinoceratoid cephalopod siphuncle segments (identified by Dr. Thomas Broadhead, University of Tennessee-Knoxville, 1979). Pyrite and silica (chalcedony and microcrystalline quartz) generally accompany the barite. These siphuncle segments are found scattered throughout the soil in a small area on the east side of the breccia body. Siphuncle segments also appear in relief on weathered outcrop surfaces from just above the Knox unconformity in this same area.

Associated with the breccia body. Barite, often as open-space fillings, is common within the breccia body at Lost Creek, especially in the upper portions of the structure. The open-space filling barite occurs as coatings around fragments of dolomite and as cement between fragments.

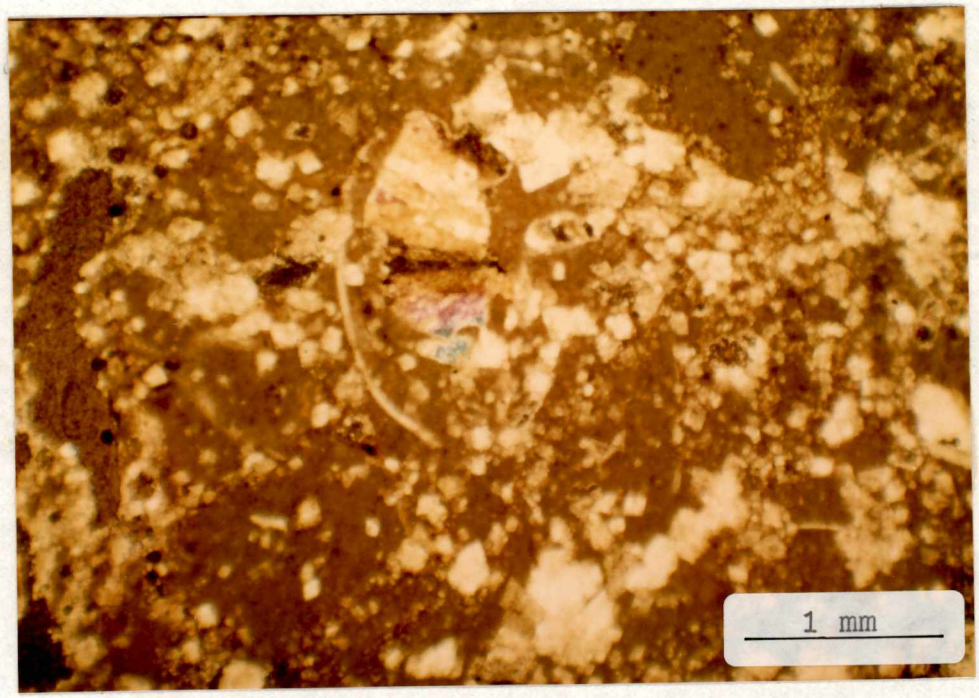


Figure 42. Barite found within the living chamber of an ostracod. The shell itself has been dissolved. Note the sharp truncation of the barite blades against the margins of the opening. Crossed nicols. Sample #77.

Barite coatings--Discrete fragments of both Type I dolomite and Type II dolomite as well as fragments containing both are commonly coated by barite (see Figure 6, page 9). Some of the dolomite, especially the finer-grained Type I dolomite, may be detrital. Scattered broken barite needles and sphalerite grains with ragged edges within the fragments may also be detrital. Some barite, Type II dolomite, and sphalerite, however, probably precipitated in place (such as the euhedral sphalerite grains that occur adjacent to ragged sphalerite grains).

The matrix between the barite-coated fragments (and non-coated fragments as well) appears to be almost identical to the fragments themselves, and indicates that brecciation was a long-lasting phenomenon of several generations and may have been pre-, syn-, and even post-ore. Brecciation pre-dating, contemporaneous with, and post-dating mineralization is a common feature of the east Tennessee zinc deposits (Hoagland, 1967). The dolomitic matrix of unmineralized east Tennessee breccias is believed to be poorly sorted clastic sediment produced by dissolution that accompanied brecciation (Hill, 1969). The detrital grains in the Lost Creek breccia fragments and matrix probably formed in a similar manner. In one sample (#1-19), clastic sphalerite has been subjected to sufficient abrasion to form rounded grains. Although dissolution might also produce rounded sphalerite grains, the textural relationships (sphalerite and dark clay swirled throughout the sample as matrix) suggest a detrital origin. Roedder (1971) suggested that the sudden collapse of a cavity during ore deposition could easily produce flow fast enough to severely abrade sphalerite in some vugs from east Tennessee zinc deposits.

Although there were apparently several generations of barite and sulfide mineralization, the bulk of sphalerite and galena deposition appears to be later than most barite. Figure 43 illustrates sphalerite that has precipitated as a coating on a barite fragment. Coatings of sphalerite are quite common around barite fragments from the portions of the breccia where sphalerite occurs in surface exposures (on the east side, near the localities of samples #169-177). The relationship of sphalerite following, and coating, earlier-formed barite is even readily determined from the outcrop. Sphalerite is also found as a coating around barite which is itself a coating around a lithic fragment.

Barite cement--Barite that occurs as a cement between fragments is more common in the Mascot portions of the breccia body, but only because of the rarity of this type of barite within the upper portions of the structure. This barite is invariably associated with very coarse (grain size of almost 1 cm) pink gangue dolomite. Both the dolomite and barite are distinctive. The dolomite, in addition to being pink and very coarse-grained, exhibits sweeping extinction and is ferroan throughout (shown by staining). Examination with the luminoscope reveals that the coarse pink dolomite is unzoned, or poorly zoned, and contrasts sharply with the multiple luminescent bands observed in typical Type II dolomite. Type II dolomite veinlets, complete with luminescent bands, are sometimes observed within breccia fragments which were later cemented by the pink dolomite.

Pink dolomite is a commonly observed gangue mineral in other Mississippi Valley-type districts, such as the Tri-State, and Copper Ridge districts (Hill, 1969; Leach, 1973). Hill (1969) reports that the pink dolomite is later than white dolomite gangue in the Copper Ridge

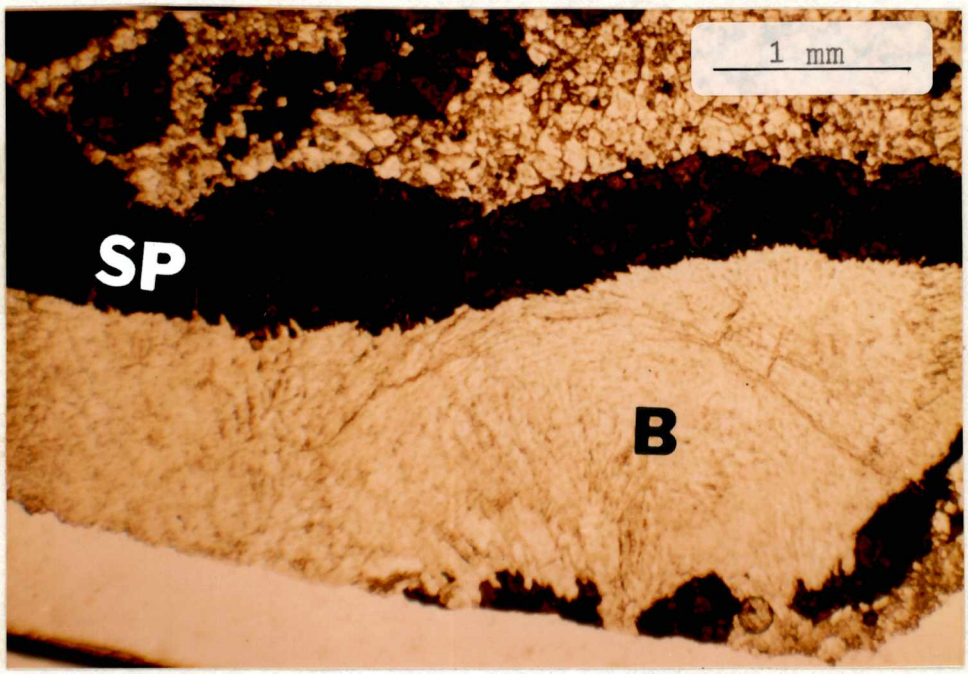


Figure 43. Sphalerite (SP) precipitated as a coating on a barite fragment (B). Sample #172.

District. It is probable that the pink dolomite at Lost Creek is also late, and perhaps should be designated as Type III dolomite.

The barite associated with the pink dolomite, as mentioned above, is also distinctive. It has precipitated in a curious feathery morphology (Figure 44). Based on laboratory synthesis of isomorphs of $BaSO_4$, curved, feathery barite dendrites may result from precipitation from very highly supersaturated solutions (Buckley, 1951). The abundant open space remaining within barite fronds is further evidence that this barite and associated pink dolomite were very late precipitates.

Pink dolomite and feathery barite always occur in the central portions of the voids created between breccia fragments. The paragenetic relationships of these minerals, compared to sulfides, is further evidence that they were the very last precipitates from the mineralizing fluids.

Where an initial crust of pyrite formed on a breccia fragment it was often followed by sphalerite and galena precipitation. These in turn were followed by the precipitation of intergrown pink dolomite and feathery barite.

The above sequence contrasts sharply with the previously demonstrated paragenetic relationships of (vein filling) barite and sulfides (page 99). Vein-filling iron sulfides (pyrite and marcasite) are always later than barite. In all thin sections and hand specimens of breccia material, pyrite, as well as sphalerite and galena, also appear to be later than barite (excluding feathery barite).

To summarize the discussion of mineralization to this point, petrographic examination aided by field exposures has proven that there

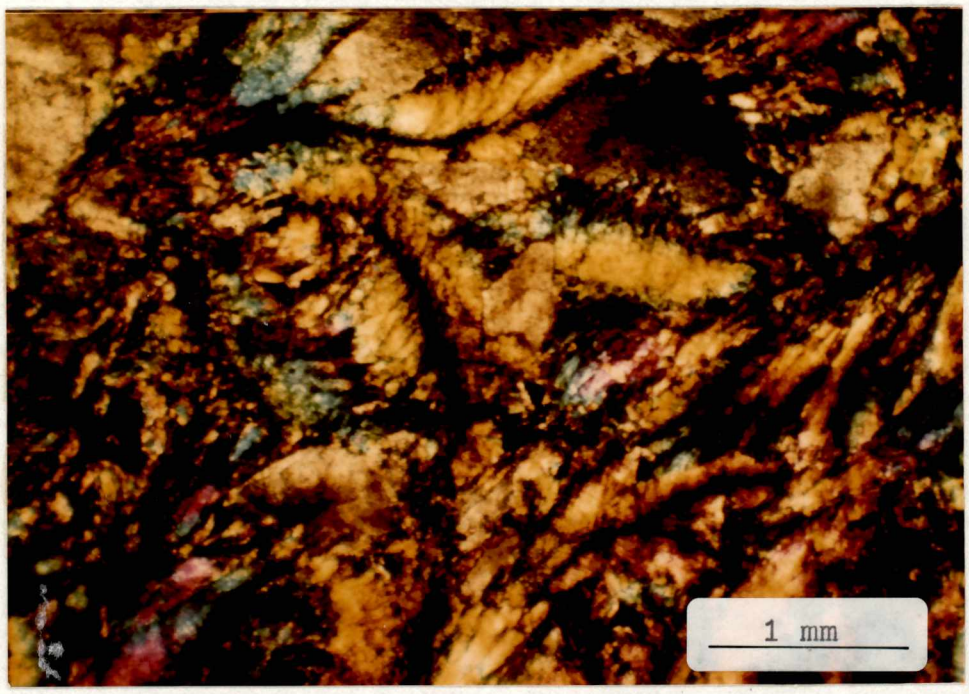


Figure 44. Feathery barite which occurs with pink, coarse-grained dolomite as late cement between breccia fragments. Crossed nicols. Sample #1-13.

were several generations of brecciation and mineralization at Lost Creek. A paragenetic sequence of events would include the following:

1. Dolomitization - Type I followed by initial Type II.

2. Brecciation, producing fragments of Type I dolomite, Type II dolomite, and mixtures of both.

3. Scattered barite and sphalerite precipitation.

4. Brecciation, producing additional fragments that sometimes contained barite and sphalerite. A detrital matrix of dolomite, barite, and sphalerite would have accumulated between fragments. It is likely that some of the scattered Type II dolomite, sphalerite, and barite actually precipitated within the detrital matrix.

5. Brecciation, producing fragments similar to those formed by the earlier episodes of brecciation, plus fragments of the detrital matrix itself.

6. Deposition of barite as coatings around any of the previously formed fragments.

7. Brecciation, producing fragments of barite from barite coatings that became separated from the lithic fragments they covered.

8. Precipitation of sphalerite as coatings around barite fragments and around barite that itself coated fragments, or on other lithic fragments.

9. Additional accumulation of detrital dolomite, barite, and sphalerite as matrix, probably accompanied by additional minor precipitation of these same minerals.

10. Late precipitation of pink (Type III) dolomite and feathery barite.

Although there is little doubt that the precipitation of these minerals marked the final pulse of mineralization, there is some uncertainty concerning the timing of the sulfides associated wtih the late dolomite and barite (see description on page 116). Are they, too, a separate late phase of (sulfide) mineralization? If so, that would imply another pulse of brecciation, needed to provide fresh rock surfaces for the sulfide precipitation. Actually, these sulfides can probably be correlated with sulfides associated with earlier-formed (non-feathery) barite, eliminating the need for yet another episode of brecciation.

The correlation is based on color banding, which implies a more limited number of generations of sphalerite precipitation relative to barite. Figure 45 shows the nature of the color banding of the sphalerite at Lost Creek. This sample (#170) is from an outcrop on the east side of the breccia body. The early sphalerite is dark in color, greenish and brownish. This was followed by orange sphalerite, which was in turn followed by light-colored sphalerite (generally pale-greenish or yellowish to almost colorless). Finally, the latest sphalerite is again orange. Compare this sequence to Figure 46 (sample #1-123) which depicts colloform sphalerite that precipitated prior to (and probably partly simultaneous with) feathery barite (visible in the interstices). Note that the sequence of color banding is similar to that shown in Figure 45, although the late orange sphalerite did not develop.

An energy-dispersive electron microprobe traverse (using a MAC 400-S microprobe available at the University of Tennessee-Knoxville) demonstrated that the Fe content of the sphalerite correlates with

Figure 45. Sphalerite color banding found at Lost Creek. Earliest sphalerite is dark in color, whereas the latest sphalerite is orange. Sample #171.

Figure 46. Colloform sphalerite which precipitated prior to (and probably partly simultaneous with) feathery barite (visible as white mineral in the interstices). Note the light-colored, euhedral sphalerite, precipitated last, that can probably be correlated with a similarly colored band in Figure 45. Sample #1-123.

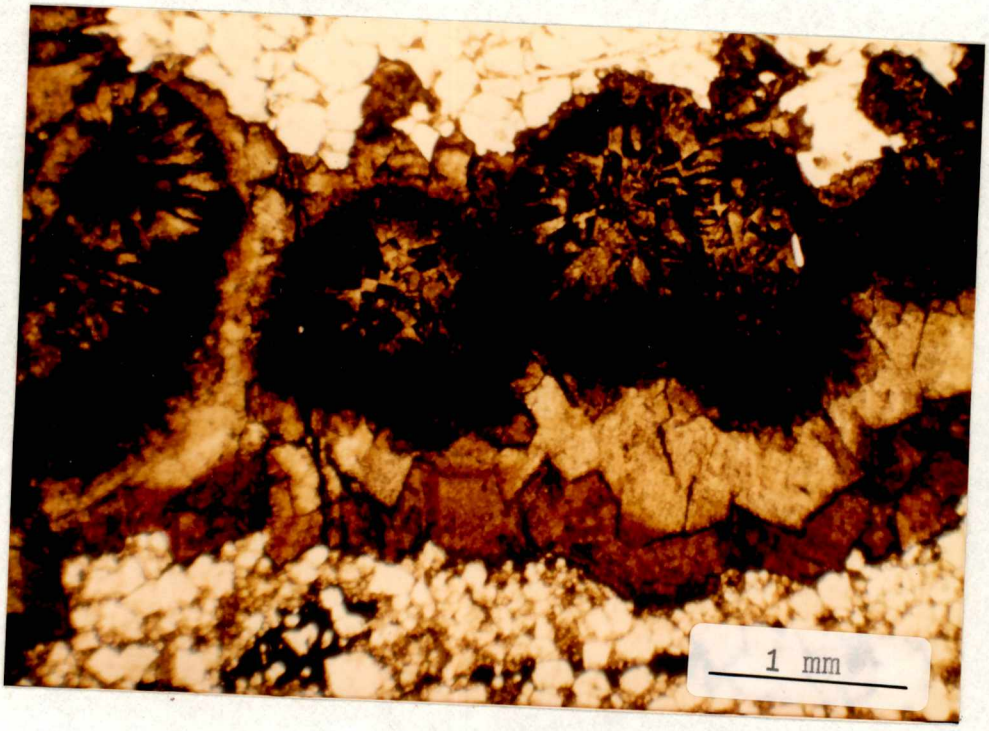


Figure 45

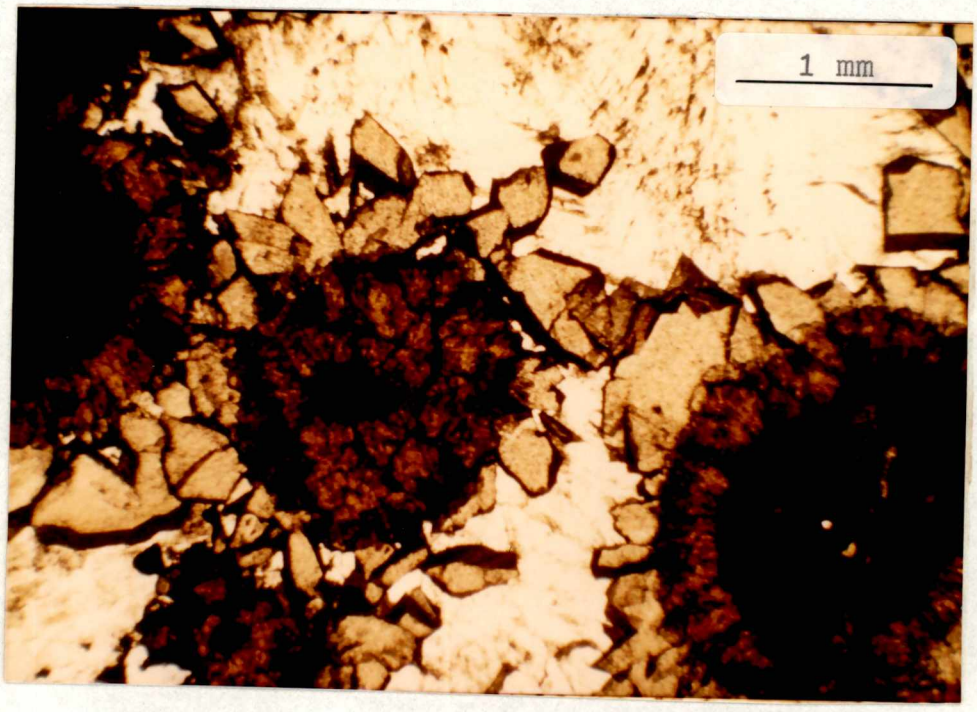


Figure 46

color, i.e., the Fe content is highest for the dark sphalerite whereas the light-colored sphalerite is practically Fe-free. This finding is in agreement with analyses by McLimans et al. (1968) who analyzed color banded sphalerites from the Upper Mississippi Valley zinc-lead district of southwest Wisconsin. However, Roedder and Dwornik (1968) found no correlation between iron content and sphalerite color banding in the Pine Point district, Northwest Territories, Canada.

Syngenetic Barite

Thin sections of Lost Creek breccia material include several examples of what may be syngenetic barite. Figure 47 (sample #168) depicts a layer of barite sandwiched between layers of intraclastic grainstone, which may represent channel deposits (see page 41). The barite blades and their orientation indicate open space growth upon the thin lime mud layer (now dolomitized by Type I dolomite) capping the lower intraclastic unit. The barite precipitation was followed by more lime mud and another surge of intraclastic material. Note the truncation of the barite blades which appear to have been broken off at the ends by the second pulse of mud and intraclasts.

Figure 47 illustrates only a small portion of the thin section made from sample #168. Barite veins that criss-cross the rock connect with the layer of barite shown in Figure 47 and indicate that the barite layer itself may be of vein filling origin. However, the morphology of the barite and its relationship to the sediment certainly argues for syngenetic precipitation. Syngenetic barite mineralization would be expected to have occurred prior to Type I dolomitization, as suggested

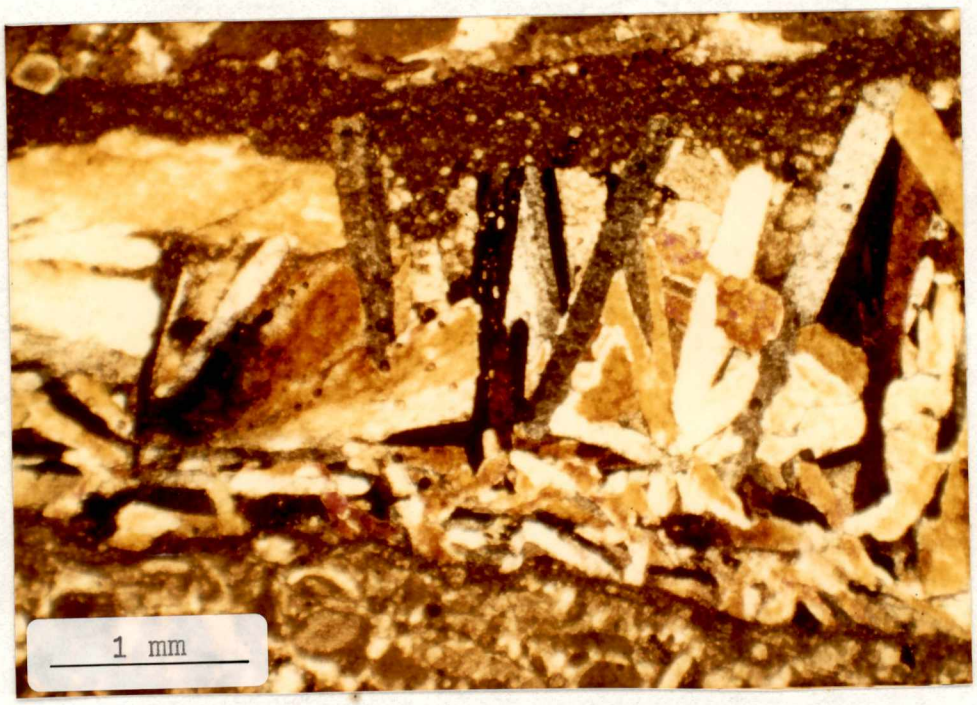


Figure 47. Possible syngenetic barite. See text (page 122) for explanation. Crossed nicols. Sample #168.

in Figure 47. This is in contrast to other barite mineralization found at Lost Creek which occurred after Type I dolomitization (see for example Figure 41, page 107).

Sample #168 was a grab sample found lying loose south of the breccia body. It may have originated considerably higher stratigraphically and perhaps represents an episode of syngenetic mineralization accompanying ore fluids that debouched onto the sea floor. Except for a few remnants, such as sample #168, most of the material recording these events would presumably have been eroded away by now. The timing of Type I dolomitization is tied to deposition and must occur fairly soon thereafter (see pages 67-80). Barite mineralization, on the other hand, ranging throughout a vertical, brecciated structure, could be epigenetic in the lower and central portions (i.e., in the Mascot Dolomite), epigenetic and diagenetic in the upper portions (i.e., in the Dot Formation), and syngenetic where mineralizing fluids escaped onto the sea floor (the record of this in the Dot Formation has been largely removed by erosion).

Additional evidence for syngenetic barite mineralization is provided by Figure 48. It depicts a large block of layered, dolomitized (by Type I dolomitization) sediment with a layer of barite that precipitated on top of the sediment (overturned in this photo). This block has been slightly warped, probably as the result of wrapping around the irregular mass of dolomitized sediment upon which the lens cap of Figure 48 rests. Note how the layer of barite itself has been disrupted and broken by this event which must have occurred during brecciation. Presumably the barite was brittle but the sediment it grew on was only partially lithified at the time of brecciation. A thin section of the



Figure 48. Barite occurrence suggestive of syngenetic precipitation. Thin section petrography has proven that barite growth was outward from the layered sediment. The entire breccia fragment has been overturned and warped, and the barite layer disrupted, by brecciation inferred to have occurred soon after deposition. Note lens cap for scale.

barite layer reveals that growth of barite blades was definitely outward (stratigraphically up, but because of overturning, down in Figure 48) from the layered sediment, and possibly syngenetic. Hemispherical upper surfaces were formed during the last stages of barite deposition when the mode of precipitation changed from relatively large blades to a mass of smaller dendritic crystals. The hemispherical structures show a thin layer of sediment capping, now dolomitized, as might be expected for syngenetic barite growing on the sea floor. These relationships indicate that not only did mineralizing fluids rise to the sea floor, but that brecciation itself may have stoped all the way to the water-sediment interface.

A thin section of another sample (#190) of bladed barite, which may also have grown syngenetically on the sea floor, reveals abundant detrital Type I dolomite and smaller broken blades of detrital barite filling the interstices between barite blades approximately 1 cm long. Some of the barite in the interstices, however, appears to be precipitated, based on the euhedral morphology and orientation perpendicular to the longer blades. Occasionally, the dolomite in the interstices will be recrystallized into larger, anhedral grains (Type II dolomite) and accompanied by iron sulfide precipitation.

It is possible that the proposed syngenetic barite described above was precipitated upon breccia fragments instead of on the sea floor. However, the flat layering of mud and barite and the growth of barite on only one surface indicates that precipitation was probably not on a breccia fragment. Actually, if brecciation extended to the sea floor, then the distinction between barite growth on the sea floor and upon a breccia fragment may become difficult if not meaningless, especially if collapse was minor.

Barite Color Banding

Barite, similarly to sphalerite, also exhibits color banding. Whereas the color of the sphalerite varies with the iron content, petrographic studies show that the color of the barite bands depends on grain size, morphology, and relationship to the host rock. The color banding is evident only in hand specimens, as it is a characteristic of aggregates of barite grains.

Dark, grayish brown, grayish red, or olive gray bands (see Figure 35, page 100) resulted from the intimate mixing of very small (as small as 50 microns) barite blades or small anhedral masses of barite with variable amounts of host rock, generally Type I dolomite. These textures, and hence color bands, can be observed both in samples believed to represent syngenetic barite growth in and on soft sediment as well as within veins where the host rock has been partially replaced along vein margins.

The morphology of pinkish barite (see Figure 35) is invariably fine-grained and dendritic. Laboratory work on synthetic crystals (Buckley, 1951) suggested dendritic growth may result not only from supersaturation (see page 116) but from inclusion of trace impurities also. Perhaps trace impurities are responsible for the pink coloration as well as the dendritic growth morphology.

White to almost clear barite forms relatively large blades characterized by open-space growth. Most of the barite observed within the breccia body is coarsely bladed white barite.

Generally, the darker bands were earlier bands and graded into the pink and white barite. The order of these later colors depended on the order of crystal morphologies of the barite. Often, the pink,

dendritic barite will follow the darker bands, and will in turn be followed by white, coarsely bladed barite. Sometimes, however, this order was reversed and large, white barite blades were followed by dendritic barite growth.

Wagner (1973) has attributed similar variations in barite type to different crystal growth rates caused by changes in the degree of supersaturation of the ore fluids. He suggested that a gradual increase in the degree of supersaturation should accelerate the rate of crystal growth, which will cause an increase in number but a decrease in the size of the barite crystals. Curved, feathery barite associated with pink dolomite (see page 116) represents growth under the highest levels of supersaturation, and perhaps can only form when the supersaturation attains a certain level thereby initiating a sudden increase in the number of crystals being formed due to spontaneous nucleation (Wagner, 1973).

Barite morphology in hand specimens probably reflects the degree of supersaturation of the ore fluid also. Generally, the barite is found as aggregates of fine to coarsely crystalline thin-bladed crystals. Blades range from less than 1 mm in length to over 1 cm, although within a given sample the crystal size of the barite is fairly uniform. The size of the barite blades is presumably related to the degree of supersaturation of the mineralizing fluid.

Hemispherical or mamillary aggregates, based on thin section petrography, are formed by dendritic barite growth. This type of barite aggregate probably represents precipitation from an ore fluid more supersaturated than that which produced the bladed barite.

Using cathodoluminescence, barite will occasionally luminesce. The luminescent color is invariably light blue, although the intensity varies from faint to quite bright. The luminescent intensity, or lack of luminescence altogether, does not seem to correlate with any other observed properties of individual barite crystals or aggregates. In fact, brightly luminescing barite may occur adjacent to blades that do not luminesce.

Sulfide Mineralization

The record of sulfide mineralization at Lost Creek is similar to the sequence of diagenesis and barite mineralization in its complexity. Sulfides that occur are pyrite, marcasite, galena, chalcopyrite, and sphalerite.

Iron sulfides (pyrite and marcasite) are ubiquitous in rocks of the Lost Creek deposit. Within the Mascot portion of the breccia, they are especially abundant and probably average at least 5% by volume. One 15-meter (45-foot) interval in the #1 drill hole contains an estimated 15% pyrite and marcasite as mineral matrix in rubble breccias.

Disseminated pyrite associated with mineralization has been described previously (page 95), as has pyrite and marcasite that occurs in veins and fractures (page 99). It has been demonstrated that there was one main pulse of sphalerite mineralization which occurred later than most barite deposition. Large amounts of iron sulfides were precipitated both before and after this main phase of sphalerite mineralization. Pyrite, however, seems to be more abundant prior to the sphalerite whreas marcasite is the primary iron sulfide deposited

subsequent to sphalerite precipitation. Marcasite generally engulfs earlier-formed pyrite (Figure 49).

Galena occurs in trace amounts in association with sphalerite. Galena deposition overlapped that of sphalerite, although much appears to be precipitated later. However, most galena is earlier than iron sulfides that precipitated subsequent to sphalerite deposition. Galena may even be replaced by marcasite.

Trace chalcopyrite seems to have precipitated throughout the main stage of sulfide deposition, although a greater percentage of it was precipitated fairly late. Chalcopyrite is found as inclusions within sphalerite, as intergrowths with sphalerite and galena, with pyrite and marcasite, and with galena and marcasite. Chalcopyrite commonly forms by exsolution from sphalerite (Ramdohr, 1969). This origin is consistent with most of the textures observed at Lost Creek.

Some very interesting sulfide textures have been seen in drill core from the #1 drill hole over the interval from 123-126 feet. Microscopic examination of polished thin sections of this rock reveals unusual botryoidal structures. The cores of these botryoids may be composed of sphalerite, galena (Figure 50), or both sphalerite and galena. The next shell is always pyrite, followed by highly fractured marcasite. The pyrite zone may be fractured also. The fragments of iron sulfides in the botryoids are generally cemented by galena. Stringers of galena that heal the fractured iron sulfide are continuous with the cores of the botryoids if they are also galena but abruptly terminate against cores composed of sphalerite.

Additional shells of intergrown sphalerite and galena follow the iron sulfide shells in some botryoids. The botryoids seem to have been

Figure 49. Twinned marcasite that precipitated subsequent to formation of pyrite (euhedral grain in center). The dark crystals are gangue dolomite. Sample #175.

Figure 50. Typical sulfide botryoid showing concentric layers of different mineralogy. The core is composed of galena. The next shell is pyrite, followed by highly fractured marcasite. Surrounding material is intergrown sphalerite and galena with abundant barite and dolomite inclusions (both very dark). Sample #1-123.

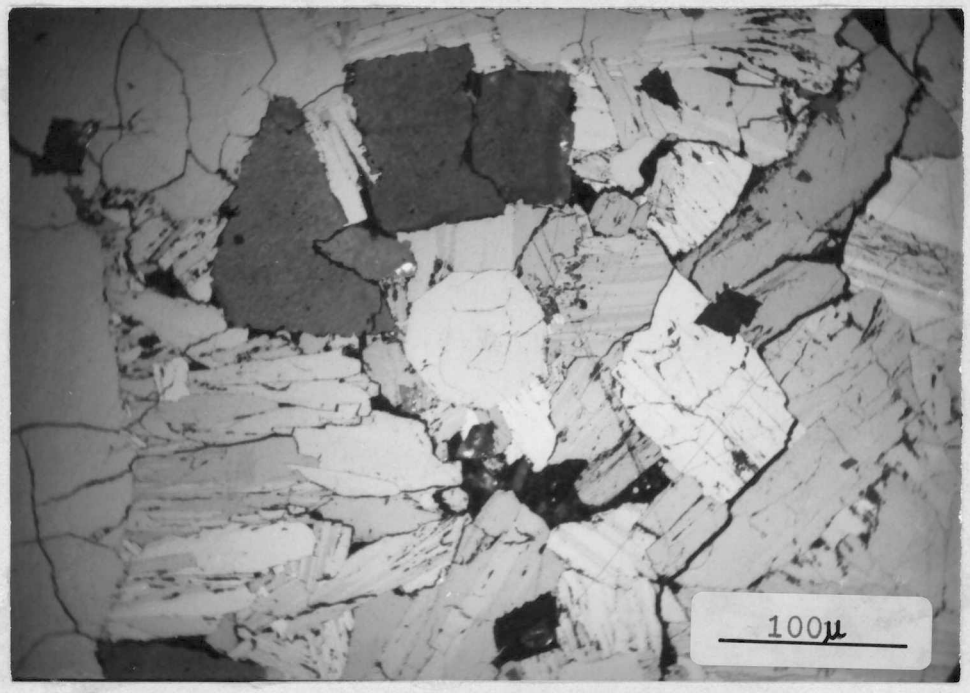


Figure 49

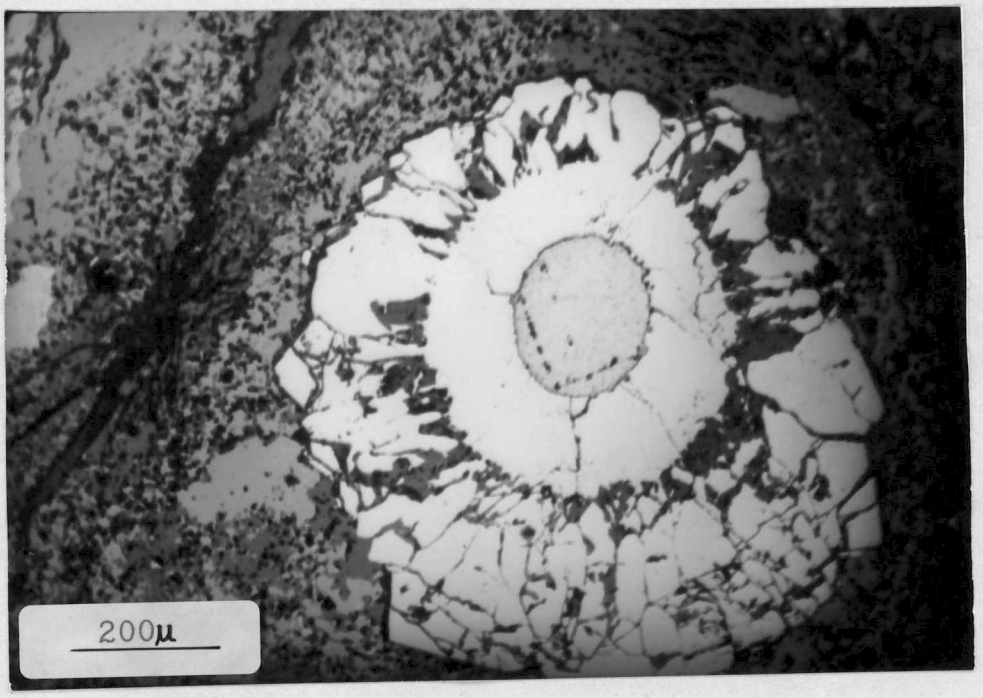


Figure 50

formed at the same time as dolomite and barite, which occur as inclusions within the sulfide shells formed later. Some later-formed sulfide shells may be so poorly developed that the sulfides appear as inclusions within non-sulfides (as in Figure 50). Some replacement of dolomite has also occurred (Figure 51).

Late fractures, healed primarily by galena and filled with abundan pyrite and marcasite fragments (and lesser numbers of sphalerite, galena, and dolomite fragments) cut irregularly across sulfides and non-sulfides alike. Some fractures, without broken fragments of other minerals, are healed primarily by barite. The timing of these late fractures, regardless of filling, may be coincident with the fracturing of the iron sulfide shells in the botryoids. Apparently, iron sulfides are relatively brittle while galena is relatively mobile and able to heal fractures.

Although not a sulfide, smithsonite is common in the weathered portion of the Lost Creek ore deposit. It is readily recognized in outcrop by a box-work texture. A sample of weathered ore containing abundant box works was analyzed by X-ray diffraction and conclusively proven to contain smithsonite. In thin section, smithsonite appears as a fine-grained, gray to colorless mineral intimately mixed with corroded sphalerite. Under cathodoluminescent light, the smithsonite is also distinctive, and luminesces a distinctive pale purple color.

Paragenesis

Studies have been made on the order of crystallization of the ore minerals in many of the deposits of Mississippi Valley-type and for districts as a whole (see, for example, Heyl et al., 1959; Hagni and

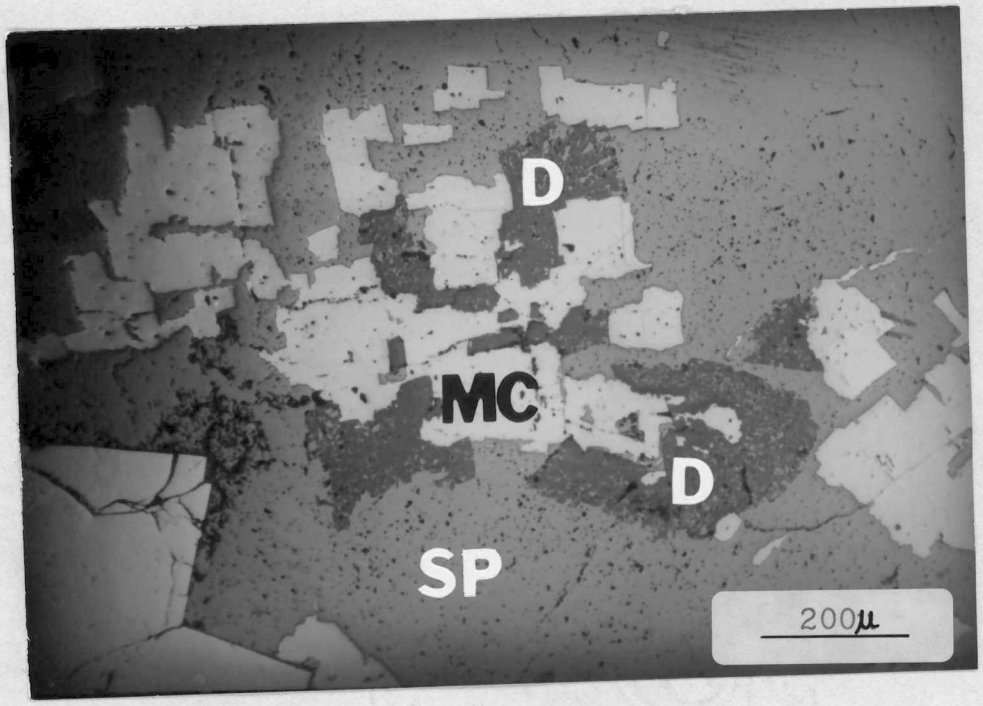


Figure 51. Replacement of large dolomite grains (D) by sphalerite (SP) and marcasite (MC). Sample #1-123.

Grawe, 1964; Hill, 1969; and Hathaway, 1969). Snyder (1968), writing on this subject said:

> It seems apparent that during the long period of mineralization, changes in metal content of solutions occurred as well as changes in conditions of deposition. A paragenetic study of a given specimen defines the situation at that point in space and time. In a different part of the district and at a different time, considerably different mineral relationships may exist and a different paragenetic order would exist.

Snyder's words ring true for the Lost Creek deposit. For example, the sulfide textures exhibited in the 123-126 foot depth zone of the #1 drill hole (see page 98) prove that the order of deposition of sulfide minerals, in detail, was very complex. Nonetheless, certain patterns and relationships emerged from a study of many samples. These have been discussed in detail in the previous sections on barite and sulfide mineralization, and are summarized in Figure 52. This figure gives the general paragenetic sequence for ore and gangue minerals associated with late diagenetic and epigenetic mineralization at Lost Creek (compare to Figure 34, page 97).

Origin and Timing of Brecciation

It has been demonstrated previously (pages 20-24) that the Lost Creek breccia resulted from collapse. Collapse was probably initiated by dissolution of host sediments, as has been suggested for other Mississippi Valley-type deposits in both eastern and central Tennessee.

Bernard (1973) noted three possible models for the formation of ore deposits associated with solution collapse structures beneath unconformities:

1. Karst-forming processes caused both development of the plumbing system and deposition of the mineralized filling.

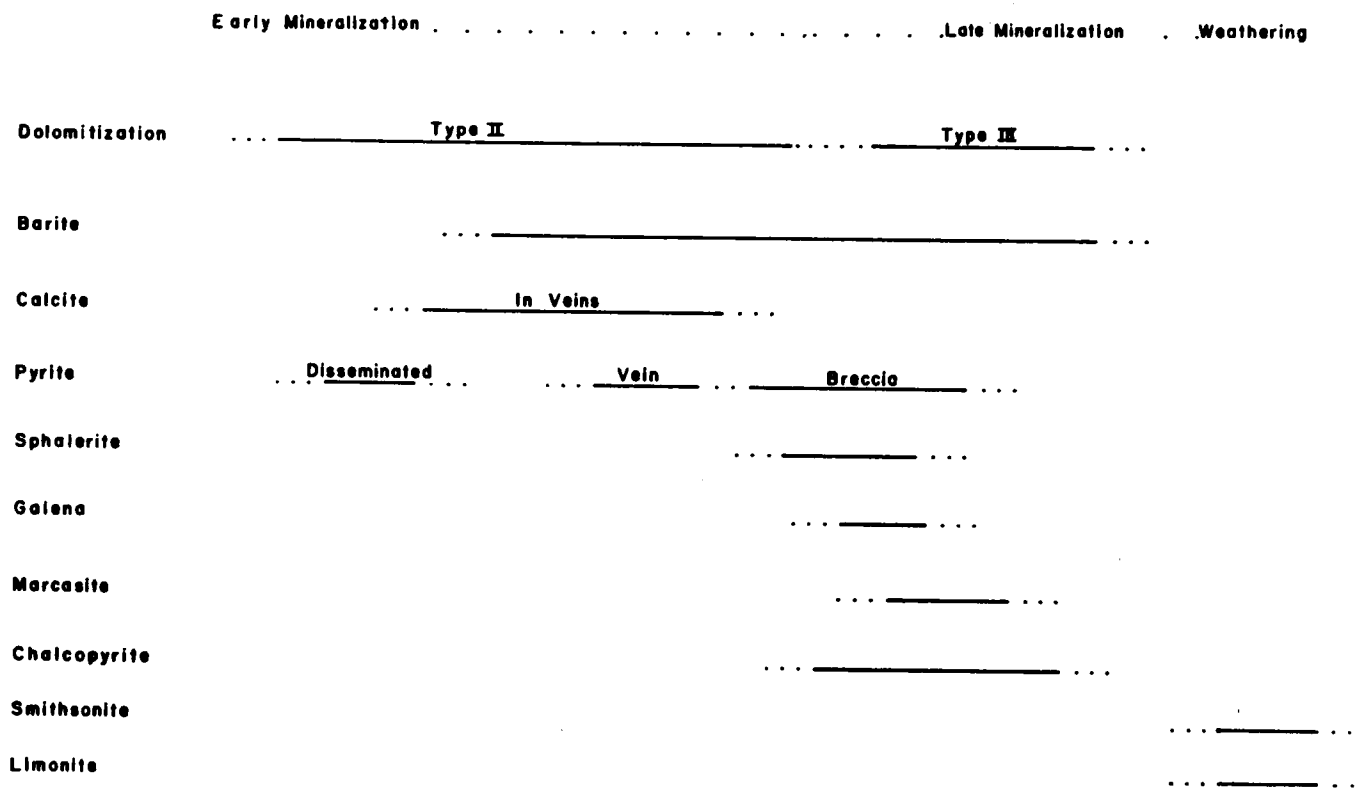


Figure 52. Paragenetic sequence for late diagenetic mineralization at the Lost Creek barite mine, expanded from Figure 34.
Note: Although mineralization within the Dot Formation can be considered at least in part, to be diagenetic, within the Mascot Formation it was entirely epigenetic. Both processes were, however, penecontemporaneous (see page 135).

2. Cavities are karstic, but the mineralization (both sulfides and non-sulfides) resulted from the influx of later hydrothermal solutions.

3. Hydrothermal solutions caused dissolution and development of cavities and deposited the mineralized filling at the same time.

The Lost Creek deposit, of course, is not confined beneath the Knox unconformity. It may have been hydrologically possible for the karst system, developed during the erosional interval of the unconformity, to have remained dynamic during earliest Middle Ordovician sedimentation. Although it may not be likely, it is therefore possible that the karstic system caused brecciation both below the Knox unconformity, within the Mascot Formation, and above the unconformity, within the Dot Formation. Nonetheless, mineralization directly caused by karst processes, according to Bernard, occurs in the deepest portions of the karstic system. This consideration eliminates Bernard's first model. The other two models could still be valid mechanisms for the formation of the Lost Creek deposit, however. Cavities, which were originally karstic, as in Bernard's second model, may have been modified and enlarged by hydrothermal solutions. A similar model has been proposed in recent years, by many workers, for the east Tennessee zinc (and possibly Sweetwater barite) deposits (Wedow, 1971). The mineralization and brecciation within the Dot Formation could have been formed by hydrothermal fluids which simply stoped their way across the unconformity. It was previously hypothesized (page 124) that mineralizing fluids may have even reached the Middle Ordovician sea floor. If so, the timing of mineralization would have been very early Middle Orodvician. Other evidence, such as the rounding and warping of breccia

fragments in the Dot breccia support this idea. Mineralization and brecciation within the Dot Formation portion of the Lost Creek deposit would therefore have been largely diagenetic (except for syngenetic deposition on the sea floor) and penecontemporaneous with epigenetic mineralization in the Mascot Dolomite beneath.

Bernard's third model could explain all of the features observed at Lost Creek also. There is no way to prove the original plumbing system was karstic. However, the close association of the deposit with the Knox unconformity is suggestive of a karst origin. Hydrothermal solutions, despite Bernard's insistence, would not be compelled to be spatially related to unconformities.

Unanswered still, however, is one of the queries raised in the introduction to this paper: Why do mineralization and brecciation transect the Knox unconformity at Lost Creek and, so far as known, only at Lost Creek in east Tennessee? Considering that the main ore zone in the east Tennessee zinc districts lies many hundreds of feet beneath the Knox unconformity, it is difficult to imagine mineralizing fluids stoping such a great vertical distance. However, if the original plumbing system were karstic, portions of the original system itself would have extended to the unconformity (or perhaps even transected the unconformity, see above). It is somewhat easier to envision the mineralizing solutions following the karstic plumbing system to the unconformity and then stoping, if the karstic system did not transect the unconformity, across 20 or 40 meters of partially lithified Dot section and onto the Middle Ordovician sea floor. The stoping action could have been caused by dissolution of the Dot sediments or, possibly, in response to foundering of limestone units within the Mascot Dolomite beneath.

Since excavation during underground mining in the east Tennessee zinc districts ceases above the ore zones, the upper portions of the breccia systems are poorly known. Crawford and Hoagland (1968), however, point out that rock matrix rubble breccias in east Tennessee may be circular or oval in plan and pipelike in section above the stratigraphic horizons of the ore zones. Their description essentially fits the shape of the Lost Creek breccia as well, and implies that the Lost Creek deposit is merely the result of the introduction of mineralizing fluids into a karst breccia above the stratigraphic zone which is normally mineralized.

Furthermore, although the Lost Creek deposit seems to be unique in eastern Tennessee, similar features have been found in central Tennessee. Drilling in middle Tennessee has located mineralized breccia systems that continue without interruption across the Knox unconformity for as much as 60 meters (200 feet) [Hoagland, 1973 (original reference not seen, see Kyle, 1976)].

Core from the Dot Formation portion of the Lost Creek breccia is markedly different from core of the brecciated Mascot. The breccia within the Dot contains abundant dark, clayey material swirled throughout the matrix. Boundaries between matrix and breccia fragments are often indistinct. In fact, similar breccias in central Tennessee (within the middle Ordovician Wells Creek Formation) are called diagenetic breccias by zinc company geologists. Although this term is meant to be descriptive, genetic implications are unavoidable since the textures that the term describes could best develop by brecciation within a semi-lithified section.

Chemistry of the Ore Fluid

Hypotheses concerning the chemistry of the fluid responsible for the deposition of the Lost Creek ores are complicated by the intimate mixing of significant amounts of sulfides with the barite. Based on fluid inclusion studies, Roedder (1971) suggested that the ore fluids that supplied the east Tennessee zinc deposits were probably deeply circulating sodium chloride-rich brines. Deposition likely occurred between 75° and 150°C. Considering the apparent close genetic ties with the east Tennessee zinc deposits, the Lost Creek ore fluid was probably very similar.

Precipitation of Ore Minerals

Speculation regarding a precipitation mechanism (or mechanisms) for the sulfides and barite at Lost Creek must be consistent with several observations:

1. The deposit is mineralogically and spatially zoned. Large quantities of sulfides are found with the Mascot Dolomite, but it contains only trace amounts of feathery (late) barite (see page 117). The overlying Dot Formation, on the other hand, contains abundant barite and only minor sulfides.

2. Within the Dot Formation, several episodes of barite and sulfide mineralization are evident (see page 118). This, in turn, indicates there were several reversals in the environment of precipitation.

3. Sparry calcite cement is intimately mixed with ferroan dolomite in vugs and voids of the Dot Formation rocks. The textural relationships suggest that precipitation of these carbonates occurred

within a mixing zone of essentially fresh water (sparry calcite precipitation) and saline water (mineralizing fluids responsible for the precipitation of the ferroan dolomite, see page 85).

Theoretical and experimental work indicates that barite can be precipitated from sodium chloride-rich solutions that are saturated with barite simply by cooling (Barnes, 1979, page 499). At Lost Creek such cooling could have been accomplished by the mixing of the ore fluids with the oxidizing formational waters of the Dot Formation. Anoxic conditions (indicated by the large volumes of sulfides) within the Mascot Dolomite may have prevented deposition of barite, despite cooling effects, until the oxidizing environment of the Dot Formation was encountered.

Another possible mechanism of precipitation involves the mixing of a barium-rich fluid (such as a connate brine) with a sulfate-rich fluid (hydrothermal fluid) (Sawkins, 1964; Leach, 1973). This hypothesis, which splits the ore fluid into two components, seems unnecessarily complicated for the Lost Creek deposit. Furthermore, it would be difficult to explain the sulfide deposition by this process.

A third model of barite precipitation calls upon the oxidation of an ore fluid containing both barium and reduced sulfur (Plummer, 1971; Wagner, 1973; Morrow et al., 1978). This method of transportation and deposition is also unlikely for the Lost Creek deposit. Oxidation of the reduced sulfur would lower the pH and produce significant dissolution of the carbonate host rocks. Although some minor replacement of dolomite has been observed at Lost Creek (see Figure 51, page 134), the barite and sulfides were generally deposited in pre-existing open spaces.

If the Lost Creek ore fluid did not contain abundant sulfide, then quantities sufficient to deposit pyrite, marcasite, sphalerite, and galena must have been supplied at the depositional site. Various processes, such as mixing of the ore fluid with H_2S-rich waters or inorganic reduction of sulfate, have been proposed to supply reduced sulfur for other Mississippi Valley-type deposits (Barton, 1967; Jackson and Beales, 1967; Anderson, 1975).

Essentially, the model that can best explain the precipitation of the Lost Creek ore is a three-fluid model. It is not very different from the two-fluid model of Mississippi Valley-type sulfide deposition first formulated by Jackson and Beales (1967). Mixing of a metal-bearing brine with H_2S-rich waters probably produced the extensive sulfide mineralization within the Mascot portion of the Lost Creek breccia structure.

In addition to metals, the Lost Creek ore fluid contained abundant barite in solution as well. Precipitation of the barite may have been produced by cooling upon mixing of the ore fluid with oxidizing formational fluids within the incompletely lithified Dot Formation sediments overlying the Mascot Dolomite. Considering that some of the barite deposition was probably syngenetic (see page 122), precipitation of barite within the Dot Formation may also have been strongly influenced by the presence of sea water derived sulfate. This would be especially true if the barium in the ore fluid was not transported as dissolved barite but as a chloride complex similar to the probable metal-transporting compounds.

Barnes (1979) issued a warning concerning precipitation mechanisms proposed for barite that is associated with sulfide minerals. In

a mixing model, the mixing ratio of the fluids would have to be adjusted rather delicately to prevent the disappearance of sulfides and the appearance of oxides (such as hematite) in the mineral assemblage.

Summary and Discussion

A final point to add to this discussion is the acknowledgment that designation of specific episodes of mineralization and especially brecciation may amount to petrographic hair-splitting. Perhaps a more realistic summation would be as follows: Type II dolomitization, brecciation, and barite mineralization were long-lasting, more or less penecontemporaneous processes. Some vug- or vein-filling Type II dolomite preceded brecciation and barite mineralization. Likewise, some barite (feathery) and Type III dolomite (pink) probably represent the last pulses of the epoch of mineralization and occurred after Type II dolomitization and brecciation had ceased.

Sulfide mineralization was also long lasting, especially iron sulfide precipitation. However, most of the sulfides (mainly sphalerite and galena) were deposited during one mineralizing episode and later than most of the barite. Calcite is found only in vein-fillings, and is not a mineralogical component of the breccia core.

The Lost Creek breccia structure formed by solution collapse. The original plumbing system was karstic, later modified and enlarged by the mineralizing fluids which stoped their away across the Knox unconformity and into the basal Middle Ordovician sediments. Evidence of diagenetic (and possibly syngenetic) brecciation and mineralization within the Dot Formation indicates mineralization was very early Middle Ordovician.

The ore fluid responsible for the transport of barium and metals was probably sodium chloride-rich and slightly acidic. The reduced sulfur necessary for precipitation of sulfides is thought to have been supplied at the depositional site. Barite deposition may have been caused by cooling that accompanied the mixing of the ore fluid with oxidizing formational waters of the Dot Formation.

CHAPTER V

SUMMARY AND CONCLUSIONS

The most important findings of this study are summarized below:

1. The depositinal regime of the Dot Formation portion of the Lost Creek section was peritidal. Among recent carbonate depositional settings, Andros Island, Bahamas, is the best, although an approximate, analogue. Similarities include a "wet" climate and the existence of a complicated, comparatively small-scale, mosaic of supratidal, intertidal, and shallow subtidal environments and subenvironments.

2. Diagenesis of the Dot sediments included many specific events which can be woven into a paragenetic sequence. Most important of these events was dolomitization. Two distinct episodes of dolomitization are recognized. The first (Type I) occurred within a mixing zone of marine and fresh waters after cementation but prior to mineralization. The second episode (Type II) of dolomitization preceded and accompanied mineralization. Tyep II dolomite can be distinguished by its coarse grain size, luminescent zonation, and ferrous iron content.

3. Mineralization within the Dot Formation can also be considered a diagenetic event (and was possibly even syngenetic in part). Mineralization, at least some brecciation, and Type II dolomitization were penecontemporaneous processes, and resulted from mixing of the mineralizing fluids with formational waters (which themselves were the product of the earlier mixing of fresh and marine waters). Barite precipitation may have been specifically controlled by the cooling and oxidation of the sulfide-rich ore fluid by the formational solutions.

Sulfides (mainly sphalerite and galena) were deposited during one mineralizing episode and later than most of the barite. The sulfides are much more common in the brecciated and mineralized Mascot Dolomite beneath the Dot Formation. Within the Mascot, mineralization was entirely epigenetic.

Recommendation for Further Work

Recommendations for additional work are directed toward two primary objectives:

1. Much stratigraphic work remains to be done in the northwestern stike belts on the Middle Ordovician units. More specifically, the Lost Creek section needs to be expanded and the paleoenvironments and sequence of diagenesis examined over a much broader area.

2. Further attention should be focussed on the Lost Creek deposit itself and must be directed toward data acquisition to confirm or deny the conclusions, based largely on petrography, reached in this study. Geochemical studies should be done. Sampling for certain studies (i.e., geochemical halo and trace elements of ore minerals) has already been completed. Fluid inclusion work could provide valuable data on the composition and temperature of the mineralizing fluids. Isotopic studies may help reveal the source or sources of the metals and sulfur introduced with the mineralizing fluids.

LIST OF REFERENCES

LIST OF REFERENCES

Adams, J. E., and Rhodes, M. L., 1960, Dolomitization by seepage refluction: Am. Assoc. Petrol. Geol. Bull., v. 44, pp. 1912-1920.

Anderson, G. M., 1975, Precipitation of Mississippi Valley-type ores: Econ. Geol., v. 70, pp. 937-942.

Aitken, J. D., 1967, Classification and environmental significance of cryptalgal limestones and dolomites, with illustrations from the Cambrian and Ordovician of southwestern Alberta: Jour. Sed. Petrol., v. 37, pp. 1163-1178.

Badiozamani, K., 1973, The Dorag dolomitization model - application to the Middle Ordovician of Wisconsin: Jour. Sed. Petrol., v. 43, pp. 965-984.

Badiozamani, K., MacKenzie, F. T., and Thorstensen, D. C., 1977, Experimental carbonate cementation: salinity, temperature, and vadose-phreatic effects: Jour. Sed. Petrol., v. 47, pp. 529-542.

Barnes, H. L., ed., 1979, Geochemistry of hydrothermal ore deposits, second edition: John Wiley and Sons, New York, 798 p.

Barrett, P. J., 1964, Residual seams and cementation in Oligocene shell calcarenites, Te Kuiti Group: Jour. Sed. Petrol., v. 34, p. 524-531.

Barton, P. B., 1967, Possible role of organic matter in the precipitation of the Mississippi Valley ores: in Brown, J. B., ed., Symposium on the genesis of stratiform lead-zinc-barite-fluorite deposits: Econ. Geol., Mon. 3, pp. 371-377.

Bathurst, R. G. C., 1975, Carbonate sediments and their diagenesis: Elsevier, New York, 658 p.

Benedict, G. L., and Walker, K. R., 1978, Paleobathymetric analysis in Paleozoic sequences and its geodynamic significance: Am. Jour. Sci., v. 278, pp. 579-607.

Bernard, A. J., 1973, Metallogenic processes of intrakarstic sedimentation in Amstutz, G. C., and Bernard, A. J. (eds.), Ores in sediments: Intern. Union Geol. Sci., Ser. A, No. 3, pp. 43-57.

Berner, R. A., 1970, Sedimentary pyrite formation: Am. Jour. Sci., v. 268, pp. 1-23.

Billings, M. P., 1972, Structural geology: Prentice-Hall, Inc., New Jersey, 606 p.

Blythe, E. W., 1967, Lithostratigraphy of the Chickamauga Group in Campbell and Claiborne Counties, Tennessee: Unpub. Master's Thesis, University of Tennessee, Knoxville, 74 p.

Bogacz, K., Dzulynski, S., Haranczyk, C., and Sobczynski, P., 1975, Origin of the ore-bearing dolomite in the Triassic of the Cracow-Silesian Pb-Zn ore district: Rocznik Polskiego Towarzystwa Geologicznego, v. 45, pp. 139-155.

Brokaw, A. L., Rodgers, J., Kent, D. F., Laurence, R. M., and Behre, C. H., Jr., 1966, Geology and mineral deposits of the Powell River area, Claiborne and Union Counties, Tennessee: U. S. Geol. Survey Bull. 1222-C, pp. C1-C56.

Buckley, H. E., 1951, Crystal Growth: John Wiley and Sons, Inc., New York, 571 p.

Burgess, W. J., 1968, Carbonate paleoenvironments in the Arbuckle Group, West Spring Creek Formation, Lower Ordovician, in Oklahoma: Unpub. ph.D. Diss., Columbia University, 165 p.

Burgess, C. J., 1979, The development of a Lower Jurassic carbonate tidal flat, Central High Atlas, Morocco. 2: Diagenetic history: Jour. Sed. Petrol., v. 49, pp. 413-428.

Carpenter, R. H., Fagan, J. M., and Wedow, H. Jr., 1971, Evidence on the age of barite, zinc, and iron mineralization in the Lower Paleozoic rocks of east Tennessee: Econ. Geol., v. 66, pp. 792-798.

Churnet, H. G., 1979, The relationships between dolomitization and sphalerite mineralization in the Lower Ordovician Upper Knox carbonate rocks of the Copper Ridge district, east Tennessee: Unpub. Ph.D. Diss., University of Tennessee, Knoxville, 237 p.

Compton, R. R., 1962, Manual of field geology: John Wiley and Sons, Inc., New York, 378 p.

Cooper, B. N., 1945, Industrial limestones and dolomites in Virginia: Clinch Valley district: Virginia Geol. Survey Bull., v. 66, 259 p.

Cooper, B. N., and Prouty, C. E., 1943, Stratigraphy of the lower Middle Ordovician of Tazewell County, Virginia: Geol. Soc. Am. Bull., v. 54, pp. 819-886.

Crawford, J., and Hoagland, A. D., 1968, The Mascot-Jefferson City zinc district, Tennessee, in Ore deposits of the United States, 1933-1967 (Graton-Sales Volume), V. 1: Am. Inst. Mining, Metall., and Petroleum Engineers, New York, pp. 242-256.

Crawford, J., Fulweiler, R. E., and Miller, H. W., 1971, Mine geology of the New Jersey Zinc Company's Jefferson City mine, in Papers on the stratigraphy of the Kingsport and Mascot Formations (Lower Ordovician) of east Tennessee: Tenn. Div. of Geol., Rept. Inv. 23, pp. 64-75.

Cullison, J. S., 1937, The geology of the Norris Reservoir region of Tennessee: Tennessee Valley Authority, unpub. rept., 138 p.

Cullison, J. S., and Scott, E. R., 1935, Norris Reservoir mineral appraisal file report, tract NR 3123: Tennessee Valley Authority, Unpub. rept.

Davies, W. E., 1951, Mechanics of cavern breakdown: National Speleological Soc. Bull., v. 13, pp. 36-42.

De Groot, J., 1967, Experimental dedolomitization: Jour. Sed. Petrol., v. 37, pp. 1216-1220.

Deffeyes, K. S., Lucia, F. J., and Weyl, P. K., 1965, Dolomitization of Recent and Plio-Pleistocene sediments by marine evaporite waters on Bonaire, Netherlands Antilles, in Pray, L. C., and Murray, R. C. (eds.), Dolomitization and limestone diagenesis: A symposium: Soc. Econ. Paleontologists and Mineralogists, Spec. Publ. 13, pp. 112-123.

Dickson, J. A. D., 1966, Caronate identification and genesis as revealed by staining: Jour. Sed. Petrol., v. 36, pp. 491-505.

Dunham, R. J., 1962, Classification of carbonate rocks according to depositional texture, in Hamm (ed.), Classification of carbonates: Am. Assoc. Petrol. Geol. Memoir 1, pp. 108-121.

Ebers, M. L., 1977, A study of gangue dolomite mineralization in the Mascot-Jefferson City zinc district, using cathodoluminescence: Unpub. Master's Thesis, University of Tennessee, Knoxville, 82 p.

Ebers, M. L., and Kopp, O. C., 1979, Cathodoluminescent microstratigraphy in gangue dolomite, the Mascot-Jefferson City district, Tennessee: Econ. Geol., v. 74, pp. 908-918.

Evamy, B. D., 1963, The application of a chemical staining technique to a study of dedolomitization: Sedimentology, v. 2, pp. 164-170.

Fagan, J. M., 1969, Geology of the Lost Creek barite mine, in Papers on the stratigraphy and mine geology of the Kingsport and Mascot Formations (Lower Ordovician) of east Tennessee: Tennessee Div. Geol. Rept. Inv. 23, pp. 40-44.

Finlayson, C. P., 1964, Mineral resources summary of the Maynardville quadrangle, Tennessee: Tennessee Div. Geol., MRS 145-SE.

Folk, R. L., 1959, Practical petrographic classification of limestones: Am. Assoc. Petrol. Geol. Bull., v. 43, pp. 1-38.

Folk, R. L., 1973, Carbonate petrography in the post-Sorbian age, in Ginsburg, R. N. (ed.), Evolving concepts in sedimentology, Johns Hopkins University Studies in Geology, No. 21: Johns Hopkins University Press, Baltimore, pp. 118-158.

Folk, R. L., 1974, The natural history of crystalline calcium carbonate: effect of magnesium content and salinity: Jour. Sed. Petrol., v. 44, pp. 40-53.

Folk, R. L., and Sidelecka, A., 1974, The "schizohaline" environment: its sedimentary and diagenetic fabrics as exemplified by Late Paleozoic rocks of Bear Island, Svalbard: Sedimentary Geology, v. 11, pp. 1-15.

Folk, R. L., and Land, L. S., 1975, Mg/Ca ratio and salinity: two controls over crystallization of dolomite: Am. Assoc. Petrol. Geol., Bull., v. 59, pp. 60-68.

Friedman, G. M., 1964, Early diagenesis and lithification in carbonate sediments: Jour. Sed. Petrol., v. 34, pp. 77-813.

Friedman, G. M., 1965, Terminology of crystallization textures and fabrics in sedimentary rocks: Jour Sed. Petrol., v. 35, pp. 643-655.

Garrett, P., 1970, Phanerozoic stromatolites: Non-competitive ecologic restriction by grazing and burrowing animals: Science, v. 169, pp. 171-173.

Gebelein, C. D., 1977, Mixing-zone dolomitization of Holocene tidal-flat sediments, southwest Andros Island, Bahamas (abs.): Am. Assoc. Petrol. Geol. Bull., v. 61, pp. 787-788.

Gildersleeve, B., 1946, Minerals and structural materials of east Tennessee: Tennessee Valley Authority, Regional Products Research Div., Rept. B.

Ginsburg, R. N. (ed.), 1975, Tidal deposits: Springer-Verlag, New York, 428 p.

Goodell, H. G., and Garman, R. K., 1969, Carbonate geochemistry of superior deep test well, Andros Island, Bahamas: Am. Assoc. Petrol. Geol. Bull., v. 53, pp. 513-536.

Grover, G., and Read, J. F., 1978, Fenestral and associated vadose diagenetic fabrics of tidal flat carbonates, Middle Ordovician New Market Limestone, southwestern Virginia: Jour. Sed. Petrol., v. 48, pp. 453-473.

Hagni, R. D., and Grawe, O. K., 1964, Mineral paragenesis in the Tri-State district Missouri, Kansas, Oklahoma: Econ. Geol., v. 59, pp. 449-457.

Hanshaw, B. B., Back, W., and Deike, R. G., 1971, A geochemical hypothesis for dolomitization by ground water: Econ. Geol., v. 66, pp. 710-724.

Hardie, L. A. (ed.), 1977, Sedimentation of the modern carbonate tidal flats of northwest Andros Island, Johns Hopkins University studies in geology No. 22: Johns Hopkins University Press, Baltimore, 196 p.

Hardie, L. A., and Garrett, P., 1977, Some miscellaneous implications and speculations, in Hardie, L. A. (ed.), Sedimentation of the modern carbonate tidal flats of northwest Andros Island, Johns Hopkins University studies in geology No. 22: Johns Hopkins Unversity Press, Baltimore, pp.

Hardie, L. A., and Ginsburg, R. N., 1977, Layering: the origin and environmental significance of lamination and thin bedding, in Hardie, L. A. (ed.), Sedimentation of the modern carbonate tidal flats of northwest Andros Island, Johns Hopkins University studies in geology No. 22: Johns Hopkins University Press, Baltimore, pp. 50-123.

Harris, L. D., 1969, Kingsport Formation and Mascot Dolomite (Lower Ordovician) of east Tennessee, in Papers on the stratigraphy of the Kingsport and Mascot Formations (Lower Ordovician) of east Tennessee: Tenn. Div. of Geol., Rept. Inv. 23, pp. 1-39.

Harris, L. D., 1971, A lower Paleozoic paleoaquifer - the Kingsport Formation and Mascot Dolomite of Tennessee and southwest Virginia: Econ. Geol., v. 66, pp. 735-743.

Hathaway, D. J., 1969, Mine geology of the New Market Zinc Company mine at New Market, in Papers on the stratigraphy of the Kingsport and Mascot Formation (Lower Ordovician) of east Tennessee: Tenn. Div. of Geol., Rept. Inv. 23, pp. 53-63.

Hayes, C. W., 1891, The overthurst faults of the southern Appalachians: Geol. Soc. Am. Bull., v. 2, pp. 141-152.

Heyl, A. V., Agnew, A. F., Lyons, E. J., and Behre, C. H., Jr., 1959, The geology of the upper Mississippi Valley zinc-lead district: U. S. Geol. Survey Prof. Paper 309, 310 p.

Hill, W. T., 1969, Mine geology of the New Jersey Zinc Company's Flat Gap mine at Treadway in the Copper Ridge district, in Papers on the stratigraphy of the Kingsport and Mascot Formations (Lower Ordovician) of east Tennessee: Tenn. Div. of Geol., Rept. Inv. 23, pp. 76-90.

Hill, W. T., and Wedow, H., Jr., 1971, An early Middle Ordovician age for collapse breccias in the east Tennessee zinc deposits as indicated by compaction and porosity features: Econ. Geol., v. 66, pp. 725-734.

Hoagland, A. D., 1967, Interpretations relating to the genesis of east Tennessee zinc deposits, in Brown, J. S. (ed.), Genesis of stratiform lead-zinc-barite-fluorite deposits: Econ. Geol., Mono. 3, pp. 52-58.

Hoagland, A. D., 1971, Appalachian strata-bound deposits: their essential features, genesis and the exploration problem: Econ. Geol., v. 66, pp. 805-810.

Hoagland, A. D., 1973, Appalachian zinc-lead and the deposits of middle Tennessee: Manuscript presented at the Geol. Soc. Am., Southeastern Section meeting, Knoxville, Tenneseee, 1973, 12 p.

Hoagland, A. D., Hill, W. T., and Fulweiler, R. E., 1965, Genesis of the Ordovician zinc deposits in east Tennessee: Econ. Geol., v. 60, pp. 693-714.

Hoffman, P., 1973, Recent and ancient algal stromatolites: seventy years of pedagogic cross-pollination, in Ginsburg, R. N. (ed.), Evolving concepts in sedimentology, Johns Hopkins University studies in geology, No. 21: Johns Hopkins University Press, Baltimore, pp. 178-191.

Hsü, K. J., and Siegenthaler, C., 1969, Preliminary experiments on hydrodynamic movements induced by evaporation and their bearing on the dolomite problem: Sedimentology, v. 12, pp. 11-25.

Illing, L. V., 1959, Deposition and diagenesis of some upper Paleozoic carbonate sediments in western Canada: 5th World Petroleum Cong. (N.Y.), sec. I, paper 2, pp. 23-52.

Jackson, S. A., and Beales, F. W., 1967, An aspect of sedimentary basin evolution, the concentration of Mississippi Valley-type ores during late stages of diagenesis: Canadian Petroleum Geology Bull., v. 15, pp. 383-435.

Keith, A., 1901, U. S. Geol. Survey Geol. Atlas: Maynardville Folio (No. 75).

Knauth, P. L., 1979, A model for the origin of chert in limestone: Geology, v. 7, pp. 274-277.

Krumbien, W. C., 1942, Physical and chemical changes in sediments after deposition: Jour. Sed. Petrol., v. 12, pp. 111-117.

Kyle, J. R., 1976, Brecciation, alteration, and mineralization in the central Tennessee zinc district: Econ. Geol., v. 71, pp. 892-903.

Land, L. S., 1970, Phreatic versus vadose meteoric diagenesis of limestones: evidence from fossil water table: Sedimentology, v. 14, pp. 175-185.

Land, L. S., 1973, Contemporaneous dolomitization of Middle Pleistocene reefs by meteoric water, north Jamaica: Bull. Marine Sci., v. 23, pp. 64-92.

Land, L. S. MacKenzie, F. T., and Gould, S. J., 1967, Pleistocene history of Bermuda: Geol. Soc. Am. Bull., v. 78, pp. 993-1006.

Land, L. S., Salem, M. R. I., and Morrow, D. W., 1975, Paleohydrology of ancient dolomites: Geochemical evidence: Am. Assoc. Petrol. Geol. Bull., v. 59, pp. 1602-1625.

Laporte, L. F., 1967, Carbonate deposition near mean sea level and resultant facies mosaic; Manlius Formation (Lower Devonian) of New York State: Am. Assoc. Petrol. Geol. Bull., v. 51, pp. 73-101.

Leach, D., 1973, A study of the barite-lead-zinc deposits of central Missouri and related mineral deposits in the Ozark region: Unpub. Ph.D. Diss., University of Missouri, 185 p.

Logan, B. W., 1974, Inventory of diagenesis in Holocene-Recent carbonate sediments, Shark Bay, Western Australia, in Logan, B. W. (ed.), Evolution and diagenesis of Quaternary carbonate sequences, Shark Bay, Western Australia: Am. Assoc. Petrol. Geol. Memoir 22, pp. 195-249.

Logan, B. W., and Semeniuk, V., 1976, Dynamic metamorphism; processes and products in Devonian carbonate rocks, Canning Basin, Western Australia: Geol. Soc. Australia Spec. Pub. No. 6, 138 p.

Longman, M. W., 1976, Depositional history, paleoecology, and diagenesis of the Bromide Formation (Ordovician), Arbuckle Mountains, Oklahoma: Unpub. Ph.D. Diss., University of Texas, Austin, 311 p.

Longman, M. W., 1980, Carbonate diagenetic textures from nearsurface diagenetic environments: Am. Assoc. Petrol. Geol. Bull., v. 64, pp. 461-487.

Love, L. G., 1964, Early diagenetic pyrite in fine-grained sediments and the genesis of sulphide ores, in Amstutz, B. C. (ed.), Sedimentology and ore genesis: Elsevier, Amsterdam, pp. 11-19.

Lovering, T. G., 1972, Jasperoid in the United States - its characteristics, origin, and economic significance: U. S. Geol. Survey Prof. Paper 710, 164 p.

Lown, D. J., 1978, Petrography, depositional environments, and carbonate diagenesis of the Lower Ordovician Mascot dolomite (K-2 to M-1 interval) near Woodbury, Cannon County, Tennessee: Unpub. Master's Thesis, University of Tennessee, Knoxville, 98 p.

Lucia, F. J., 1972, Recognition of evaporite-carbonate shoreline sedimentation, in Rigby, J. K., and Hamblin, W. K., (eds.), Recognition of ancient sedimentary environments: Soc. Econ. Paleontologists and Mineralogists, Spec. Pub. 16, p. 160-191.

Lyle, J. R., 1977, Petrography and carbonate diagenesis of the Bonneterre Formation in the Viburnum Trend area, southeast Missouri: Econ. Geol., v. 72, pp. 420-434.

Maher, S. W., 1970, Barite resources of Tennessee: Tenn. Div. Geol., Rept. Inv. 28, 40 p.

Maher, S. W., and Finlayson, C. P., 1965, Investigation of miscellaneous mineral deposits in east Tennessee: Tenn. Acad. Sci. Jour., v. 40, pp. 44-47.

McCormick, J. E., Evans, L. L., Palmer, R. A., and Rasnick, F. D., 1971, Environment of the zinc deposits of the Mascot-Jefferson City district, Tennessee: Econ. Geol., v. 66, pp. 757-762.

McLimans, R. K., Barnes, H. L., and Ohmoto, H., 1980, Sphalerite stratigraphy of the Upper Mississippi Valley zinc-lead district, southwest Wisconsin: Econ. Geol., v. 75, pp. 351-361.

Meyers, W. J., 1974, Carbonate cement stratigraphy of the Lake Valley Formation (Mississippian), Sacramento Mountains, New Mexico: Jour. Sed. Petrol., v. 44, pp. 837-861.

Meyers, W. J., and Lohmann, K. C., 1978, Microdolomite-rich syntaxial cements: proposed meteoric-marine mixing-zone phreatic cements from Mississippian limestones, New Mexico: Jour. Sed. Petrol., v. 48, pp. 475-488.

Miller, R. L., and Brosgé, W. P., 1954, Geology and oil resources of the Jonesville district, Lee County, Virginia: U. S. Geol. Survey Bull., v. 990, 240 p.

Misik, M., 1971, Observations concerning calcite veinlets in carbonate rocks: Jour. Sed. Petrol., v. 41, pp. 450-460.

Morrow, D. W., Krouse, H. R., Ghent, E. D., Taylor, G. C., and Dawson, K. R., 1978, A hypothesis concerning the origin of barite in Devonian carbonate rocks of northeastern British Columbia: Canadian Jour. of Earth Sciences, v. 15, pp. 1391-1406.

Mossler, J. H., 1971, Diagenesis and dolomitization of Swope Limestone (Upper Pennsylvanian) of southeast Kansas: Jour. Sed. Petrol., v. 41, pp. 961-970.

Murray, R. C., and Lucia, F. J., 1967, Cause and control of the dolomite distribution by rock selectivity: Geol. Soc. Am. Bull., v. 78, pp. 21-35.

Neal, W. J., 1969, Diagenesis and dolomitization of a limestone (Pennsylvanian of Missouri) as revealed by staining: Jour. Sed. Petrol., v. 39, pp. 1040, 1045.

Nickel, E., 1978, The present status of cathodoluminescence as a tool in sedimentology: Minerals Science and Engineering, South Africa, v. 10, No. 2, pp. 73-100.

Oder, C. R. L., and Miller, H. W., 1945, Stratigraphy of the Mascot-Jefferson City zinc district: Am. Inst. Min. Met. Eng. Tech. Pub. 1818, 9 p.

Ohle, E. L., 1959, Some considerations in determining the origin of ore deposits of the Mississippi Valley-type: Econ. Geol., v. 54, pp. 769-789.

Oldershaw, A. E., 1971, The significance of ferroan and non-ferroan calcite cements in the Halkin and Wenlock limestones (Great Britain), in Bricker, O. P. (ed.), Carbonate cements: The Johns Hopkins Press, Baltimore, pp. 225-229.

Park, W. C., and Schot, E. H., 1968, Stylolites: Their nature and origin: Jour. Sed. Petrol., v. 38, pp. 175-191.

Penhallegon, W. J., 1938, Barite in the Tennessee Valley region: Tennessee Valley Authority Geol. Bull. 9.

Plummer, L. N., 1975, Mixing of sea water with calcium carbonate ground water, in Whitten, E. H. T. (ed.), Quantitative studies in geological sciences: Geol. Soc. Am. Memoir 142, pp. 219-238.

Plummer, A. N., 1971, Barite deposition in central Kentucky: Econ. Geol., v. 66, pp. 252-258.

Posey, H. H., 1979, Brecciation, mineralization, and facies relationships of Cambro-Ordovician carbonates in the Arbuckle Mountains and Southern Oklahoma aulacogen, Oklahoma: Unpub. Master's Thesis, University of Missouri, Rolla, 119 p.

Pray, L. C., and Murray, R. C. (eds.), 1965), Dolomitization and limestone diagenesis, a symposium: SEPM Spec. Pub. 13, Tulsa, Oklahoma, 180 p.

Ramdohr, P., 1969, The ore minerals and their intergrowths: Pergamon Press, Oxford, 1174 p.

Rickard, D. T., 1970, The origin of framboids: Lithos, v. 3, pp. 269-293.

Roedder, E., 1971, Fluid-inclusion evidence on the environment of formation of mineral deposits of the southern Appalachian Valley: Econ. Geol., v. 66, pp. 777-791.

Roedder, E., and Dwornik, E. J., 1968, Sphalerite color banding: lack of correlation with iron content, Pine Point, Northwest Territories, Canada: American Mineralogist, v. 53, pp. 1523-1529.

Roehl, P. O., 1967, Stony Mountain (Ordovician) and Interlake (Silurian) facies analogs of recent low-energy marine and subaerial carbonates, Bahamas: Am. Assoc. Petrol. Geol. Bull., v. 51, pp. 1979-2032.

Rodgers, J., 1953, Geologic map of east Tennessee with explanatory text: Tenn. Div. Geol. Bull., v. 58, pt. II, 168 p.

Runnells, D. D., 1969, Diagenesis, chemical sediments, and the mixing of natural waters: Jour. Sed. Petrol., v. 39, pp. 1188-1201.

Safford, J. M., 1869, Geology of Tennessee: Nashville, 585 p.

Sawkins, F. J., 1964, Ore genesis in the North Pennine ore field in the light of fluid inclusion studies: Econ. Geol., v. 61, pp. 385-401.

Shinn, E. A., 1973, Carbonate coastal accretion in an area of longshore transport, NE Qatar, Persian Gulf, in Purser, B. H. (ed.), The Persian Gulf: Springer-Verlag, New York, pp. 179-192.

Shinn, E. A., Ginsburg, R. N., and Lloyd, R. M., 1965, Recent supratidal dolomite from Andros Island, Bahamas, in Pray, L. C., and Murray, R. C. (eds.), Dolomitization and limestone diagenesis: a symposium: Soc. Econ. Paleontologists and Mineralogists, Spec. Publ. 13, pp. 112-123.

Shinn, E. A., Lloyd, R. M., and Ginsburg, R. N., 1969, Anatomy of a modern carbonate tidal-flat, Andros Island, Bahamas: Jour. Sed. Petrol., v. 39, pp. 1202-1228.

Sibley, D. F., 1979, Dolomitization of Plio-Pleistocene carbonate sediments, Bonaire Netherlands Antilles (abs.): Am. Assoc. Petrol. Geologists, Soc. Econ. Paleontologists and Mineralogists Annual Mtg., p. 164.

Snyder, F. G., 1968, Geology and mineral deposits, midcontinent United States, in (Graton-Sales volume), Ore deposits of the United States: Am. Inst. Mining Metall. Petrol. Engineers, New York, pp. 257-286.

Steinen, R. P., 1974, Phreatic and vadose diagenetic modification of Pleistocene limestone: petrographic observations from subsurface of Barbados, West Indies: Am. Assoc. Petrol. Geol. Bull., v. 58, pp. 1008-1024.

Swingle, G. D., 1964, Elevation of the Chickamauga limestone to group status in east Tennessee (abs.): Tenn. Acad. Sci. Jour., v. 39, No. 2, p. 66.

Tebbut, G. E., Conley, C. D., and Boyd, D. W., 1965, Lithogenesis of a distinctive carbonate rock fabric: Contributions to geology, University of Wyoming, v. 4, pp. 1-13.

Twenhofel, W. H., 1939, Principles of sedimentation: McGraw-Hill, New York, 610 p.

Ulrich, E. O., 1911, Revision of the Paleozoic systems: Geol. Soc. Am. Bull., v. 22, pp. 281-680.

Wagner, R. J., 1973, Stratigraphic and structural controls and genesis of barite deposits in Washington County, Missouri: Unpub. Ph.D. Diss., University of Michigan, 265 p.

Walker, K. R., A brief introduction to the ecostratigraphy of the Middle Ordovician of Tennessee (Southern Appalachians, U.S.A.) in Ruppel, S. C., and Walker, K. R. (eds.), The ecostratigraphy of the Middle Ordovician of the Southern Appalachians (Kentucky, Tennessee, Virginia), U.S.A.: A field excursion, pp. 12-17.

Walker, K. R., and Laporte, L. F., 1970, Congruent fossil communities from Ordovician and Devonian carbonates of New York: Jour. Paleontology, v. 44, pp. 928-944.

Wanless, H. R., 1979, Limestone response to stress: pressure solution and dolomitization: Jour. of Sed. Petrol., v. 49, pp. 437-462.

Wedow, H., Jr., chm., 1971, A paleoaquifer and its relation to economic mineral deposits: The Lower Ordovician Kingsport Formation and Mascot Dolomite. A Symposium: Econ. Geol., v. 66, pp. 695-810.

Wilson, R. C. L., 1966, Silica diagenesis in Upper Jurassic limestones of southern England: Jour. Sed. Petrol., v. 36, pp. 1036-1049.

Wolfe, M. J., 1970, Dolomitization and dedolomitization in the Senonian chalk of Northern Ireland: Geol. Mag., v. 107, pp. 39-49.

Zenger, D. H., 1972, Significance of supratidal dolomitization in the geologic record: Geol. Soc. Am. Bull., v. 83, pp. 1-12.

APPENDIX

APPENDIX

CONSTRUCTION OF STRATIGRAPHIC FRAMEWORK

The method of erecting the stratigraphic framework used in this study was subject to errors from the following sources:

1. Plane table survey error--Standard survey techniques (Compton, 1962, pp. 88-112) were used in determining the relative elevations and precise map locations of most control points. Other control points were added from these plane table control points with a steel tape and Brunton compass. Overall, the elevations of control points were probably determinted with an accuracy of $\pm$.3 meter. Locations are probably accurate within $\pm$1 meter. Figure A-1 gives the locations, with assigned numbers, for all control points used in construction of the stratigraphic framework.

2. Error in strike and dip measurements--Repeated rechecking, especially of shallowly dipping beds, has probably kept errors in measurement to a minimum. Stratigraphic calculations in all cases were made using the measured attitude closest to the control points.

3. Natural variations in outcrop attitudes--These stratigraphic calculations assume perfectly planar strata of constant dip. Many natural processes have acted upon the sediments from the time of deposition until the present to complicate this assumption. Factors that must be considered include such things as the possible occurrence of depositional dip, structural complications both regional and local in scope, and local solution activity.

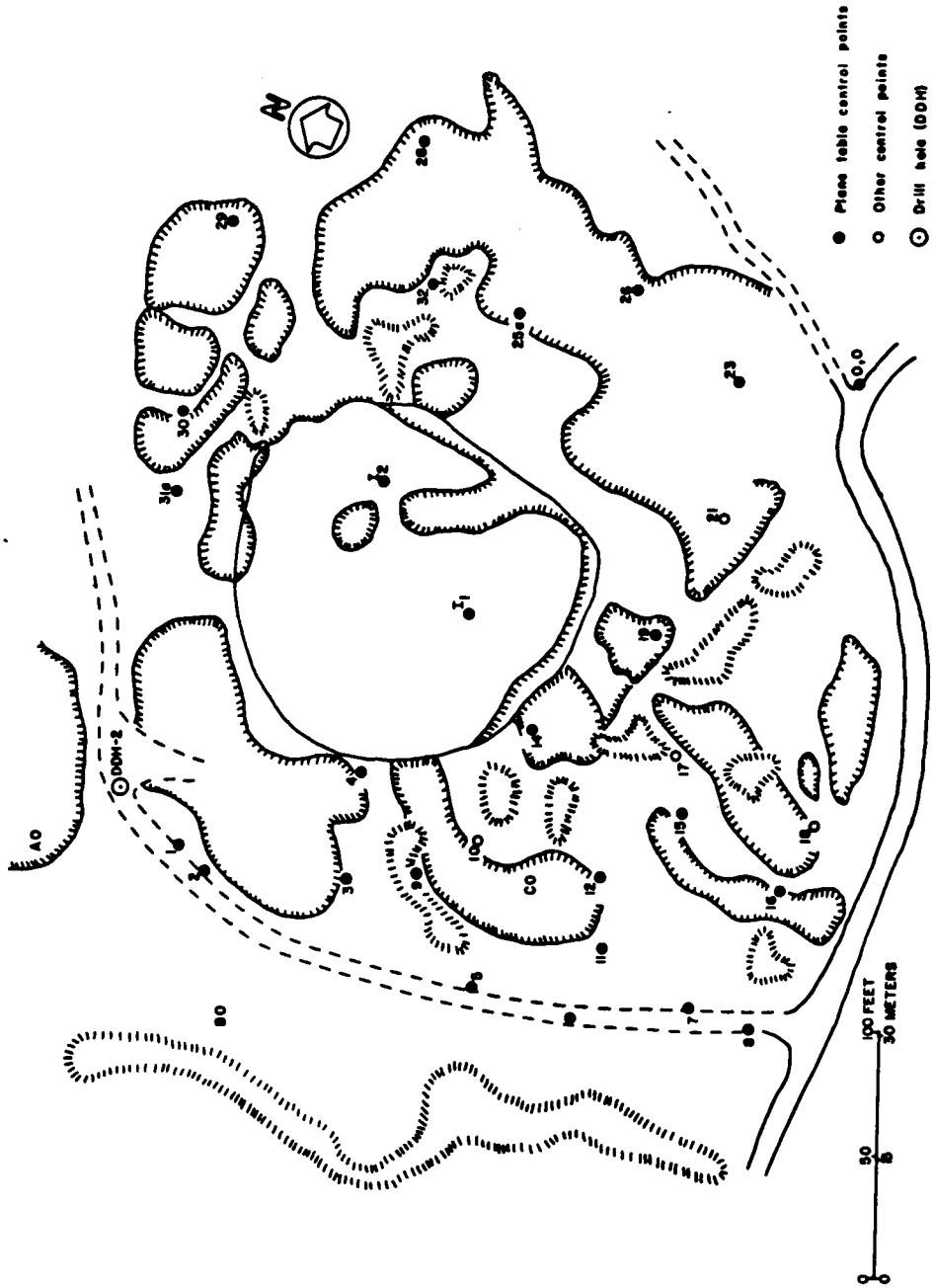


Figure A-1. Control points used in construction of stratigraphic framework.

Primarily as a result of variables such as those listed above, determination of relative stratigraphic positions for two control points generally yielded a range of values. These determinations were made graphically using English system measurements. Metric values are, however, shown on the lithofacies diagram (see Figure 14, page 36) which represents a synthesis of field work, these stratigraphic calculations, and thin section petrography.

Cross sections were prepared into which the bedding attitudes of control points were projected. Simple measurements on the cross sections perpendicular to bedding yielded relative stratigraphic positions. An example is given in Figure A-2. As can be seen, control point #2 is not less than 7 feet or more than 12 feet below control point #3 over the interval considered (which is equal to the ground distance between the two points). Stratigraphic positions of control points were calculated in a sequential fashion. For instance, once the relative positions of #1 and #2 control points were established, then #2 and #3 were compared, #3 and #4, and so on.

The relative stratigraphic positions of samples were determined by measuring their stratigraphic position relative to the closest control point. Lithologic comparisons and thin section petrography were sometimes able to better define the relative stratigraphic positions of control points, and hence served as an internal check of the accuracy of the overall stratigraphic framework. As an example, the possible calculated stratigraphic range between control points #2 and #3 is 7-12 feet, #3 being 7-12 feet above #2. The stratigraphic positions of several rock samples, measured from control point #3, are greater than 7 feet below the #3 horizon. Therefore, if the range between #2 and #3 is the

Control point	Elevation (relative)	Distance between points	Attitude	Trend of section line	Angle of intersection of strike line and section line	Apparent dip
#2	25.7		N58E,16SE		86	16
		54'		N28°W		
#3	17.2		N58E, 21SE		86	21

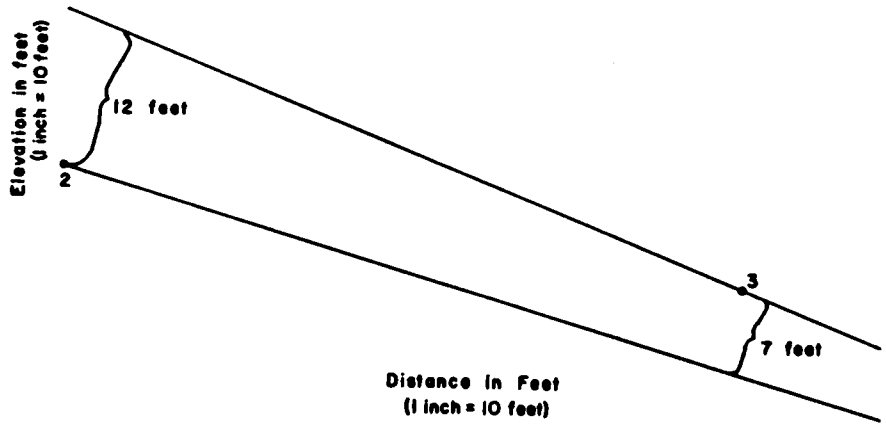


Figure A-2. Example of graphical determination of stratigraphic position.

minimum, i.e., 7 feet, these rock samples will overlap samples collected with reference to control point #2. In this example, lithologic and thin section comparisons indicated that a full 12 feet of stratigraphic section between control points #2 and #3 is probably justified.

The inherent weaknesses in modifying the stratigraphic framework in this fashion are many, not the least of which is the fact that lateral variations in environment and lithologic type are to be expected at any point in time across the environmentally complex Middle Ordovician Lost Creek tidal flats. Still, this would seem to be the best method for eliminating ranges and selecting single values for relative stratigraphic positions of the control points.

A comparison of the varying stratigraphic positions of the Knox unconformity at Lost Creek, using the above methods, indicates at least 12 meters (40 feet) of relief developed over a ground distance of 76 meters (250 feet).

VITA

Roger Thomas Steinberg was born in Lancaster, Pennsylvania, on February 4, 1952. He attended elementary school in Quarryville, Pennsylvania, and was graduated from Solanco High School, also in Quarryville, in June 1970. The following September he entered Wake Forest University. In September 1971 he transferred to the University of Tennessee, Knoxville, and received a Bachelor of Arts degree with High Honors in Geology in June 1974.

In the fall of 1974 he accepted a graduate assistantship at the University of Tennessee, Knoxville, and began study toward a Master's degree in Geology. This degree was awarded in June 1981.

During the period from 1974 to 1980 the author held several temporary and summer jobs with companies engaged in mineral exploration. He also worked as a carpenter for a year and a half.

Mr. Steinberg is a member of Sigma Gamma Epsilon and the Society of Mining Engineers of AIME. He is currently employed by The Hanna Mining Company, St. Louis, Missouri.